Mathematical models of biofilm growth and food particle degradation in the gastrointestinal tract

A thesis presented in partial fulfillment of the requirements for the degree of

Doctor of Philosophy

in

Nutrition

at

Massey University

Palmerston North

New Zealand

Amy S. Van Wey Lovatt

2013

ABSTRACT

This thesis focuses on two important aspects of digestion: soluble nutrient loss during gastric digestion and the fermentation of digesta by intestinal bacteria.

The bioaccessibility of nutrients within a food matrix has become of increasing interest as it is the precursor of bioavailability. pH directly affects enzymatic reactions and has a significant effect on the soluble loss from the food matrix. Analysis of the propagation of acidic water in two model foods showed that the diffusion of the fluid depends on both the pH and the food matrix. Mathematical models were developed to describe the soluble particle loss during gastric digestion at various pH levels and to predict the likely rate of soluble particle loss during digestion

Food components that are indigestible in the upper gastrointestinal (GI) tract are likely substrate for the microbiota of the large bowel. The proximity of the microorganisms to one another provides the potential for cross-feeding and competition for nutrients. A modification of a mathematical model was used to characterize the growth kinetics of 18 *Bifidobacterium* strains. This model was extended to describe nutrient competition and cross-feeding between *Bacteroides thetaiotaomicron* and two *Bifidobacterium* species and was able to predict their coculture growth dynamics based on their respective monoculture growth kinetics.

While it has been known that the GI tract harbors a diverse bacterial population, biofilms were only recently observed to be associated with the digesta. Biofilm growth is critically dependent on the nutrient availability. Mathematical models that describe nutrient transport within biofilms have made three simplifying assumptions: the effective diffusion coefficient (EDC) is constant, is that of water, and/or is isotropic. Using a Monte Carlo simulation, EDC values were determined, both parallel and

perpendicular to the substratum, within 131 single species, three-dimensional biofilms, constructed from confocal laser scanning microscopy images. This study showed that diffusion within bacterial biofilms was anisotropic and depth dependent. A new reaction-diffusion model is proposed to describe the nutrient concentration within a bacterial biofilm that accounts for the depth dependence of the EDC.

This thesis enhances our current knowledge in nutrition and microbiology by providing more accurate models that describe food degradation due to acidic hydrolysis and bacterial fermentation.

ACKNOWLEGMENTS

There are many people with whom I owe my gratitude for their guidance, support and encouragement. I would like to begin by thanking my many supervisors, all of whom were available every time I needed them: Warren McNabb, Nicole Roy, Adrian Cookson, Tanya Soboleva, Paul Moughan, and Paul Shorten. In particular, I would like to thank Nicole Roy for her continued encouragement to publish my work and unfailing effort to convert me from American to Kiwi English (who would have thought it would be such a challenge to learn to use a "s" in place of a "z"); Adrian Cookson for teaching me that it is quite acceptable to give deadlines to supervisors; Paul Moughan and the Riddet Institute, Centre of Research Excellence, for granting me the Earle Food Research Fellowship, which provided me with three years funding and opportunities to attend both national and international conferences; Warren McNabb for his willingness to continue to fund me and my project after my scholarship ended and for not being offended when I referred to him as "my figure head, like the Queen of England to New Zealand"; Tanya for being tough, which pushed me to work a bit harder; and finally Paul Shorten, my go to guy who not only encouraged me throughout my PhD process but was my constant sounding board and would at times "round me in" when I had "lost the plot".

A big thanks goes out to Romain Briandet and Arnaud Bridier. Without their contribution (the growth and CLSM images of over 100 microbial biofilms) I would not have been able to show that diffusion within biofilms is anisotropic. A big thanks also goes to Robert Wieliczko for teaching me the basics in order for me to complete the experiments necessary to model the degradation of food particles and to Pauline Hunt for her critical and artistic eye in helping me to improve some of my figures.

I would like to thank the many friends I have met at the Ruakura Research Centre and the Riddet Institute. Without their friendship, living in a foreign country would not have been so enjoyable. To Margy Madsen and Chantelle Petrone, my longtime friends who encouraged me throughout my entire academic career and pushed me to continue when times were tough and I wanted to throw in the towel.

Most of all, I would like to thank my family. Without the encouragement of my parents I may have never applied for the PhD project in New Zealand. More so, I would like to thank them for a lifetime of continued emotional support and guidance. I would like to thank my son for learning to make a life for himself in New Zealand and for his subtle support over these years, despite his fears, disappointment, and anger for moving him across the world (during his teenage years) and away from our wonderfully supportive family. Last, I would like to thank my husband, Simon Lovatt, for refusing to marry me until my PhD was submitted. What a motivator!

Contents

List of Figures

List of Tables

List of Abbreviations

Acid-Base (AB)

autoinducer 2 (AI-2)

chronic fatigue syndrome (CFS)

confocal laser scanning microscopy (CLSM)

degree of polymerization (DP)

Derjaguin-Landau-Verwey-Overbeek (DLVO)

effective diffusion coefficient (EDC)

extended DLVO (XDLVO)

extracellular polymeric substances (EPS)

fluorescence correlation spectroscopy (FCS)

fluorescence return after photo bleaching (FRAP)

fructose equivalents (FE)

gastrointestinal (GI)

gastric fluid (GF)

inflammatory bowel disease (IBD)

Lifshitz-van der Waals (LW)

Markov chain Monte Carlo (MCMC)

short chain fatty acids (SCFA)

simulated gastric fluid (SGF)

translocated intimin receptor (Tir)

Publications

Van Wey, A. S., Cookson, A.L., Roy, N.C., McNabb, W.C., Soboleva, T.K., Shorten, P.R. (2011) Bacterial biofilms associated with food particles in the human large bowel. *Molecular Nutrition and Food Research* **55** (7); 969-978

Van Wey, A. S., Cookson, A.L., Soboleva, T.K., Roy, N.C., McNabb, W.C., Bridier, A. Briandet, R., Shorten, P.R. (2012) Anisotropic nutrient transport in three-dimensional single species bacterial biofilms. *Biotechnology and Bioengineering* **109** (5); 1280-1292

Van Wey, A. S., Cookson, A.L., Roy, N.C., McNabb, W.C., Soboleva, T.K., Wieliczko, R.J., Shorten, P.R. (Submitted) A mathematical model of the pH and food matrix composition on fluid transport into foods: An Application in gastric digestion and cheese brining. *Food Research International*

Van Wey, A. S., Cookson, A.L., Roy, N.C., McNabb, W.C., Soboleva, T.K., Shorten, P.R. (Submitted) Monoculture parameters successfully predict the coculture growth of *Bacteroides thetaiotaomicron* and *Bifidobacterium*. *ISME Journal*

Van Wey, A.S. and Shorten, P.R. (Accepted) Mathematical models of food degradation in the human stomach. In: Boland M, Golding M, Singh H (eds). *Food Structures, Digestion and Health.* Elsevier.

Chapter 1 Introduction

1.1. Background

Diet is often considered the major driver influencing nutrition; however the diet is only one aspect of human nutrition. In order for a healthy individual to make use of the nutrients within their diet, the nutrients must first become bioaccessible (released from the food matrix) and bioavailable (absorbed and used by the host). Thus, the ability of the gastrointestinal (GI) tract to function efficiently is a component of both the effectiveness of bioaccessibility and bioavailability of nutrients.

The bioaccessibility of nutrients begins with mastication and the secretion of salivary enzymes (amylase and lingual lipase), which soften and fragment the food into smaller particles. This fragmentation increases the overall surface area to volume ratio, which improves digestion within the stomach. The increased surface area to volume ratio provides additional contact area for gastric fluid (GF) to absorb into the food particle; this absorption of GF tenderizes the food matrix and increases the bioaccessibility of the nutrients within the food matrix. These nutrients are then transported into the small bowel for absorption and then become bioaccessible. For particles that are still too large to be passed to the small bowel, peristaltic contractions squeeze the food bolus and create retropulsive flow patterns which moves the food bolus from the antrum to the proximal region of the stomach. This movement, in conjunction with the force of the contractions, contributes to additional fracturing of food components and also causes erosion of the food matrices as the particles come into contact with other foods within the bolus.

Within the small bowel, additional proteases (trypsin, chymotrypsin, carboxypeptidase, etc.), pancreatic lipase and bile salts are secreted which are absorbed into the food matrix. Here most of the protein and fat contents of food are leached into the lumen of the small bowel then transported through the intestinal epithelium for utilization by the host. Components of the food matrix that are indigestible by the host are then passed into the large bowel. While it is commonly believed that all available nutrients have been absorbed in the small bowel and thus the host has received all possible benefits from the diet, this is not the case.

Historically, it has been believed that the function of the large bowel is to absorb water and salts before the removal of the undigested food components. However, over the past 30 years the focus of scientific research on the interaction between the commensal intestinal bacteria and the host has demonstrated that the large bowel has a much broader role in human health. The large bowel provides a nutrient rich environment in which a diverse bacterial population thrives. It is estimated that there are 10^{14} bacteria cells within the digestive tract (Luckey 1972), composed of over 1000 distinct bacterial species (Hooper and MacPherson 2010). As the bacteria ferment the non-digested food components, they produce metabolites that are essential for human health. Indeed, intestinal bacteria provide the major source of metabolites such as folic acid.

1.2. Dissertation Overview

This thesis aims to mathematically model some of the key components of human digestion. Here the focus is on specific topics in which there is a significant gap in the current literature in order to elucidate the key physiological factors involved in nutrient bioavailability. In particular, this thesis focuses on two significant aspects of digestion.

Primarily, this thesis focuses on the interaction between the commensal bacteria and food particles in the human large bowel. The effects of gastric pH and food matrix composition on the digestion of food within the human stomach are also considered in this thesis. This gastric digestive aspect was instigated in order to understand how bacteria metabolize non-digested food components in that extracellular enzymes may degrade food particles in a manner similar to the way nutrients are released from a food matrix by gastric fluid. The interaction between the commensal bacteria and food particles in the human large bowel is also dependent on the food particle size and composition, which in turn are dependent on digestion in the stomach.

It may be argued that food particle size and composition also depends upon the digestive process in the small bowel. Such a statement is true; however, the commensal intestinal bacteria are primarily saccharolytic and thus preferentially ferment dietary fiber such as resistant starch and non-starch polysaccharides. The rapid transit time of dietary fiber, combined with the low bacterial population within the small bowel, minimizes the impact of particle degradation by the small bowel commensal bacteria. Essentially, the substrates preferred by the commensal bacteria will pass from the stomach through the small bowel having only been altered by the gastric environment. Thus, gastric digestion, rather than small bowel digestion, plays a significant role in determining the particle size and composition of the food matrix that will be fermented by the commensal bacteria in the large bowel.

Chapter 2 includes a review of gastric digestion, the effects of the components of the food matrix on digestibility and the mathematical models currently in the literature which relate to the degradation of food particles within the human stomach. Most of the section reviewing gastric digestion and the models related to gastric digestion will be published, as a book chapter, in the book titled *Food Structures, Digestion and Health*

(Van Wey and Shorten Accepted). Chapter 2 also reviews the current literature with regards to bacterial biofilms associated with food particles in the human large bowel. This review was published in *Molecular Nutrition and Food Research* (Van Wey et al 2011). Mathematical models of biofilm growth and nutrient transport within biofilms are reviewed along with current methods for determining nutrient transport within biofilms. Much of this section has been published in *Biotechnology and Bioengineering*. Lastly, Chapter 2 summarizes the literature on the substantial impact of bacterial metabolites on human health, the relevance of considering oligofructose and inulin as substrates for the commensal intestinal bacteria, as well as an analysis of the mathematical models within the literature that focus on microbial competition/cross-feeding. This section is based on the introduction in the manuscript submitted to *ISME Journal.* [Please see the List of Publications for details].

In Chapter 3, the effects of gastric pH and food matrix composition, on the digestion of food within the human stomach, are considered. Within this chapter, the effects of gastric pH and food composition on the propagation of the wetting front of simulated gastric fluid without pepsin or mucin in two food models (carrot and Edam cheese) are measured and analyzed. A model to describe the non-linear rate of soluble particle loss during digestion at various constant pH levels is developed, which incorporates the non-linear propagation of the acidic water into the food matrix. In addition, a model to predict the likely rate of soluble particle loss during digestion in the stomach is developed, which accounts for the change of pH during the digestion time period. The content of Chapter 3 has been submitted to *Food Research International* for publication (Van Wey et al Submitted-b).

In Chapter 4, models of the metabolism of fructose, oligofructose and inulin by the commensal intestinal bacteria are described. Within this chapter, a model that draws

upon the previously proposed dynamic, mechanistic mathematical model of Amaretti et al (2007) to describe the mechanisms for substrate consumption and subsequent microbial growth and metabolite production for bacteria grown in monoculture is developed. This model is modified to describe the preferential degradation of oligofructose for monoculture microbial growth.

In addition to the aforementioned models, a model is developed to describe competition between two bacterial species for a particular substrate as well as cross-feeding resulting from the breakdown products from extracellular carbohydrate hydrolysis by one of the bacterial species. This competitive/cross-feeding model incorporates the primary metabolites produced by both bacterial species. The competition/cross-feeding model is used to explore and predict the growth dynamics between *Bacteroides thetaiotaomicron* LMG 11262 and *Bifidobacterium longum* LMG 11047 and *Bacteroides thetaiotaomicron* LMG 11262 and *Bifidobacterium breve* Yakult as compared to experimental coculture data.

Chapter 4 can be considered a macroscopic view of the formation of heterogeneous bacterial biofilms within the human GI tract. The work in Chapter 4 has been submitted for publication in *ISME Journal* (Van Wey et al Submitted-a).

In Chapter 5, a microscopic view of bacterial biofilms is employed to investigate the transport of nutrients within a bacterial biofilm. Within this chapter, (1) a method is developed to determine the effective diffusion coefficient (EDC) within 131 distinct, single species, three-dimensional bacterial biofilms; (2) the level of anisotropic transport within bacterial biofilms is characterized; (3) the relationship between the porosity of the biofilm and the EDC is determined; and (4) a model for nutrient transport within a bacterial biofilm growing on a nutrient-providing substratum is

constructed. The work presented in Chapter 5 has been published in *Biotechnology and Bioengineering* (Van Wey et al 2012).

DRC 16

MASSEY UNIVERSITY
GRADUATE RESEARCH SCHOOL

STATEMENT OF CONTRIBUTION TO DOCTORAL THESIS CONTAINING PUBLICATIONS

(To appear at the end of each thesis chapter/section/appendix submitted as an article/paper or collected as an appendix at the end of the thesis)

We, the candidate and the candidate's Principal Supervisor, certify that all co-authors have consented to their work being included in the thesis and they have accepted the candidate's contribution as indicated below in the *Statement of Originality*.

Name of Candidate: Amy S. Van Wey

Name/Title of Principal Supervisor: Warren McNabb

Name of Published Research Output and full reference:

Van Wey, A. S., Cookson, A.L., Roy, N.C., McNabb, W.C., Soboleva, T.K., Shorten, P.R. (2011) Bacterial biofilms associated with food particles in the human large bowel. Molecular Nutrition and Food Research 55 (7); 969-978

In which Chapter is the Published Work: Chapter 2

Please indicate either:

- The percentage of the Published Work that was contributed by the candidate:

  and / or

- Describe the contribution that the candidate has made to the Published Work:

  The candidate did the necessary research for the manuscript and prepared the manuscript for publication.

Amy S. Van Wey — Candidate's Signature — 23/05/2013 — Date

Warren McNabb — Principal Supervisor's signature — 23/05/2013 — Date

DRC 16

MASSEY UNIVERSITY
GRADUATE RESEARCH SCHOOL

STATEMENT OF CONTRIBUTION TO DOCTORAL THESIS CONTAINING PUBLICATIONS

(To appear at the end of each thesis chapter/section/appendix submitted as an article/paper or collected as an appendix at the end of the thesis)

We, the candidate and the candidate's Principal Supervisor, certify that all co-authors have consented to their work being included in the thesis and they have accepted the candidate's contribution as indicated below in the *Statement of Originality*.

Name of Candidate: Amy S. Van Wey

Name/Title of Principal Supervisor: Warren McNabb

Name of Published Research Output and full reference:

Van Wey, A.S. and Shorten, P.R. (Submitted) Mathematical models of food degradation in the human stomach. In: Boland M, Golding M, Singh H (eds). Food Structures, Digestion and Health. Elsevier.

In which Chapter is the Published Work: Chapter 2

Please indicate either:

- The percentage of the Published Work that was contributed by the candidate:

  and / or

- Describe the contribution that the candidate has made to the Published Work:

  The candidate did the necessary research, mathematical modeling, and preparation for portion of the manuscript which is included in the thesis.

Amy S. Van Wey — Candidate's Signature — 23/05/2013 — Date

Warren McNabb — Principal Supervisor's signature — 23/05/2013 — Date

GRS Version 3– 16 September 2011

DRC 16

MASSEY UNIVERSITY
GRADUATE RESEARCH SCHOOL

STATEMENT OF CONTRIBUTION
TO DOCTORAL THESIS CONTAINING PUBLICATIONS

(To appear at the end of each thesis chapter/section/appendix submitted as an article/paper or collected as an appendix at the end of the thesis)

We, the candidate and the candidate's Principal Supervisor, certify that all co-authors have consented to their work being included in the thesis and they have accepted the candidate's contribution as indicated below in the *Statement of Originality*.

Name of Candidate: Amy S. Van Wey

Name/Title of Principal Supervisor: Warren McNabb

Name of Published Research Output and full reference:

Van Wey, A. S., Cookson, A.L., Roy, N.C., McNabb, W.C., Soboleva, T.K., Wieliczko, R.J., Shorten, P.R. (Submitted) A mathematical model of the pH and food matrix composition on fluid transport into foods: An Application in gastric digestion and cheese brining. Food Research International.

In which Chapter is the Published Work: Chapter 3 and part of Chapter 2

Please indicate either:

- The percentage of the Published Work that was contributed by the candidate:

  and / or

- Describe the contribution that the candidate has made to the Published Work:

  The candidate did the necessary research, labwork, mathematical modeling, and preparation for this manuscript .

Amy S. Van Wey — Candidate's Signature — 23/05/2013 — Date

Warren McNabb — Principal Supervisor's signature — 23/05/2013 — Date

GRS Version 3– 16 September 2011

DRC 16

MASSEY UNIVERSITY
GRADUATE RESEARCH SCHOOL

STATEMENT OF CONTRIBUTION TO DOCTORAL THESIS CONTAINING PUBLICATIONS

(To appear at the end of each thesis chapter/section/appendix submitted as an article/paper or collected as an appendix at the end of the thesis)

We, the candidate and the candidate's Principal Supervisor, certify that all co-authors have consented to their work being included in the thesis and they have accepted the candidate's contribution as indicated below in the *Statement of Originality*.

Name of Candidate: Amy S. Van Wey

Name/Title of Principal Supervisor: Warren McNabb

Name of Published Research Output and full reference:

Van Wey, A. S., Cookson, A.L., Roy, N.C., McNabb, W.C., Soboleva, T.K., Shorten, P.R. (Submitted) Monoculture parameters successfully predict the coculture growth of Bacteroides thetaiotaomicron and Bifidobacterium. ISME

In which Chapter is the Published Work: Chapter 4 and portions of Chapter 2

Please indicate either:

- The percentage of the Published Work that was contributed by the candidate:

  and / or

- Describe the contribution that the candidate has made to the Published Work:

  The candidate did the necessary research, mathematical modeling, and preparation for this manuscript .

Amy S. Van Wey — Candidate's Signature — 23/05/2013 — Date

Warren McNabb — Principal Supervisor's signature — 23/05/2013 — Date

DRC 16

MASSEY UNIVERSITY
GRADUATE RESEARCH SCHOOL

STATEMENT OF CONTRIBUTION
TO DOCTORAL THESIS CONTAINING PUBLICATIONS

(To appear at the end of each thesis chapter/section/appendix submitted as an article/paper or collected as an appendix at the end of the thesis)

We, the candidate and the candidate's Principal Supervisor, certify that all co-authors have consented to their work being included in the thesis and they have accepted the candidate's contribution as indicated below in the *Statement of Originality*.

Name of Candidate: Amy S. Van Wey

Name/Title of Principal Supervisor: Warren McNabb

Name of Published Research Output and full reference:

Van Wey, A. S., Cookson, A.L., Soboleva, T.K., Roy, N.C., McNabb, W.C., Bridier, A. Briandet, R., Shorten, P.R. (2012) Anisotropic nutrient transport in three-dimensional single species bacterial biofilms. Biotechnology and Bioengineering 109 (5); 1280-1292

In which Chapter is the Published Work: Chapter 5 and part of Chapter 2

Please indicate either:

- The percentage of the Published Work that was contributed by the candidate:

  and / or

- Describe the contribution that the candidate has made to the Published Work:

  The candidate did the necessary research for the manuscript, all of the mathematical modeling within the manuscript, and prepared the manuscript for publication. Arnaud Bridier and Romain Briandet cultured the biofilms, provided the CLSM images and a summary of the methods for culturing and staining the biofilms which was incorporated in the Materials and Methods section (5.3.1).

Amy S. Van Wey — Candidate's Signature — 23/05/2013 — Date

Warren McNabb — Principal Supervisor's signature — 23//05/2013 — Date

Chapter 2 Literature Review

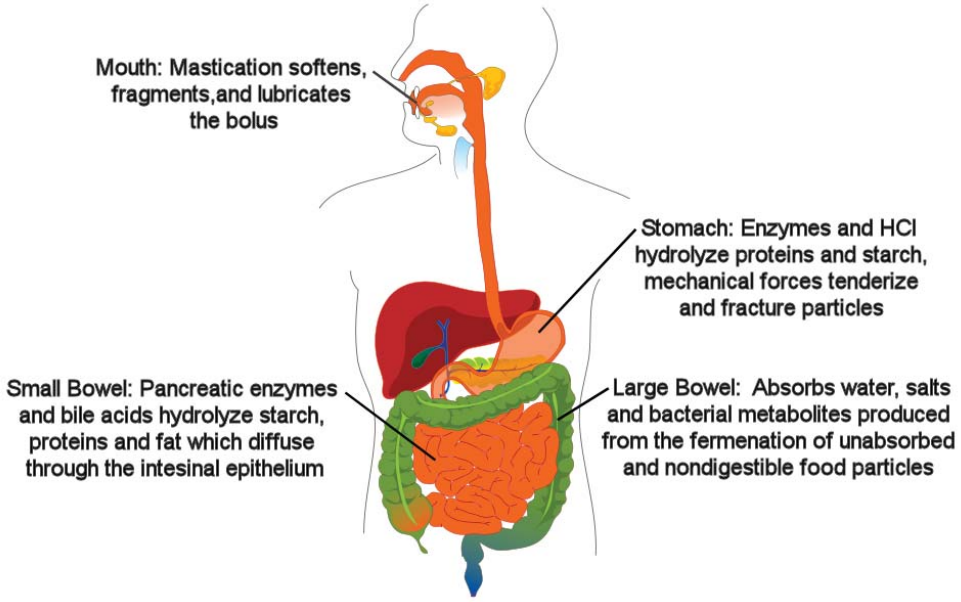

Figure 2.1 Highlights of the human digestive process which begins with mastication and ends with bacterial fermentation of undigested food particles in the large bowel.

2.1. Food Degradation as a Result of Gastric Digestion

Digestion begins with the mastication of food particles [Figure 2.1]. While mastication is not essential to the chemical breakdown of food particles in the stomach (Davenport 1982), it is beneficial in that mastication mixes the food with the saliva which lubricates and softens the foods. Additionally, a key enzyme in saliva, α-amylase, aids in the digestion of starch during gastric digestion when the pH of the gastric contents is greater than three (Bornhorst and Singh 2012). Most importantly, the

process of mastication reduces the particle size which increases the surface area of the particles allowing for more contact with and increased absorbance of gastric fluid upon entering the stomach.

The human stomach is a dynamic and complex system, where the degradation of food particles is the result of mechanical forces and chemical reactions. Peristaltic movements in the stomach compress the food bolus which may lead to fracturing of particular food matrices. The peristaltic movements also move the viscous food bolus in a retropulsive flow pattern. This movement leads to shearing and erosion of the individual food surfaces through contact with other food components in the bolus. In addition to mechanical forces, acidic hydrolysis and enzymatic reactions cause leaching of nutrients from the food matrix to be absorbed in the small bowel. Food digestion kinetics are not limited to mechanical forces, but also depend on food structures, particle size, meal volume and composition, viscosity, pH, temperature and enzymatic reactions.

Food particles are broken down by the processes of erosion, fragmentation, and tenderization (Kong and Singh 2009a, Kong and Singh 2009b, Kong et al 2011, Kong and Singh 2011). These processes are shown in Figure 2.2. Erosion describes the process of the gradual wearing away of the food surface when the applied stresses are less than that required to fracture or break the food particle. Fragmentation describes the breaking of food particles into two or more similar sized particles. The process of tenderization occurs as a result of the transport of gastric juice into the food particle and the resulting softening of the food matrix. In general, the process of tenderization increases the rate of erosion and fragmentation. The transport of gastric juice into food particles also facilitates leaching of solids into the gastric medium.

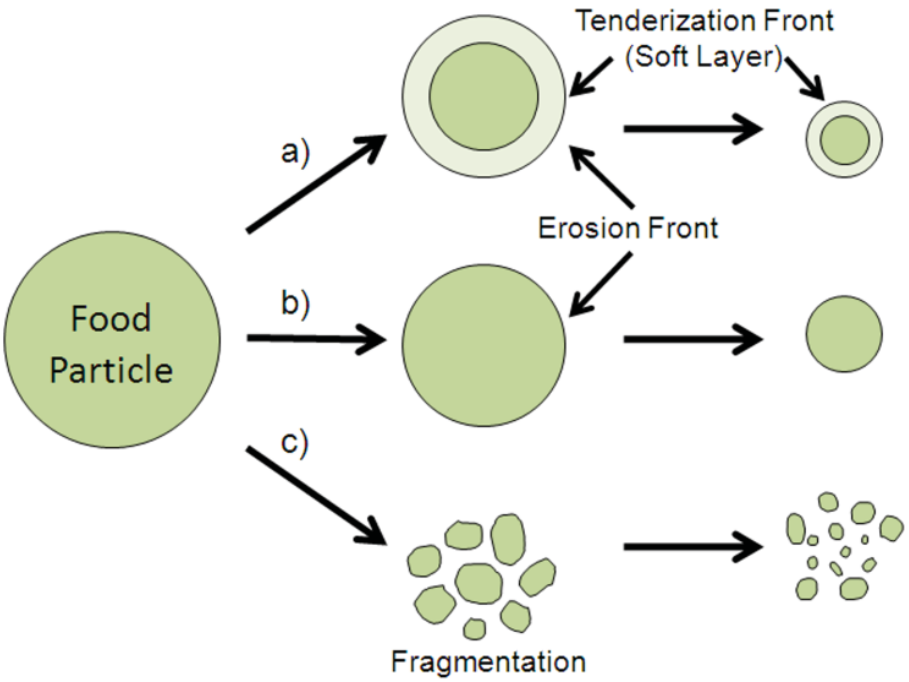

Figure 2.2 The three processes of food particle degradation: (a) tenderization, (b) erosion and (c) fragmentation.

2.1.1. Effects of the Components of the Food Matrix on Gastric Digestion

The food matrix composition has a marked effect on the degradation of the food particle and may restrict or enhance enzymatic reactions. The digestibility of proteins in various foods (legumes, cereals, milk products, chicken and kiwifruit) can be dependent upon the protein secondary structure, in particular the *β*-sheets (Bublin et al 2008, Carbonaro et al 2012, Guo et al 1995). These same secondary structures are found in *β*-lactoglobulin, which has been shown to be resistant to proteolysis by both pepsin and trypsin (Guo et al 1995).

While it is expected that the amount of protein in a food matrix would have an effect on the ability of pepsin to hydrolyze peptides, the amount of fat in the food matrix

can also have a marked effect on protein digestibility. In a double-blind placebo-controlled food challenge that tested for the allergenicity of peanuts in a recipe with low and high fat content, it was found that the high fat content resulted in a low oral allergenic effect (Grimshaw et al 2003). It was surmised that the lack of early oral warning signs (i.e. anaphylactic response) was due to a concealing effect by the fat in the high-fat food matrix, which reduced the bioaccessibility of the proteins. The ability of fat to restrict the bioaccessibility of foods during gastric digestion has also been shown in studies with vitamin B_{12} encapsulated in a water-in-oil-in-water double emulsion (Giroux et al 2013). In the study only 4.4% of vitamin B_{12} was released after 120 minutes of gastric digestion. Thus, the fat content of foods will have an effect on the digestibility, and hence, bioaccessibility of nutrients.

2.1.2. Mathematical Models of Gastric Digestion

There are remarkably few mathematical models in the literature that describe food degradation in the human stomach.

2.1.2.1. Mathematical Models of Fluid and Food Particle Flow in the Stomach

The area that has received the most attention is that of modeling the motility and geometry of the human stomach (Ferrua et al 2011). These models are based on computation fluid dynamics (CFD). CFD has also been used in industrial/engineering contexts to model particle-fluid flow, particle-fluid interactions, particle-particle interactions, particle-wall interactions and particle erosion (which has been described as a function of the particle impact velocities) (Li et al 2009).

Many of these models have described the stomach geometry and motility in two dimensions for simplicity; however, Ferrua & Singh (2010) using a 3-D model have shown that the flow of gastric contents is three dimensional and that the 2-D models

cannot account for the differences in velocity and flow patterns as described with a 3-D model. In particular, the 2-D model cannot reproduce the retropulsive flow pattern and eddy structures predicted by the 3-D model. The 3-D model predicted "that the strongest fluid motions developed in the antropyloric region, and that a slow but constant flow recirculation occurred between the proximal and distal regions of the stomach" (Ferrua et al 2011).

While the 3-D model has provided good insight into the function of peristaltic contractions and the movement of the stomach contents, it has yet to be expanded to describe the shearing or fracturing of food components in the human stomach or the leaching of nutrients from the food matrix.

2.1.2.2. Empirical Models of Wet Mass Retention During Gastric Digestion

The first mathematical models to describe the degradation of a food matrix have primarily focused on the wet mass retention ratio of the food (wet sample weight after digestion time t divided by the initial wet sample weight). The wet mass retention ratio has been observed to follow three distinct profiles (delayed sigmoidal, sigmoidal and exponential, Figure 2.3), yet all three profiles can be described using one equation:

$$y(t) = (1 + k\beta t)\exp(-\beta t) \qquad 2.1$$

where k and β are constants found using regression (Kong and Singh 2008, Kong and Singh 2009b). The sigmoidal profile can be described by an initial slow disintegration stage, followed by an exponential disintegration profile. The delayed sigmoidal profile occurred in foods with low moisture content. In these foods, the absorption of gastric fluid increased the wet weight of the food to such an extent that it exceeded the degradation rate, which resulted in a wet mass retention ratio greater than 1. The delayed sigmoidal profile can be seen with studies of raw and roasted almonds; in this case the wet mass retention ratio increased, as a result of gastric fluid absorption, even

though the dry solid mass decreased over the same digestion time (Kong and Singh 2009a).

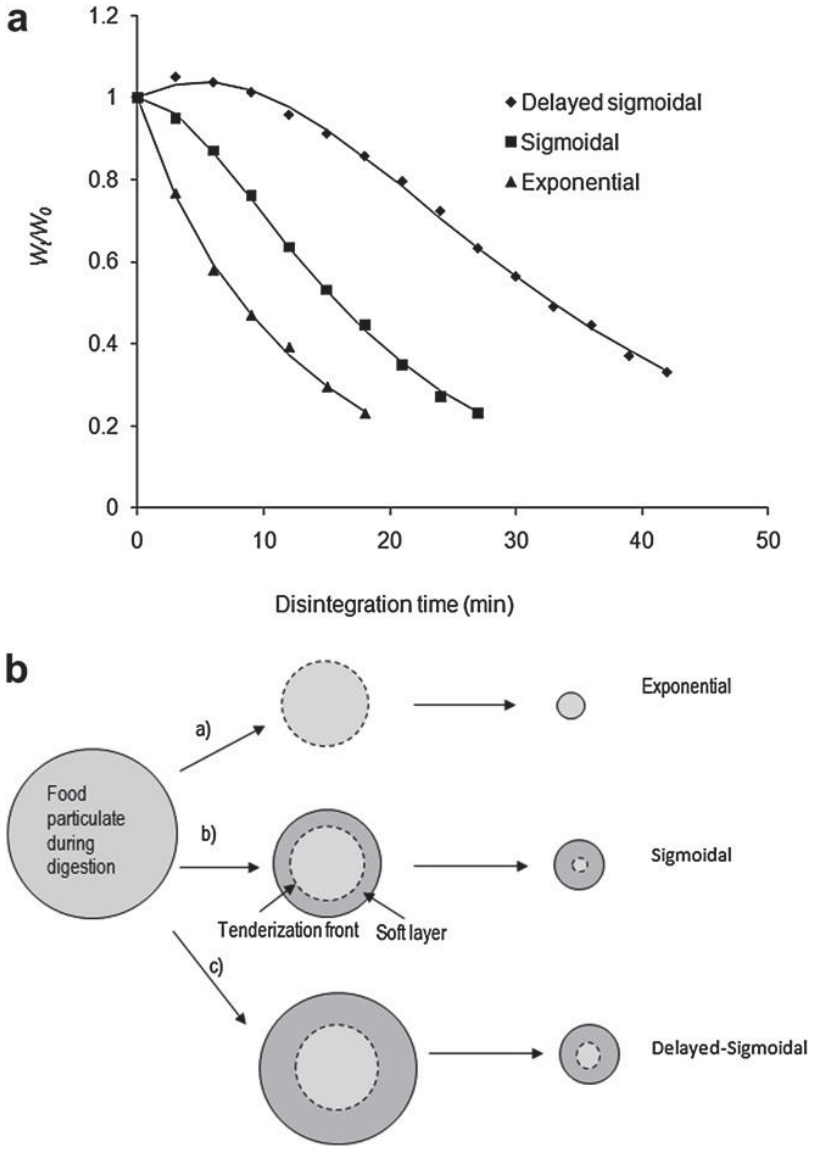

Figure 2.3 (a) Three different profiles describing the wet mass retention rate during gastric digestion. (b) Diagram depicting how gastric fluid absorption influences the wet mass retention rate profiles and subsequent erosion of the food matrix during gastric digestion (Ferrua et al 2011). Reprinted with permission from *Trends in Food Science & Technology*.

While it is useful to have a simple model that can be fit to the data using regression methods, this model does not provide additional understanding of the underlying processes facilitating degradation as it is an empirical model rather than a mechanistic model. The use of the wet mass ratio may more accurately describe some of the satiation properties of a food matrix by revealing insight into how meal volume changes during the digestive process, rather than depicting the bioaccessibility of nutrients within a food matrix.

2.1.2.3. Empirical Models of Dry Solid Loss during Gastric Digestion

In order to ascertain the bioaccessibility of nutrients from a food matrix, it is important to be able to determine the dry solid loss during the digestive process. The loss of the dry solid would constitute the soluble and insoluble nutrients which have leached into the gastric medium and thus are available for absorption in the small bowel. There has been only one mathematical model in the literature to describe solid loss. Kong and Singh (2011) described soluble solid loss using an empirical model. Specifically, they used a Weibull function to describe the ratio of dry solid loss at time, *t*, hours of digestion:

$$\frac{S_0 - S(t)}{S_0} = 1 - \exp\left(-at^b\right) \qquad 2.2$$

where S_0 is the initial dry solid weight and $S(t)$ is the solid weight after *t* hours of digestion and *a* and *b* are constants fit by regression (Kong and Singh 2011). However, this description of the dry solid loss does not adequately describe the solid loss after an extended time (e.g. 36 hours). This equation assumes that complete degradation will occur at some time, which is not necessarily the case. Additionally, this equation does not provide any insight into the mechanisms responsible for the solid loss; for example the diffusion of the gastric fluid or the pH of the fluid.

In the same work, Kong and Singh (2011) used the first term of Fick's second law of diffusion for an infinite cylinder to determine the effective diffusion coefficient (EDC) of simulated gastric fluid into raw carrot at different pH values (Eq. 2.3).

$$\frac{S_0 - S(t)}{S_0} = \sum_{n=1}^{\infty} \frac{4}{\beta_n^2} \exp\left(\frac{-\beta_n^2 D_{eff} t}{R^2}\right) \qquad 2.3$$

Based on this equation, Kong and Singh (2011) determined that for pH 5.3, the EDC was constant, however at pH 3.5 and 1.8, they calculated two EDC values. They explain the two calculated values characterize two stages of diffusion without any clear explanation of the phenomena. A better explanation is that Eq. 2.3 does not adequately describe the diffusion of the simulated gastric fluid because the EDC is a function of time rather than a constant. Such an hypothesis is more consistent with other studies of porous media (Crank 1975, Davey et al 2002, Gomi et al 1996, Yamamoto 1999).

2.2. Digestion within the Small Bowel

Particulate size, macronutrients (fat, protein, starch), meal viscosity and temperature are a few of the factors which contribute to the rate of gastric emptying (Davenport 1982, Goetze et al 2007, Siegel et al 1988). Of these, particulate size is directly dependent upon the mechanical forces and chemical reactions within the stomach. Liquids tend to empty rapidly from the stomach into the duodenum, whereas solids often show a lag phase where initial, slow stomach emptying is followed by a more rapid linear phase (Siegel et al 1988). The rate of emptying is directly related to the particle size in that particles remain within the stomach until they reduce in size to less than ~2 mm (Davenport 1982, Marciani et al 2001).

Upon entering the duodenum, the chime is mixed with mucus, pancreatic enzymes and bile acids. These substances increase the pH of the chime to approximately

6, which allows enzymes such as amylase to be activated. Pancreatic enzymes are primarily responsible for proteolysis and carbohydrate catabolism whereas lipolysis is facilitated by both pancreatic lipase and bile salts. Even though the duodenum is a fraction of the length of the jejunum and ileum combined (20 cm as compared to 7-8 m), it is within the duodenum that most of the chemical processes of intestinal digestion occurs (Davenport 1982).

Nutrient absorption primarily takes place within the duodenum and jejunum, and bile salts are absorbed through diffusion in the duodenum and jejunum and through active transport in the ileum. Water, electrolytes and soluble nutrients (such as minerals and vitamins) freely diffuse through the tight junctions between the epithelial cells. The diffusion of water and electrolytes can be bi-directional depending on the osmotic and electrochemical gradient; however the permeability of the small bowel to water and electrolytes decreases linearly from the duodenum and jejunum to the ileum (Davenport 1982).

Large lipids, such as triglycerides, are broken down into monoglycerides and free fatty acids by the pancreatic lipase. The monoglycerides and free fatty acids then aggregate with bile slats forming micelles. Micelle formation provides a conduit to improve the diffusion of monoglycerides and free fatty acids into the epithelium cells (Carey et al 1983).

Protein digestion is complex and occurs in four locations: the stomach, intestinal lumen, brush border (microvilli covered surface of the epithelium) and cytoplasm of the mucosal cells (Carey et al 1983). Pepsin, an enzyme in gastric fluid, begins the digestive process of proteins and results in polypeptides of various lengths and some free amino acids which are readily absorbed in the small bowel. The polypeptides produced from pepsin proteolysis are further digested in the lumen of the small bowel by pancreatic

enzymes such as trypsin, chymotrypsin and elastase. While proteolysis in the lumen may result in some free amino acids, the aforementioned enzymes typically act on the interior peptide bonds resulting in smaller polypeptides. As these polypeptides come into contact with the brush border of the epithelium, additional enzymes (aminopeptidases and dipeptidases) release amino acids through the hydrolysis of the polypeptide at the carboxy and amino end. Unlike lipids, the resulting amino acids, dipeptides, tripeptides, and some amino acids of length four are then actively transported into the epithelium cells. Here the final step of proteolysis occurs as small peptides are broken down into amino acids by cytoplasmic peptidases (Carey et al 1983, Davenport 1982).

Carbohydrate catabolism is similar to proteolysis. Polysaccharide digestion begins in the mouth, with the secretion and mixing of saliva which contains α-amylase. Further digestion of starch by α-amylase in the stomach depends upon the mixing of the contents and the pH, as α-amylase is inactivated when the pH drops below ~3 (Bornhorst and Singh 2012). Pancreatic α-amylase further hydrolyzes polysaccharides in the intestinal lumen, resulting in oligosaccharides such as maltose, maltotriose, and branched polymers containing between 6 and 8 glucose molecules (Carey et al 1983, Davenport 1982). Like protein breakdown, the brush border contains a number of oligosaccharidases which are responsible for the further hydrolysis of oligosaccharides. While these oligosaccharidases are associated with the entire small bowel brush border, the concentration of the enzymes is greatest in the mid to distal jejunum and upper ileum (Davenport 1982). Monosaccharides released through the hydrolysis of oligosaccharides by the enzymes in the brush border are not necessarily immediately absorbed by the small bowel, but may return to the lumen. Unlike protein absorption, not all monosaccharides are actively transported into the epithelium cells. Glucose and

galactose are actively transported, whereas fructose is transported through diffusion; thus glucose absorption is approximately 3-6 times faster than fructose (Davenport 1982).

Transit of nutrients though the small bowel is governed by two types of mechanical forces: segmental and peristaltic contractions. Segmental contractions mix the chyme and the digestive juices as well as expose the chime to the intestinal barrier, increasing nutrient absorption. Two types of segmental contractions may occur: eccentric and concentric. Eccentric contractions occur in segments less than 2 cm long and have little effect on the intraluminal pressure; therefore, during such contractions the chyme is not forced out of the segment yet mixing of the chyme within the segment may occur. Concentric contractions (in segments > 2 cm) generate enough luminal pressure to completely empty the segment of chyme. Such contractions may cause simultaneous retropulsive and forward movement of the chyme; however, the increased frequency of the contractions in the duodenum and subsequent decrease in frequency throughout the jejunum and ileum ensures that on average the chyme is directed towards the colon (Davenport 1982, Toms et al 2011). Peristaltic contractions move in a progressive wave distally from the duodenum to the ileum (Koch et al 2012). These successive contractions of longitudinal and circular muscle function primarily to move the digesta (in particular dietary fiber) through the small bowel and into the large bowel to be fermented by the commensal intestinal bacteria.

2.3. Bacterial Biofilms Associated with Food Particles in the Human Large Bowel

In developed countries, some individuals are experiencing personal health deterioration due to busy and often sedentary lifestyles that include an over

consumption of energy-dense, nutritionally-poor convenience foods (Granato et al 2010). This is evident by the prevalence of obesity, cardiovascular diseases, and diabetes in developed countries (Flegal et al 2010, Ginter and Simko 2010, Panico and Mattiello 2010). The decline of health, combined with new developments in nutritional science and media attention focused upon the link between diet and health has resulted in a higher demand for foods which improve human health (Granato et al 2010).

Many functional foods target the growth of intestinal bacteria since it has become widely accepted that the maintenance of commensal bacterial populations are necessary for intestinal (and overall) health. Due to the beneficial effects of commensal bacteria, the formulation and utilization of probiotics, prebiotics and synbiotics have been at the forefront of nutritional research (Tallon 2009). Probiotics are defined as "live microbial feed supplements that beneficially affect the host by improving its intestinal microbial balance" (Saulnier et al 2009). Synbiotics are the combination of probiotic(s) and prebiotic(s), "selectively fermented ingredients that allow specific changes, both in the composition and/or activity in the gastrointestinal microbiota that confers benefits upon host well-being and health" (Saulnier et al 2009).

Bacteria within the large bowel have been found to affect host function by producing short chain fatty acids (SCFA) (Albrecht et al 1996, Macfarlane and Macfarlane 2007, Younes et al 2001), synthesizing vitamins (Albrecht et al 1996, Burgess et al 2009, Conly et al 1994, Glancey et al 2007, Madhu et al 2009), modulating the immune system (Borruel et al 2002, Furrie et al 2005, Macfarlane et al 2009, Saulnier et al 2009) and acting as inhibitors of colonization by potentially pathogenic bacteria (Coconnier et al 1993, De Ruyter et al 1996, Lievin et al 2000).

The surface area of the human bowel (400 m^2) combined with an ideal temperature and an abundance of nutrients provides an environment in which anaerobic

and facultative anaerobic bacteria thrive (MacDonald and Monteleone 2005). It is estimated that there are 10^{14} bacteria cells within the digestive tract, which is 10 times the number of cells that constitute the human anatomy (Luckey 1972). The short transit time (2-4 hours) causes a rapid flow of material through the small bowel, inhibiting bacterial colonization (Macfarlane and Dillon 2007), whereas the transit time within the large bowel, 1-3 days, provides an ideal environment for bacterial growth and fermentation [Figure 2.4]. There are over 1000 distinct bacterial species (Hooper and MacPherson 2010) with 30–40 species comprising up to 99% of the total population (Hooper et al 2002). This may be an underestimate since only 10-50% of the bacteria are cultivable (Kurokawa et al 2007, O'Toole and Claesson 2010, Suau et al 1999). While the bacterial population of the adult human intestinal tract is heterogeneous and

\

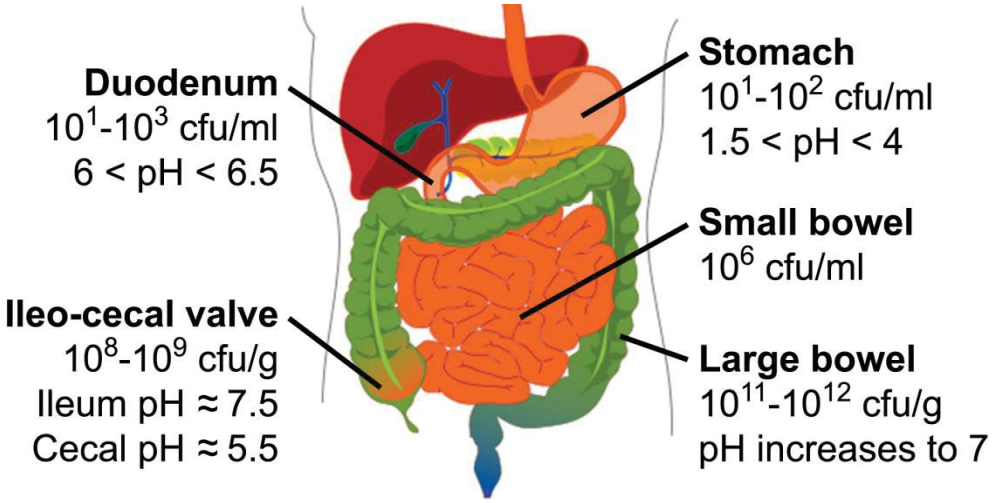

Figure 2.4 Bacterial counts in the gastrointestinal tract, including the stomach (Macfarlane and Dillon 2007), duodenum (O'May et al 2005) and small bowel (Saulnier et al 2009) (colony forming units/ml luminal contents) and at the ileo-cecal valve (Macfarlane and Dillon 2007) and within the large bowel (colony forming units/g luminal contents) (Guarner and Malagelada 2003). Reprinted with permission from *Molecular Nutrition and Food Research*.

individual specific (due to health, diet, age, and environment), their metabolism and overall function are similar (Kurokawa et al 2007) and are unique to the intestinal environment.

Given the prevalence of bacterial biofilms associated with food particles in ruminants, it was assumed that bacteria formed biofilms on digesta within the human intestinal tract, and in particular within the colon (Costerton et al 1983). However, the first reports of bacterial biofilms associated with food particles in human fecal matter were by Macfarlane and colleagues (Macfarlane et al 1997, Macfarlane and Macfarlane 2006, Probert and Gibson 2002). Due to the difficulty of studying digesta within the human large bowel, little is known about the mechanisms used for bacterial attachment or growth on food particles *in vivo*. The majority of our knowledge has been gained from *in vitro* experimentation utilizing fecal inocula or single bacterial species. However, studies of the large intestinal contents of sudden death victims have shown higher levels of SCFA in the proximal colon (cecum and ascending colon) indicating carbohydrate fermentation (Cummings et al 1987, Macfarlane et al 1992). Although biofilms constitute only 5% of the bacterial population in human fecal samples (Macfarlane and Macfarlane 2006), high levels of acetate within the proximal colon, which is readily produced by heterogeneous bacterial biofilms (Leitch et al 2007, Macfarlane and Macfarlane 2006, Macfarlane and Dillon 2007), implies that either bacterial biofilms are prolific in this site or that the formation of a biofilm leads to increased production of acetate.

With the possibility of biofilms being prevalent in the large bowel, extensive research into the effects and functionality of digesta-associated biofilms is necessary. To assist in this endeavor, the following sections will cover current knowledge of bacterial biofilms associated with food particles in the human large bowel, examine the

established mathematical models depicting bacterial attachment, nutrient transport and microbial cross-feeding/competition for nutrients and to elucidate key areas for further research.

2.3.1. Health Benefits Associated with the Commensal Intestinal Bacteria

The commensal intestinal bacteria have been found to have a substantial impact on not only intestinal health, but the overall health of the host. The primary SCFA produced by the commensal bacteria are butyrate, acetate and propionate. Butyrate provides an energy source for the intestinal epithelial cells, improves the mucosal integrity of the intestinal wall, and regulates gene expression and cell growth (Macfarlane and Cummings 1991, Nepelska et al 2012). The role of SCFA in human health is not restricted to the intestinal tract. Acetate is utilized as an energy source by the heart, brain and skeletal muscles (Macfarlane and Cummings 1991). Propionate enhances satiety by regulating hormones responsible for stomach emptying and appetite and is associated with the inhibition of cholesterol, triglyceride and fatty acid synthesis in the liver (Hosseini et al 2011); the effects suggest that propionate may play a role in obesity in humans.

In addition to SCFA production, commensal bacteria have been associated with the maturation and modulation of the human immune system. In particular, certain lactobacilli and bifidobacterial strains have been shown to decrease symptoms associated with immunoglobulin E (IgE)-associated allergies, such as allergic rhinitis, asthma, and atopic dermatitis (Özdemir 2010). Additionally, recent studies have linked intestinal inflammation and commensal bacteria population imbalances (reduced bifidobacteria and/or lactobacilli) to inflammatory bowel disease (IBD) (Macfarlane et al 2009) and chronic fatigue syndrome (CFS) (Lakhan and Kirchgessner 2010).

Furthermore, the use of prebiotics, probiotics or synbiotics have been shown to reduce the levels of inflammatory cytokines in patients with IBD (Furrie et al 2005) and reduce anxiety symptoms in CFS patients (Rao et al 2009). The awareness of the potential benefits of the commensal bacteria and their metabolites has led to the development of probiotics, prebiotic and functional foods that not only address digestive, but overall human health.

2.3.2. Effects of Diet on the Microbial Composition

Until recently, human newborn intestinal tracts were believed to be sterile at birth and bacterial colonization was influenced by the mode of delivery (cesarean versus vaginal delivery), premature delivery and exposure to intensive care units, feeding (breast fed versus formula fed), and sanitation (Jiménez et al 2008a, O'Toole and Claesson 2010, Penders et al 2006, Perez et al 2007). While these factors influence the bacterial population in neonates, recent research suggests that bacteria inhabit the fetal intestinal tract *in utero* (Jiménez et al 2005, Jiménez et al 2008b, Satokari et al 2009) and that breast milk supplies both oligosaccharides and commensal bacteria that have prebiotic and probiotic effects, respectively, in the infant (Jiménez et al 2008a, Perez et al 2007).

While the metabolic requirements for most of the enteric bacteria and the metabolites produced by these bacteria are unknown (Jacobs et al 2009), current metagenomic studies of bacteria from fecal samples have shown that the intestinal bacteria of adult, weaned and unweaned children primarily function as carbohydrate transporters and metabolizers (Kurokawa et al 2007). There was a notable difference between the collective genomes of the microbiota (microbiome) of weaned children or adults as compared to the microbiome of unweaned infants, which may be attributed to the role played by bacteria in transport and uptake of simple sugars from breast milk.

A recent study comparing the fecal bacteria of European children, fed a Westernized diet high in sugar, animal fat and energy dense foods, and the fecal bacteria of rural African children, fed a diet high in plant polysaccharides, demonstrated differences in the bacterial population once breastfeeding was replaced by solid foods (De Filippo et al 2010). The ratio of *Firmicutes* to *Bacteroidetes* were particularly different; *Bacteroidetes* such as *Prevotella* and *Xylanibacter* with cellulolytic and xylanolytic plant polysaccharide degradation genes were most prevalent in the rural African children. Similar disparities in the ratio of *Firmicutes* to *Bacteroidetes* have been recorded in obese versus lean individuals (Ley et al 2006). De Filippo et al (2010) propose that the ratio of *Firmicutes* to *Bacteroidetes* may be used as an indicator for future obesity risk and that this disparity may result from diets rich in fat, animal protein and sugar rather than diets high in plant carbohydrates and resistant starch (De Filippo et al 2010).

The dominant phyla in fecal samples are *Firmicutes* and *Bacteroidetes* (Kurokawa et al 2007). *Firmicutes*, in particular *Ruminococcus* species from *Clostridium* cluster IV, have been found to adhere to and form biofilms on particulates such as plant polysaccharides, resistant starch and mucin (Leitch et al 2007, Walker et al 2008). This difference in substrate association and utilization by *Firmicutes* and *Bacteroidetes* was also reported by Mirande et al (2010) who compared dietary fiber degradation by *Bacteroides xylanisolvens* SB1A and *Roseburia intestinalis* XB6B4 (Mirande et al 2010). It is surmised that *Firmicutes* are more efficient at fermenting insoluble carbohydrates (Ley et al 2006), whereas many *Bacteroides* species, which demonstrate substrate versatility (Hooper et al 2002, Leitch et al 2007), may rely on soluble oligosaccharides and polysaccharides released by the breakdown of insoluble polysaccharides (Walker et al 2008) when in a competitive environment. The ability of

some bacterial species to ferment metabolites produced by or released by another species is called microbial cross-feeding, which is a defining factor in the heterogeneity of bacterial biofilms.

Currently, most studies investigating the influence of diet on the commensal enteric bacteria have primarily investigated the effects of prebiotics or synbiotics (Macfarlane et al 2008). Additionally, these studies focus on how particular food components affect specific bacterial species rather than changes in phylum distribution. It is important to note that fecal samples are often used to enumerate and distinguish bacterial species in human studies. This however may not be an accurate representation of the bacterial population in specific areas of the bowel.

The information obtained from sudden death victims has been helpful in confirming the degradation of indigestible carbohydrates within the colon, as well as in determining the metabolites produced by the commensal bacteria (Cummings et al 1987, Macfarlane et al 1992). Additionally, the microbiota is capable of proteolysis, which is evidenced by the occurrence of branch chained fatty acids in the human distal colon (Cummings and MacFarlane 1997). Therefore it is reasonable to expect that the bacterial populations associated with the digesta will change over time and may be determined by the substrates available within the digesta. The bacterial population in fecal samples may reflect the bacterial population within the transverse and descending colon rather than the cecum and ascending colon, where carbohydrate fermentation primarily takes place. This has been substantiated by a study comparing the cecal and fecal bacteria of healthy humans. Marteau et al (2001), using 16 rRNA probes which target *Bacteroides* and *Clostridium* groups found that strict anaerobic bacteria represented 44% of the fecal bacterial rRNA and only 13% of the cecal bacterial rRNA. Similarly, Marteau et al (2001) found that the facultative anaerobes *Escherichia coli* and

the *Lactobacillus-Enterococcus* group represented 50% of the cecal and 7% of the fecal bacteria rRNA (Marteau et al 2001). Thus, when gaging the impact of a dietary supplement or functional food on the commensal intestinal bacteria, the use of bacterial counts from fecal samples may not provide an accurate representation of the microbial population composition in the ascending or transverse colon.

2.3.2.1. Polysaccharides with Prebiotic Effects

Given that the commensal bacteria more readily metabolize resistant starch and non-starch polysaccharides, products such as inulin and oligofructose are commonly used food ingredients in functional foods. Neither inulin nor oligofructose are hydrolyzed in the stomach or absorbed in the small bowel, yet they are completely fermented by the commensal bacteria in the large bowel (Cherbut 2002, Ramnani et al 2010). *In vivo* studies have shown that inulin and oligofructose have a bifidogenic effect, or increase the number of certain *Bifidobacterium* species, and in many cases there is also an increase of *Lactobacillus* (Bouhnik et al 1999, Costabile et al 2010, Gibson et al 1995, Meyer and Stasse-wolthuis 2009, Ramnani et al 2010). In addition to the prebiotic effect, these ingredients add to the functionality of some foods, such as dairy products, frozen desserts, table spreads, baked goods, breakfast cereals and salad-dressings, as fat and sugar replacers (Brownawell et al 2012, Franck 2002). When inulin is thoroughly hydrated it forms a gel with a spreadable texture and can act as a stabilizer for foams and emulsions in ice creams, table spreads and sauces (Franck 2002). Although oligofructose has one third the sweetness of sucrose, oligofructose can enhance fruit flavors when used in combination with other alternative sweeteners, such as aspartame and acesulfame K (Franck 2002). The addition of oligofructose decreases the aftertaste of the alternative sweetener and provides an improved mouth feel (Franck 2002).

Given the bifidogenic effect of fructans, *Bifidobacteria* are often combined with fructans as a synbiotic because of their beneficial effects to the host; however, *in vitro* studies have shown that many *Bifidobacteria* are unable to break down and metabolize sugars with a degree of polymerization greater than 8 (Falony et al 2009b, Rossi et al 2005). Given that bacteria do not live in isolation, but are often found as mixed species biofilms (Macfarlane and Macfarlane 2006), the bifidogenic effect of fructan prebiotics may be a result of microbial cross-feeding (Falony et al 2009a).

2.3.2.2. Mathematical Models Predicting Coculture Dynamics and Microbial Cross-Feeding

Only a few coculture experiments that specifically characterized bacterial cross-feeding and nutrient competition have been reported (Falony et al 2006, Falony et al 2009a) and often do not report the bacterial growth, metabolites and substrate degradation associated with each strain during coculture (Belenguer et al 2006, Chassard and Bernalier-Donadille 2006, Degnan and Macfarlane 1995, Duncan et al 2004). These data are essential to determine bacterial interactions and the parameter values for macroscopic mathematical models of interacting microbial populations. Additionally, there are currently few mathematical models that describe either bacterial cross-feeding or nutrient competition, most of which are empirical rather than mechanistic models.

The Lotka-Voterra model (or variations thereof), which describes species competition, has been applied to describe mixed microbial populations (Eqs 2.4a,b) (Cornu et al 2011, Mounier et al 2008). Here, r_i represents the growth rate of the i^{th} bacterial strain, x_i, α_{12} is the effect species 2 has on species 1, similarly, α_{21} is the effect that species 1 has on species 2, and K_i represents the carrying capacity for the i^{th} bacterial strain.

$$\frac{dx_1}{dt} = r_1 x_1 \left(1 - \frac{x_1 + \alpha_{12} x_2}{K_1}\right) \quad 2.4a$$

$$\frac{dx_2}{dt} = r_2 x_2 \left(1 - \frac{x_2 + \alpha_{21} x_1}{K_2}\right) \quad 2.4b$$

Cornu et al (2011) found that the Lotka-Voterra model (Eqs. 2.4a,b) was unable to predict the mixed microbial populations (*Listeria monocytogenes* verses other microflora) in salted diced bacon using parameters based on pure culture experiments. While Mounier et al (2008) found that the Lotka-Voterra model provided insight into the interactions between various yeast and bacteria during cheese making, the model depicted interactions between specific bacteria and yeast that could not be explained by the experimental results.

Wintermute and Silver (2010) proposed a simple dynamic, empirical model to describe the level of cooperation between two auxotrophic *Escherichia coli* mutants (Eqs. 2.5a,b). Each mutant was unable to synthesize an essential metabolite (amino acids, nucleotides or cofactors) or components of the glycolysis and respiration pathways necessary for the growth of the bacterium.

$$\frac{dA}{dt} = C_B \left(\frac{B}{A+B}\right)\left(1 - \frac{A+B}{K}\right) \quad 2.5a$$

$$\frac{dB}{dt} = C_A \left(\frac{A}{A+B}\right)\left(1 - \frac{A+B}{K}\right) \quad 2.5b$$

In the Eqs. 2.5a,b, the variables *A* and *B* represent the concentration of the two different bacterial strains, C_A and C_B represent the level of cooperation on the part of strain *B* and *A*, respectively, (i.e. C_B is a numerical measure for the amount of benefit strain *A* receives per bacterium *B*) and *K* represents the logistic carrying capacity of the batch culture. In this model *A* and *B* are measured in terms of optical density. The first factor in Eq. 2.5a demonstrates that there is an increased growth in strain *A* when strain

B increases; however, in this model the benefits from strain *B* must be divided amongst all bacteria. Here cooperation implies that the paired strain provides a metabolite which is necessary for the other strain to grow (i.e. provides a metabolite that the bacterium cannot synthesize).

This model predicts that the growth of strain *A* will increase when partnered with a cooperative strain (i.e. dA/dt increases as C_B increases). Additionally, the growth of strain *A* will increase when *A* provides a low level of cooperation with strain *B* as a result of decreased numbers of strain *B* and hence more metabolite available for *A* to utilize; however, if the cooperation of strain *A*, C_A, is high, then strain *B* dominates the batch culture, reducing the growth rate of strain *A*. One drawback of this model is that it assumes that both bacteria must contribute to the fitness of the other. If either C_A or C_B are equal to zero then there is no growth of bacterial strain *B* or *A*, respectively.

Equations 2.5a,b are related to the model described by Bull and Harcombe (2009) (Eq. 2.6a,b). The model proposed by Bull and Harcombe (2009) allows for the growth of the individual species independent of any cooperation or cross-feeding between the two species. This is accomplished by the inclusion of growth constant terms, r_A and r_B, that do not rely on the population of the other species. This inclusion also allows for the possibility of one bacterial species benefiting from the other without any reciprocal cross-feeding. To guarantee that the benefit from cross-feeding does not approach infinity for small values of *A* (both strains are in terms of density), the addition of k_A provides a dampening effect that makes the cross-feeding resource proportional to *B* for vanishing values of *A*. This similarly applies to *B*.

$$\frac{dA}{dt} = A\left(r_A + C_B \frac{B}{A + k_A}\right)\left(1 - \frac{A+B}{K}\right) \qquad 2.6a$$

$$\frac{dB}{dt} = B\left(r_B + C_A \frac{A}{B + k_B} \right)\left(1 - \frac{A+B}{K} \right) \qquad 2.6b$$

Neither model (Eqs. 2.5 or 2.6) is suitable for explicitly describing and understanding the nature of the interactions between microbial populations because they do not incorporate the mechanisms that influence those interactions. For instance, there is no explicit reference to the metabolites which are responsible for the benefits, nor the substrate required for bacterial growth by either one or the other bacterium which facilitates the production of the nebulous metabolite.

At present there are a few published models that have extended/modified the microbial population model of Baranyi and Roberts (1994). The model proposed by Baranyi and Roberts (1994) is used to describe the observed lag, exponential and stationary phase of a single bacterium (Eqs. 2.7a-c). In Eqs. 2.7a-c, N represents the concentration of the bacterial population at time t, $\mu_{\max}$ is the maximum specific growth rate, $N_{\max}$ represents the maximum population of the bacteria, and Q represents the physiological state of the cells at any given time, which accounts for the lag phase.

$$\frac{dN}{dt} = \mu_{\max} N\left(\frac{Q}{1+Q} \right)\left(1 - \frac{N}{N_{\max}} \right) \qquad 2.7a$$

$$\frac{dQ}{dt} = \mu_{\max} Q \qquad 2.7b$$

$$N(t=0) = N_0, Q(t=0) = Q_0 \qquad 2.7c$$

A number of models have modified or extended Eqs. 2.7a-c to include the effects of mechanistic processes, such as metabolite production, substrate depletion and changes in pH that may limit microbial growth (Janssen et al 2006, Poschet et al 2005, Van Impe et al 2005). These models extend the Baranyi and Roberts (1994) model by modifying the last factor in Eq. 2.7a, since a fixed value for the maximum concentration

of bacteria, N_{max}, cannot describe growth inhibition due to substrate limitations (i.e., different substrate concentrations will result in a different N_{max}) nor toxic products produced by a competitive bacterium (Van Impe et al 2005). These models also included an additional differential equation to describe either the production of a metabolite, substrate depletion or changes in pH, as a function of the bacterial population. Only one of the models incorporated substrate limitations (Van Impe et al 2005), which is a key factor in mono- and coculture microbial growth.

A dynamic, mechanistic model has been proposed to demonstrate bacterial growth (determined by optical density) and the subsequent butyrate production as a result of lactate utilization (Muñoz-Tamayo et al 2011):

$$\frac{dx_{la}}{dt} = Y\rho_{la} \qquad 2.8a$$

$$\frac{ds_{la}}{dt} = -\rho_{la} \qquad 2.8b$$

$$\frac{ds_{ac}}{dt} = Y_{ac}\rho_{la} \qquad 2.8c$$

$$\frac{ds_{bu}}{dt} = Y_{bu}\rho_{la} \qquad 2.8d$$

where

$$\rho_{la} = k_m \frac{s_{la}x_{la}}{K + s_{la}}. \qquad 2.8e$$

The model variables are optical density of bacteria, x_{la}, (which is assumed to be proportional to the bacterial concentration) and concentration of metabolites, *s*, (lactate (la), acetate (ac) and butyrate (bu)). The parameters are the rate of consumption of lactate, k_m, the Monod constant, *K*, the yield of biomass from lactate consumption, *Y*, and the yield, Y_i, of metabolites from lactate consumption (acetate $i = ac$ or butyrate $i = bu$). A drawback to this model is it does not incorporate either the bacterium that

produced the lactate or the substrate hydrolyzed by the lactate-producing bacterium. Thus the model does not provide a comprehensive description of coculture growth kinetics.

2.3.3. Bacterial Biofilm Formation

Bacterial biofilms are a conglomeration of bacteria adhered to either a biotic or abiotic surface and are distinguished from adherent microcolonies by the evidence of a slime coating the bacterial consortia. This slime or extracellular polymeric substances (EPS) can be comprised of polysaccharides, proteins, DNA and lipids that are associated primarily through ionic interactions (Gristina 2004). Additionally, 90-99% of the biofilm water content lies within the EPS (Flemming et al 2005). The water within the biofilm is not uniformly distributed due to the spatial distribution of bacteria and the overall structure of the biofilm.

Biofilms are ubiquitous in nature. Biofilms may be found not only in the human intestinal tract, but in the gastrointestinal (GI) tract of all animals, associated with heart valves and catheters, within river beds and streams, drinking water pipes, in foods and food processing plants, and in waste water systems. Biofilms can be homogeneous, consisting of only one bacterial or microbial species, or heterogeneous, consisting of multiple bacteria or microbial species. In some instances bacterial biofilms are beneficial, as in the commensal intestinal bacteria and biofilms in waste water treatment systems (Dereli et al 2012); however, bacterial biofilms may be pathogenic and result in complicated infections, as in the case of biofilm growth in the lungs of cystic fibrosis patients and biofilm growth on biomedical implants within humans, or biofilms may cause spoilage in the case of biofilms associated with food or food processing equipment. Biofilms are so prolific that it is now believed that biofilm formation is the preferred means of survival and maintenance for bacteria in dynamic systems.

In any environment, biofilm formation follows a five step process: (1) surface conditioning, (2) initial, reversible attachment to the conditioning film, (3) irreversible attachment, (4) accumulation or growth and (5) detachment (Boland et al 2000) [Figure 2.5].

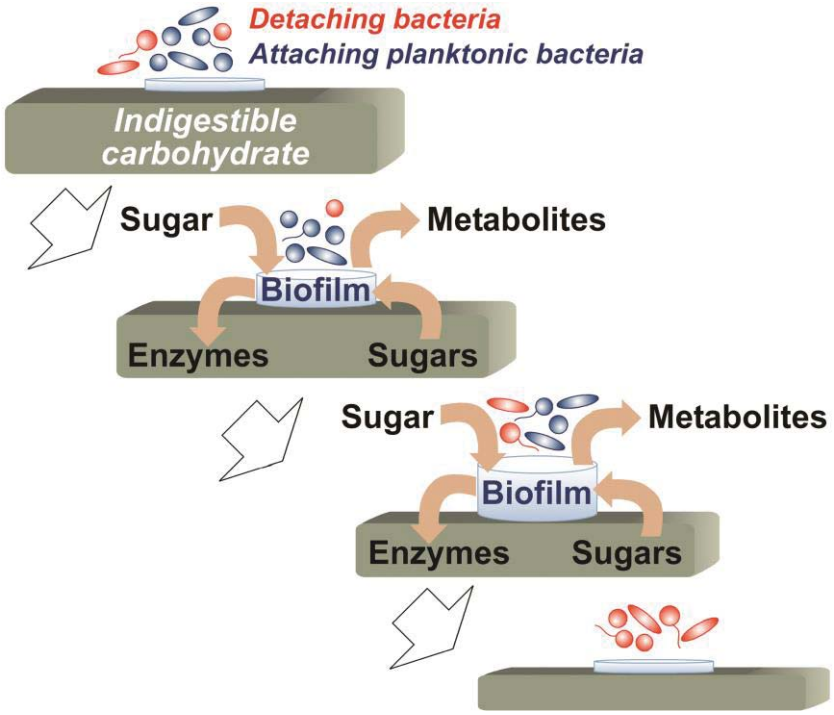

Figure 2.5 A conceptual schema of food degradation in relation to biofilm biomass accumulation. Initial attachment of bacteria to a food particle, biofilm growth via cell division and recruitment of planktonic bacteria, biofilm maturation as food particle nutrients are degraded and the dispersal of bacterial from the nutrient depleted particle.

2.3.3.1. Surface Conditioning

Regardless of the environment, surface conditioning is the precursor to biofilm formation. Surface conditioning is the adsorption and accumulation of small molecules to a surface. Surface conditioning has been observed primarily in studies of bacteria in marine environments, bacteria associated with biomaterials, and dental caries. Prior to

bacterial attachment, water, ions, proteins, lipids, glycoproteins and polysaccharides become attached to and accumulate on biomaterials and tissues within humans (Chamberlain 1992, Gristina 2004). Conditioning alters the surface and impacts the affinity of bacteria to the surface (Dunne 2002, Neu 1996). Currently, information pertaining to specific diets and their influence on surface conditioning is lacking in the literature; however, it is probable that surface conditioning occurs on food particles within the GI tract due to the complexity of the digesta, which includes partially degraded or indigestible food particles, digestive enzymes, epithelial cells, mucus, and microbial metabolites. *In vitro* studies have provided evidence that many human extracellular components are targeted by bacteria for adhesion (Dunne 2002). Ions, such as calcium and magnesium (De Kerchove and Elimelech 2008), and glycoproteins, such as fibronectin (Liu et al 2007b), may improve bacterial attachment. In the case of oral biofilms, the coverage of the tooth by glycoproteins (pellicle formation) is required for the attachment of bacteria (Rüdiger et al 2002).

2.3.3.2. Initial and Irreversible Attachment

Initial and irreversible attachments are not necessarily distinguishable phases in biofilm development. Initial attachment is thought to be affected by the hydrophobicity, cell size, and the electric charge of both the bacterial cell and conditioned surface (Jass et al 1997) as well as environmental factors such as receptor sites (such as glycoproteins) (Gristina 2004), nutrient availability, fluid dynamics and competing bacteria. These mechanisms may be relatively weak and detachment may occur. Thus, the subsequent or simultaneous adherence of proteins found on cellular membranes and ends of filamentous cell appendages, such as fimbriae or pili, as well as the secretion of EPS, binds the bacteria irreversibly to the substratum (Gristina 2004).

Given the difficulty of human studies of GI digesta movement, insights have been gained from animal experiments. Lentle and Janssen (2008) suggested that laminar mixing (in the small bowel) may result from simultaneous circular and longitudinal contractions (Lentle and Janssen 2008). These contractions may be able to generate radial mixing with the flow dependent upon the viscosity of the digesta, in that increased amounts of indigestible carbohydrate reduces radial mixing. Little is known about the mixing of contents within the human cecum, though it is reasonable to assume that the mixing of the digesta is minimal given that indigestible carbohydrates make up the majority of the digestive material. Moreover, as the digesta progresses through the digestive tract it changes from a pseudoplastic fluid (in the small bowel) to a solid (in the transverse colon) due to absorption of water (Lentle and Janssen 2010). Dehydration of the digesta and reduced frequency of radial constriction and peristalsis result in little to no churning of the digesta in the transverse and distal colon (Lentle et al 2005). This implies that the motility of non-flagellated/nonpilated bacteria in the large bowel is largely due to diffusion rather than fluid transport.

Generally, both the bacteria and the conditioned substratum are negatively charged (Gristina 2004), although surface conditioning by ions may create a neutrally charged substratum (De Kerchove and Elimelech 2008). A combination of van der Waal and hydrophobic forces, and possibly chemical interactions with closely associated cells (electrostatic, hydrogen and covalent bonding) may allow the bacterial cells to overcome repulsive force from surfaces (Goller and Romeo 2008, Jass et al 1997, Jenkinson et al 2003). In addition to environmental factors and molecular mechanisms, flagella enable bacteria to overcome repulsion, although continued motility after attachment can hinder biofilm formation (Goller and Romeo 2008, Jenkinson et al 2003).

Given the diversity of environmental factors, many bacteria have the ability to express different adhesins. Biofilm formation by Gram-negative bacteria such as *Enterobacteriaceae* is facilitated by proteins on either curli fimbriae or Type 1 fimbriae, depending on environmental factors (Cookson and Woodward 1999, Cookson et al 2002, Goller and Romeo 2008). In experiments using intestinal tissue obtained from either the distal duodenum or duodenum-jejunal junction in children, the adherence of enteropathogenic *E. coli* required the direct contact of an outer surface protein, intimin, with the mucosa (Hicks et al 1998). Enteropathogenic *E. coli* secretes several effector proteins into the host cell and embeds a secreted protein, translocated intimin receptor (Tir), into the host cell membrane, generating a receptor for intimin (Hicks et al 1998).

While the use of flagellum and pili may be essential for attachment of bacteria to human tissue, Kurokawa et al (2007) reported that motility is not required for commensal enteric bacteria to persist within the lumen of the colon (Kurokawa et al 2007). They suggested that flagellated bacteria, which are immunogenic, may be easily targeted and eliminated by the immune system.

2.3.3.3. Bacterial Attachment to Food Particles

The attachment mechanisms used by pathogenic bacteria have been studied extensively and there are numerous studies focusing on colonization inhibition via surface conditioning of biomedical devices. However, very little is known about the mechanisms used by commensal bacteria to attach to resistant starch, indigestible non-starch polysaccharides, oligosaccharides, proteins and lipids within the intestinal lumen or how surface conditioning effects attachment. The particular mechanism required for attachment to resistant starch has been elucidated for only a few strains of enteric bacteria. Surface cellular proteins appear to facilitate attachment to particular substrates, resistant starch, which has been substantiated by studies involving *Bacteroides*

thetaiotaomicron (Shipman et al 1999, Shipman et al 2000), four additional intestinal *Bacteroidetes* (Xu et al 2007), *Bifidobacterium adolescentis* and *Bifidobacterium pseudolongum* (Crittenden et al 2001).

The mechanisms used to bind the enteric microbiota to either milk oligosaccharides, lipids or proteins are not well understood. Given the high proportion of carbohydrates in the digesta (Macfarlane and Cummings 1991) and the emphasis on carbohydrate metabolism by the enteric bacteria (Kurokawa et al 2007), it is not surprising that studies have focused on the utilization of resistant starch and dietary fiber by the intestinal microbiota. However, oligosaccharides, present at 10-20 grams/liter in human milk, are a primary substrate for *Bifidobacterium* within the infant intestinal tract (Wada et al 2008). In the infant large bowel, bacteria may attach to and metabolize available milk oligosaccharides. Therefore, the inclusion of milk oligosaccharides in further studies investigating the attachment mechanisms of enteric bacteria to carbohydrates would be invaluable and may provide additional insights into the formation of bacterial biofilms in the lumen of the infant GI tract.

Although the availability of protein in the large bowel is approximately one fifth that of carbohydrates (Macfarlane and Cummings 1991), enteric bacteria metabolize protein within the distal region of the large bowel. Additionally, it has been hypothesized that the metabolites from proteolytic fermentation may increase the risks of colon cancer and IBD (Jacobs et al 2009, O'Keefe 2008). Thus there is a need to both ascertain which species metabolize protein and determine the binding mechanisms used by the enteric bacteria.

Lipid metabolism primarily takes place in the small bowel, however approximately 5-10% (0.3-0.6 grams/day) of bile acid escapes reabsorption in the distal ileum (Begley et al 2006, Jones et al 2004). There is evidence to support that, in

humans, deconjugation of bile acids begins in the small bowel (Go et al 1988) and continues in the cecum and colon (Eyssen 1973, Hamilton et al 2007, Ridlon et al 2006, Thomas et al 2001). Studies detected bile salt hydrolase activity, the ability to deconjugate bile salts, in *Bifidobacterium*, *Lactobacillus*, *Enterococcus*, *Clostridium* and *Bacteroides* spp. (Begley et al 2006). The function of bile salt hydrolase activity is still unknown, but it has been suggested that the bacteria incorporate cholesterol and/or bile into the bacterial cell membrane which could strengthen the membrane and alter the charge of the bacterium. Such modifications of the bacterial cell membrane may increase their ability to survive areas of the GI tract that have a low pH. Although the fecal bacteria have the ability to hydrolyze bile salts, our current understanding of the human large bowel microbiome shows that the genes required for lipid transport and metabolism are under-represented (Kurokawa et al 2007); however, this is likely due to the relatively low levels of bile acids that enter the colon and that only ~0.0001% of the total colonic microbiota are estimated to be capable of converting primary bile acids to secondary bile acids (Ridlon et al 2006). Regardless, if indeed bile salt hydrolase activity results in a change of the net charge of the bacterial cell membrane, this may have an impact on the attachment process of these bacteria to food particles within the large bowel. Further studies are needed.

2.3.3.4. Theoretical Models for Bacterial Attachment

In vitro and *in vivo* experimentation is complemented by mathematical modeling. There are three accepted theories that describe attachment of charged molecules or cells to a substratum in a liquid environment: Derjaguin-Landau-Verwey-Overbeek (DLVO), Lifshitz-van der Waals (LW) Acid-Base (AB) approach to thermodynamic theory and extended DLVO (XDLVO) theory (Missirlis and Katsikogianni 2007).

DLVO theory was originally developed to describe the behavior of colloidal particles with a surface in a liquid environment. DLVO theory assumes that the total interaction energy, or energy of adhesion, is dependent upon the separation distance between the surface and particle and is described as the sum of energies from LW interactions and electrostatic repulsion (Hermansson 1999). DLVO theory was adopted to explain the attachment of bacteria, which are similar in size to colloids, to a surface as this process can follow two steps: reversible and irreversible attachment (Hermansson 1999, Hori and Matsumoto 2010) [Figure 2.6]. However, not all bacteria appear to follow this two-step process. The production of EPS and flagellum may also influence bacterial attachment at relatively long ranges (100 nm) (Boks et al 2008, De Kerchove and Elimelech 2008, Fletcher 1988, Goulter et al 2009, Long et al 2009),

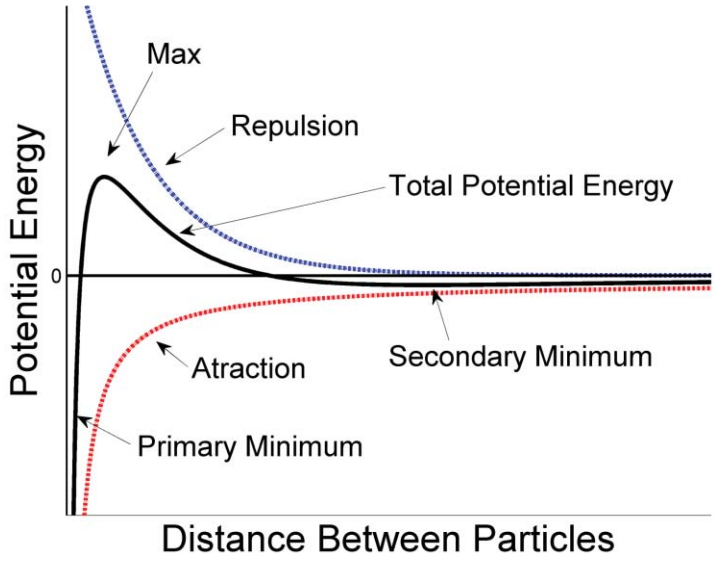

Figure 2.6 Schematic drawing of DLVO theory. Repulsion (blue dotted curve) occurs from the overlap of electric double layers of both the substratum and bacteria, whereas permanent or induced dipoles attract (red dotted line) the bacteria to the substratum. When the total potential energy (black line) is at the secondary minimum reversible attachment occurs, whereas irreversible attachment happens at the primary minimum.

which is not accounted for in the DLVO theory. According to DLVO theory, bacterial attachment should not occur at such distances but bacteria with EPS and/or flagellum are readily able to attach at distances up to 100 nm (Boks et al 2008, De Kerchove and Elimelech 2008, Fletcher 1988, Goulter et al 2009, Long et al 2009). Furthermore, DLVO does not account for attraction due to hydrophobic interactions, which can be 10-100 times stronger than those from LW (Katsikogianni and Missirlis 2004, Pashley et al 1985). The LW-AB thermodynamic theory for bacterial attachment was developed to overcome these shortcomings.

Van Oss et al (1986) proposed the LW-AB thermodynamic theory in which the AB component accounted for the observation that hydrophobic bacterial cells readily attach to a hydrophobic substratum and that hydrophilic bacterial cells prefer a hydrophilic substratum. The thermodynamic LW-AB approach considers that the total free energy of adhesion is the sum of LW (apolar) interactions and AB (polar) interactions (i.e. all possible electron-donor/electron-acceptor interactions) (Van Oss et al 1988) at the substratum-liquid interface, substratum-bacterial interface and the bacterial-liquid interface (Missirlis and Katsikogianni 2007). The AB interactions are often referred to as hydrophobic/hydrophilic interactions due to potential hydrogen bonding. The LW-AB theory does not consider the distance dependence of the LW or AB interactions nor does it account for reversible attachment, as the model requires a cell-substratum interface.

Given the respective merits of DLVO and LW-AB theory, Van Oss extended the DLVO theory by incorporating AB interactions in the total energy of bacterial-substratum interactions (Van Oss 1989). Therefore, XDLVO theory can be considered a combination of DLVO and LW-AB theories (Missirlis and Katsikogianni 2007).

There is increasing evidence to suggest that all three theories do not adequately describe bacterial attachment within the context of the human GI tract (Bayoudh et al 2009, De Kerchove and Elimelech 2008, Hori and Matsumoto 2010, Liu et al 2007b, Missirlis and Katsikogianni 2007, Pashley et al 1985, Schneider 1996). Studies have shown that LW-AB and XDLVO theories are more accurate than DLVO, which may be due to the incorporation of AB interactions in both the XDLVO and LW-AB models. As mentioned earlier, hydrophobic interactions can be 10-100 times stronger than those of LW interactions when the cell-substratum distance is within 5 nm (Katsikogianni and Missirlis 2004, Pashley et al 1985). Additionally, experiments studying bacterial attachment found that surface conditioning by particular ions, such as magnesium and calcium, can alter the charge of the substratum so that electrostatic and LW interactions have an insignificant influence on bacterial attachment (Bayoudh et al 2009, De Kerchove and Elimelech 2008, Hori and Matsumoto 2010, Pashley et al 1985). Thus, the incorporation of AB interactions in the theoretical models of bacterial attachment appears to be necessary (Liu et al 2007a).

Bacterial attachment is a very complex process. While these models describe aspects of the physicochemical properties of bacterial attachment, they do not, however, incorporate biological factors. The lack of inclusion of biological factors in the above models may contribute to the discrepancy between model predictions and experimental observations. Currently, these models are used to describe the attachment of bacteria to surfaces in a variety of environments. A critical analysis of the agreement of XDLVO and LW-AB theories with experiments may provide valuable insights. Given the complexity of the various environments in which bacteria grow and the environmental specific attachment methods employed by bacteria, a universal model may not be feasible or appropriate.

2.3.4. Biofilm Growth and Detachment

Once irreversible attachment to a substratum has been established, biofilm maturity is facilitated by the generation of daughter cells (Costerton et al 1987) and the recruitment of bacteria from the surrounding medium. Both cellular proteins and the production of EPS appear to help bind the bacteria to the substratum and aid in cell-to-cell adherence (Bayston 1999, Costerton et al 1987). Biofilm associated protein homolog, Bap, and accumulation associated protein, Aap, are surface proteins that are thought to mediate biofilm formation via cell-to-cell contact with some *Staphylococcus* strains (Sandiford et al 2007). In oral *Streptococcus*, bacterial cell-cell aggregation or coaggregation is thought to be attributed to either lectin-saccharide or protein-protein interactions (Hasty et al 1992).

Presently the role of the EPS remains equivocal. For example, components of the EPS can aid binding of bacteria to conditioned surfaces (Koo et al 2010, Sutherland 2001b, Vu et al 2009), may be necessary for biofilm formation by providing structural stability and protection from shear forces in hydrodynamic environments (Koo et al 2010, Marvasi et al 2010, Sutherland 2001b) and may promote both aggregation and co-aggregation by providing receptor sites to which bacteria can bind (Donlan 2002, Koo et al 2010, Marvasi et al 2010, Sutherland 2001b). The role of the EPS is not restricted to biofilm formation and structural integrity, but may supply nutrients for utilization by non-competing bacteria (Sutherland 2001a) and act as a storage receptacle for nutrients to abate variation in nutrient availability (Sutherland 2001a). Additionally, the EPS may increase resistance to antimicrobials (Mah and O'Toole 2001), provide protection from gastric acid (Zhu and Mekalanos 2003) and reduce susceptibility to the human immune system (Peters et al 2012). Given the diverse observations, it is likely that the EPS is

multifunctional and that functional components will vary depending on the types of bacteria associated within the biofilm and environmental factors.

Biofilms do not experience unrestricted growth. The development of the biofilm is restricted by nutrient availability, removal of waste, interactions with the immune system and quorum sensing.

2.3.4.1. Nutrients and Growth

It is accepted that the mechanism employed for nutrient transport into the biofilm is diffusion (Wanner et al 2006); thus, nutrient gradients develop within the biofilm. This in turn, affects the growth rate of the bacteria within the biofilm. It is well documented that bacteria within biofilms, primarily near a non-organic substratum, exhibit a quiescent state brought on by the general stress response from nutrient and oxygen deprivation, changes in pH and the buildup of toxic by-products (Dunne 2002), whereas bacteria on the outer layer of the biofilm, where nutrients are easily accessible, express a growth and metabolic rate similar to planktonic (free floating) bacteria (Anderl et al 2003). However, this is not necessarily the case for biofilms attached to food particles because the substratum acts as a substrate. In this scenario, bacteria closely associated with the substratum and those on the periphery (closest to the intestinal lumen) have more access to nutrients [Sandra MacFarlane, pers. comm.] and thus would demonstrate the greatest growth rate. In contrast to biofilms in other environments, biofilms growing on a nutrient providing substratum will penetrate into the substratum while also spreading along the substratum and growing outward. The penetration of the biofilm into the food matrix may provide further protection from shear forces while increasing the surface area of the biofilm thereby improving substrate availability.

2.3.4.2. Quorum Signaling: Structure, Virulence, and Detachment

Bacteria within biofilms demonstrate a number of phenotypic differences from their planktonic counterparts. One such difference is the production of signaling molecules by both Gram-negative and Gram-positive bacteria, which appear to be regulated by bacterial cell population density (Hammer and Bassler 2003). Acyl-homoserine lactones and post-translationally processed peptides, in Gram-negative and Gram-positive bacteria respectively, have been implicated in the regulation of biofilm development, biofilm structure, virulence and cell detachment (the fifth stage of biofilm development) (Rhoads et al 2007).

Current studies exploring the mechanisms of quorum sensing in bacterial biofilms have focused on pathogenic bacteria. Biofilm-associated *Vibrio cholerae* have been shown to be 1000-fold more resistant to acid than planktonic bacteria (Zhu and Mekalanos 2003), allowing them to survive the low pH of the stomach. *V. cholerae* biofilm formation is initiated by the quorum-sensing regulator LuxO while maintenance is dependent upon the HapR regulator (Zhu and Mekalanos 2003). Once within the bowel, detachment from the biofilm, which is regulated by HapR, is necessary for dispersal and maximal colonization of the small bowel (Zhu and Mekalanos 2003).

Quorum sensing appears to be necessary for differentiation, maintenance and detachment of *Pseudomonas aeruginosa* biofilms. Although this bacterium is not found within the GI tract, it has been well studied and many of the architectural and biofilm-related processes of *P. aeruginosa* may be similar to intestinal bacteria. There are two recognized cell-to-cell signaling systems in *P. aeruginosa*: *lasI-lasR* and *rhlR-rhlI* (Davies et al 1998). The *lasI-lasR* system initiates biofilm formation via the synthesis of the quorum sensing signal N-3-oxododecanoyl-L-homoserine lactone ($N3OC_{12}$-HSL),

whereas the *rhlR-rhlI* system influences biofilm structure, maintenance and detachment (Barken et al 2008, Boles et al 2005, Davey et al 2003).

E. coli K-12 may rely on the EPS component colanic acid for structural differentiation. Strains deficient in colanic acid produced densely packed, thin (approximately 2 cell depth), uniform biofilms similar to *P. aeruginosa* biofilms lacking in $N3OC_{12}$-HSL. Biofilms with colanic acid formed complex, 3-dimensional pillars (26 μm high) (Danese et al 2000). Given the similarity of colanic acid deficient *E. coli* biofilms and the *P. aeruginosa lasI* mutant biofilms, Danese et al (2000) hypothesize that quorum sensing may play a role in colanic acid production.

The autoinducer 2 molecule (AI-2), associated with the *luxS*, gene has been proposed to be a common signaling molecule for inter and intra-species communication. Tannock et al (2005) found that the *luxS* mutant strain of *Lactobacillus reuteri* was capable of colonizing and forming biofilms in the forestomach epithelium of mice; however the biofilms were thicker than the wild type. It was concluded that the synthesis of AI-2 requires the *luxS* gene, based on the significant difference in AI-2 activity in mutant mice as compared to the wild type. Tannock et al (2005) reasoned that the increased thickness in the mutant strain biofilms was a result of the lack of AI-2 molecule, which may be necessary for regulation of bacterial proliferation.

Lactobacillus rhamnosus GG (ATCC 53103), a probiotic strain, has been shown to possess a *luxS* gene, required for A1-2 synthesis (Lebeer et al 2007). The insertion of a tetracycline resistance marker gene disrupted the function of the *luxS* gene, which suppressed the synthesis of AI-2. Lebeer et al (2007) found that the mutant strain had a reduced ability to form biofilms in AOAC medium; however when AI-2 was added to the medium, the mutant strain could not form biofilms analogous to the wild strain. The addition of cysteine significantly increased biofilm formation, however wild type levels

were not achieved (Lebeer et al 2007). These findings suggest that the decrease in biofilm formation may be attributed to metabolic pathways regulated by *luxS* rather than by the signaling molecule AI-2.

Presently, the specific processes involved in the structural formation and detachment of commensal enteric bacterial biofilms attached to food particles have yet to be ascertained. However, it is likely that both quorum sensing and nutrient availability will influence both the structural formation and detachment of bacterial biofilms attached to digesta.

2.3.4.3. Nutrient and Molecule Transport in Biofilms

Biofilms are ubiquitous in nature. The transport of nutrients or molecules within biofilms (microbial, yeast, bacteria or mixed) is better understood than any other topic discussed thus far in the literature review. Most of our understanding stems from the investigation of biofilms associated with waste management.

Existing experimental methods, such as pulse field gradient nuclear magnetic resonance with (McLean et al 2008) or without confocal laser scanning microscopy (CLSM) (Beuling et al 1998, Renslow et al 2010), microelectrodes (Beyenal and Lewandowski 2002, Rasmussen and Lewandowski 1998), fluorescence return after photobleaching (FRAP) (Bryers and Drummond 1998, Waharte et al 2010), and fluorescence correlation spectroscopy (FCS) (Briandet et al 2008), have been used to calculate the effective diffusion coefficient (EDC) parallel to the substratum in biofilms. Such studies have shown that the EDC can vary at different locations within the biofilm (Beyenal and Lewandowski 2002, Bryers and Drummond 1998, Renslow et al 2010, Yang and Lewandowski 1995) and have resulted in EDCs that range from 5% to 95% of that in water (Beuling et al 1998, Wood and Whitaker 2000).

Although information on transport parallel to the substratum is useful, three-dimensional modeling simulations and *in situ* experimental studies have shown that transport of nutrients perpendicular to the substratum is critically relevant to biofilm function. In the case of low velocity flow in the bulk liquid environment (De Beer et al 1996), or when the chemical is only produced or consumed by the bacteria within the biofilm (Picioreanu et al 2004), the concentration gradient is normal to the substratum; however, in the latter case, this may depend upon the biofilm morphology since multidimensional gradients may occur in biofilms which are highly porous and channeled. Furthermore, in multi-species biofilms the concentration gradient may be multidimensional if the chemical facilitates microbial cross-feeding (Picioreanu et al 2004). Thus there is a need for estimating the EDC in biofilms both parallel to and perpendicular to the substratum.

2.3.4.4. Effective Diffusion Coefficient

Despite the evidence that nutrient transport is multidimensional, to date, mathematical models have made three simplifying assumptions with regards to the transport of particles within a biofilm: 1) the EDC is constant (Alpkvist and Klapper 2007, Chang et al 2003, Hermanowicz 2001, Rahman et al 2009, Rajagopalan et al 1997, Xavier et al 2004); 2) the EDC is that of water (Alpkvist and Klapper 2007, Kreft et al 2001, Rajagopalan et al 1997, Xavier et al 2004); and 3) the EDC is isotropic (the same in directions parallel and perpendicular to the substratum) (Alpkvist and Klapper 2007, Chang et al 2003, Rahman et al 2009, Xavier et al 2004).

There is one paper which describes the relationship between nutrient transport perpendicular to the substratum and distance from the substratum. Using microelectrodes, Beyenal and Lewandowski (2002) measured local effective diffusivity profiles at multiple locations within biofilms to estimate the EDC. In this study,

biofilms consisting of *Pseudomonas aeruginosa* (ATCC 700829), *Pseudomonas fluorescens* (ATCC 700830) and *Klebsiella pneumonia* (ATCC 700831) were grown on flat plate reactors at various constant flow velocities. As seen in Figure 2.7, they found a linear relationship between the EDC and the distance from the substratum. They surmised that the linear decrease in the EDC towards the substratum is due to an increased heterogeneity within the biofilm. They also found that the slope of the linear relationship differed based on the flow conditions in which the bacteria were grown, in that the slope of the EDC in biofilms grown at low or high flow velocities was lower than biofilms grown at moderate flow velocities. Taking into consideration the external mass transfer (dependent on flow velocity) and the resulting EDC, Beyenal and

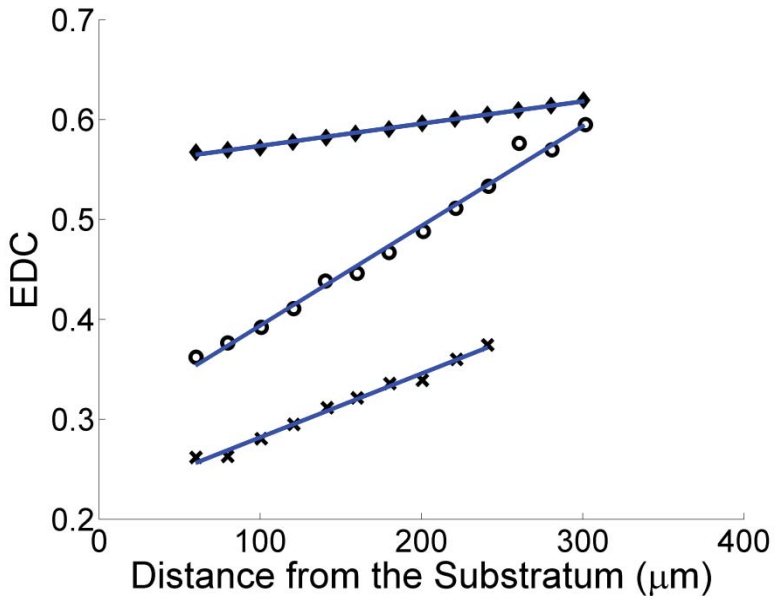

Figure 2.7 The effective diffusion coefficient (EDC) as a function of distance from the substratum for biofilms grown at selected flow velocities: 8cm/s (diamonds), 7.5 cm/s (circles) and 28 cm/s (crosses) (Beyenal and Lewandowski 2002). Image reconstructed using automatic image capturing software. Reprinted with permission from *Biotechnology and Bioengineering*.

Lewandowski (2002) hypothesized that the EDC gradient in biofilms is related to the biofilm density, as the biofilm structure has been shown to alter as a result of various flow velocities.

While the linear relationship, between the EDC and the distance from the substratum, observed by Beyenal and Lewandowski (2002) may seem satisfactory, this linear relationship does not consider the behavior near to, or far from, the substratum. A complete profile is necessary to determine an accurate relationship between the EDC and distance from the substratum.

2.3.4.5. Relationship Between Biofilm Porosity or Density and Nutrient Transport

There are a multitude of models describing the relationship between either biofilm porosity (volume fraction of the biofilm that is liquid) or biofilm density and nutrient diffusion within the biofilm (Beuling et al 2000, Fan et al 1990, Ho and Ju 1988, Horn and Morgenroth 2006, Kapellos et al 2007, Libicki et al 1988, Maxwell 1892, Mota et al 2002, Phillips 2000, Wood et al 2002). For a review of mathematical models see Wang and Zhang (2010). Some are heuristic fits to data (i.e. trial and error), whereas others are derived using theoretical arguments based on simplified biofilm geometry [Table 2.1]. It is not clear which of these models is most suitable for describing the effect of biofilm structure on nutrient transport within the biofilm.

Many models partition the biofilm into two distinct components where one component is comprised of biomass (bacteria and EPS) and the other of water (Alpkvist and Klapper 2007, Hermanowicz 2001, Wanner et al 2006, Wood and Whitaker 2000). The biofilm can then be considered a porous media. The biomass within the biofilm reduces the rate of diffusion of particulates parallel to the substratum via steric hindrance (De Beer et al 1997, Guiot et al 2002). However, the distribution of biomass may be heterogeneous (Bridier et al 2010) and the diffusion parallel to the substratum

may be different to the diffusion perpendicular to the substratum. For example, if the biomass is compact with multiple column like structures growing perpendicular to the substratum (Bridier et al 2010, Danese et al 2000), one would expect that the columns of bacteria would hinder the transport of particles parallel to the substratum to a greater degree than perpendicular to the substratum [Figure 2.8]. Thus I hypothesize that the EDC in biofilms is anisotropic, with a level of anisotropy that is dependent on the biofilm structure.

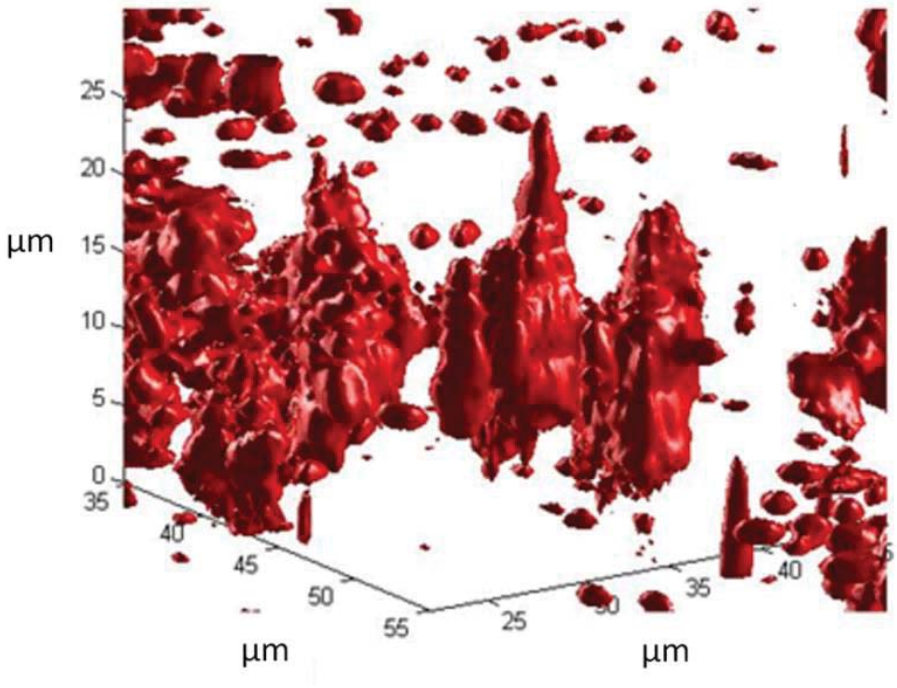

Figure 2.8 A partial view of a *Salmonella enterica* biofilm created from stacked CLSM images in MATLAB, demonstrating column like structures that form in biofilms. The z-axis represents the distance (μm) from the substratum (microtiter plate).

Table 2.1 Mathematical models describing the relationship between biofilm porosity, **ε**, or density, ρ , and the EDC, D_{eff} . Note, D_W is the diffusion coefficient in water.

Model	**Reference**
$\frac{D_{eff}}{D_W} = \frac{2\varepsilon}{3-\varepsilon}$	(Maxwell 1892)
$\frac{D_{eff}}{D_W} = \frac{\varepsilon}{\tau^2}$	(Epstein 1989)[a]
$D_{eff} = 1 - \frac{0.43\rho^{0.93}}{11.19 + 0.27\rho^{0.09}}$	(Fan et al 1990)
$\frac{D_{eff}}{D_W} = a + b\rho$	(Horn and Morgenroth 2006)[b]
$\frac{D_{eff}}{D_W} = \exp\left(-0.84 f^{1.09} - a(1-\varepsilon)^b\right)$ $f = (1-\varepsilon)(1+\lambda)^2$ $a = 3.727 - 2460.\lambda + 0.822\lambda^2$ $b = 0.358 + 0.366\lambda - 0.0939\lambda^2$	(Phillips 2000)[c]

(a) Here the tortuosity, τ , is defined as the ratio of the average pore length to the length of the porous medium along the major flow or diffusion axis. (b) the parameters *a* and *b* are found by linear regression. (c) In the context of biofilms, λ is the ratio of the radius of the diffusing solute to the pore ratio. Since the model description was used to estimate diffusion of solutes in muscle fiber, λ is assumed to be constant and the parameter values (*a* and *b*) may not be suitable for biofilms as seen in the work by Kapellos et al (2007).

2.4. Concluding Comments

As our knowledge of food/bacteria/host interactions increases, it is becoming clear that there is enormous potential in the development of functional foods. With the increasing incidence of intestinal related conditions, allergies and food intolerances, there is a growing awareness by the public for alternative methods to improve general health. To maximize the potential health benefits from functional foods, it is essential that we develop a deeper understanding of (1) how gastric digestion alters the food matrix; (2) how to predict the proportion of the food matrix which remains after digestion in the stomach and small bowel, as well as the composition of the remaining food matrix; (3) how diet impacts bacterial attachment to the digesta in the small and large bowel; (4) how diet impacts the bacterial colonization of the bowel; and (5) how bacteria work in a consortium to degrade food particles within the small and large bowel.

The human stomach is a dynamic and complex system. Here, the few models in the literature pertaining to gastric digestion have been outlined. In terms of mathematical modeling, it is only in its early development; however the building blocks to fully understand how the stomach works to degrade food particles are slowly being put together. Of course, future food degradation experiments which specifically consider the effects of the food matrix components on erosion and fragmentation, changes in food particle distribution during digestion and the rate of emptying, the effects of temperature on degradation, and the diffusion of gastric fluid as a function of pH are critical to advance the current mathematical models.

The value of understanding food/microbial interactions has only just gained substantial notice in scientific research. Until recently, research has focused on pathogenic bacteria, most of which are associated with the intestinal epithelium rather

than the digesta. Additionally, studies of the commensal bacteria associated with the intestinal lumen and digesta have concentrated on enumeration, classification, determination of preferred substrates of known species and potential metabolites released via carbohydrate fermentation, and to a lesser extent protein metabolism and bile acid hydrolysis.

It is clear that this area of research is still in its infancy. Many of the microbial species associated with the GI tract, and in particular associated with the digesta, have yet to be identified. While the enteric microbiota is capable of metabolizing a variety of dietary and endogenous compounds, the mechanisms required for attachment to these substrates has only been determined for a few bacterial strains and primarily to resistant starch. When testing the current theoretical models for bacterial attachment, there is clear evidence that these models do not accurately reflect bacterial attachment in this dynamic system. Quorum signaling, in pathogenic bacteria, has been recognized as a necessary process by which biofilm formation, structure and detachment is regulated, although as yet, these pathways have not been determined in the commensal microbiota.

In terms of modeling bacterial growth and biofilm development, the scientific community has made significant gains. However, as pointed out in the literature review, the level of anisotropy of nutrient transport in biofilms has yet to be determined, primarily due to the methods in which the effective diffusion coefficient is determined. Furthermore, complete models which predict bacterial competition and cross-feeding have yet to be developed. Much of the challenge in building reliable predictive models is the lack of data required to validate the models. There is a substantial need for future coculture and multi-culture bacterial experiments which explicitly measure growth kinetics at relatively frequent time intervals.

Currently there is little knowledge of this unique, complex and highly important, physiological system–the human gastrointestinal tract the interactions between food/bacteria/host. This is an exciting field of study for those in nutrition, microbiology and mathematical modeling.

2.5. Aims of Research

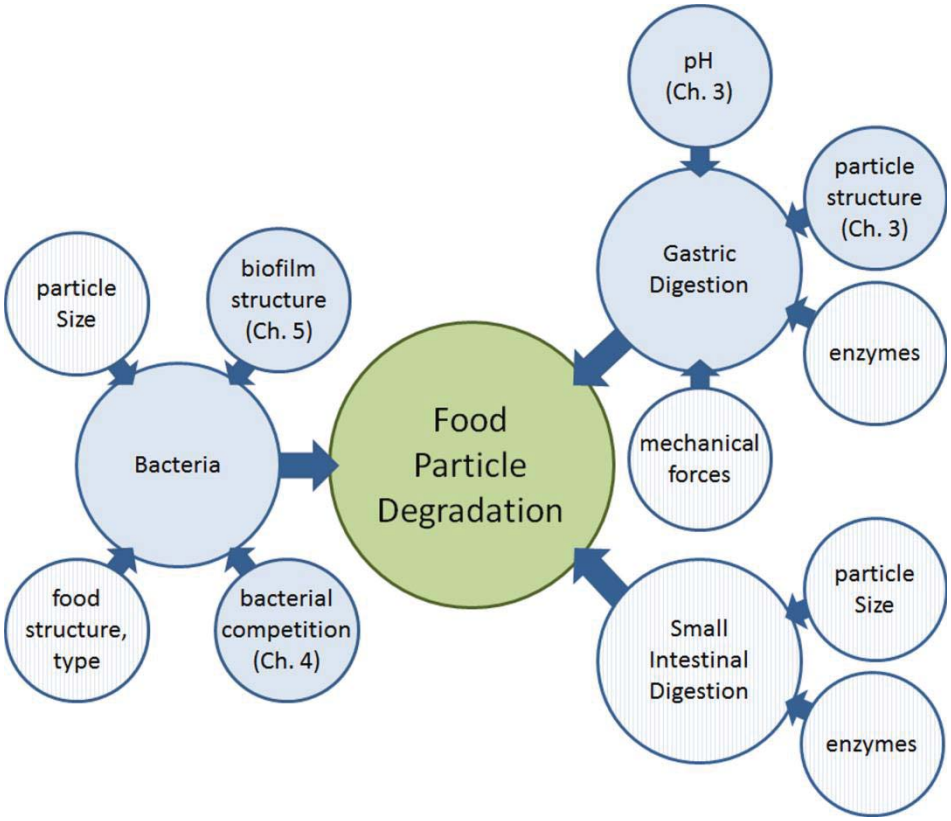

There are many challenges associated with understanding the complex interactions in the human digestive tract. *In vivo* observation and experimentation is often difficult, expensive or even impossible. For example, it is difficult to accurately measure the rate of production of metabolites by bacteria within biofilms. In an *in vivo* situation, the rate of production of metabolites by the commensal bacteria may be difficult to directly quantify because, soon after they are produced, the majority of

metabolites diffuse through the intestinal epithelium to be utilized by the body. The difficulties of *in vivo* experimentation necessitate the use of alternative methods for measurement, prediction and understanding. *In vitro* experimental systems and mathematical models are useful adjunct tools for this purpose.

From one point of view, mathematical models are similar to *in vitro* experiments, in that both allow phenomena to be studied in a "model system" or simplified scenario of the biological system of primary interest. Mathematical models can be used to provide insight and understanding to the information obtained through *in vitro* and *in vivo* experimentation. Mathematical models can be used to 1) provide a systematic framework to link experiments, 2) form the basis of a statistical tool to estimate physical variables that are difficult to measure directly (such as metabolite production rates), 3) make predictions and 4) formulate new biological hypotheses to be tested by new experiments.

The literature review has highlighted a number of areas in which mathematical models could be used to provide better insight into the mechanisms responsible for the degradation of food particles within the human digestive tract. As mentioned in section 2.1.2.3, there has yet to be a mechanistic model proposed in the current literature to describe solid loss as a result of gastric digestion. To understand the complexities of gastric digestion and to build models which accurately describe the underlying digestive mechanisms, it is essential to determine the effects of different factors (food structure, preparation, particle size, meal volume and composition, viscosity, pH, and temperature) on gastric digestion prior to investigating the interactions between those factors. Here, only the effect of pH on digestion is considered as the pH directly affects enzymatic reactions, varies over the digestive time, and has been shown to have a significant effect on the amount of soluble loss from the food matrix.

The hypothesis driving the work in Chapter 3 is that the rate of diffusion of the fluid into a food particle is not only dependent upon the concentration of the fluid diffusing into the food particle, but is also dependent on the pH of the fluid and the structure of the food matrix. Furthermore, these dependencies contribute to the increased rate of soluble loss and protein degradation in particles submerged in gastric fluid with low pH. The aim is to demonstrate this dependency by developing a dynamic, mechanistic mathematical model that describes the soluble loss of a food particle due to degradation by acidic hydrolysis in the human stomach using raw carrot and Edam cheese as model food systems.

Chapter 4 is motivated by the hypothesis that a mathematical model of microbial growth can be used to predict coculture growth kinetics based on monoculture growth kinetics. The aim of Chapter 4 is four fold: (1) to develop a model that draws upon the previously proposed dynamic, mechanistic mathematical model of Amaretti et al (2007) to describe the mechanisms for substrate consumption and subsequent microbial growth and metabolite production for bacteria grown in monoculture, (2) to extend the model to describe the preferential degradation of oligofructose during growth of a single bacterial strain in monoculture, (3) to adapt the model to describe competition between two bacterial species for a particular substrate as well as cross-feeding resulting from the breakdown products of extracellular carbohydrate hydrolysis by one of the bacterial species, and (4) to explore and predict the growth dynamics between *Bacteroides thetaiotaomicron* LMG 11262 and *Bifidobacterium longum* MG 11047 and *B. thetaiotaomicron* LMG 11262 and *Bifidobacterium breve* Yakult as compared to experimental coculture data using the model described in the third aim of Chapter 4.

The work in Chapter 5 is driven by the hypothesis that nutrient transport in biofilms is anisotropic. The aim of this chapter is four fold: (1) to utilize an alternative

method for determining the EDC in real three-dimensional bacterial biofilms, (2) to determine the level of anisotropic nutrient transport in biofilms, (3) to ascertain the relationship between the porosity of the biofilm and the EDC and (4) to construct a model of nutrient transport within a bacterial biofilm growing on a nutrient-providing substratum.

Chapter 3 A Mathematical Model of the Effect of Gastric Fluid pH on Food Degradation in the Human Stomach

3.1. Abstract

The question of bioaccessibility of nutrients within a food matrix has become of increasing interest in the fields of nutrition and food science as bioaccessibility is the precursor to bioavailability. By analyzing the propagation of the wetting front of simulated gastric fluid (SGF) without pepsin or mucin in raw carrot core and Edam cheese as model systems, the diffusion of the acidic water is shown to be dependent on the pH of the gastric fluid and the food matrix. Utilizing the diffusion rates found at various pH levels (1.50, 2.00, 3.50, 4.30, 5.25 and 7.00), a model is developed to describe the measured non-linear rate of soluble particle loss during digestion at various constant pH levels. Additionally, a model is developed to predict the likely rate of soluble particle loss during digestion in the stomach where pH decreases with time. This model can be used to help understand and optimize the relationship between food structure/composition and food degradation in the human stomach, which may help in the development of novel foods with desired functionality.

3.2. Introduction

In food science and nutrition the question of the bioaccessibility of a food (the fraction of a nutrient released from a food matrix) is of increasing interest. In order for a

nutrient to become bioavailable (absorbed by and used by the host), it must first become bioaccessible through the processes of mastication, stomach digestion, and enzymatic reactions within the small bowel. Both the degree of particle loss and the amount of remaining material is critical to human health; in that the leached soluble fraction is readily available for absorption in the small bowel and the remaining insoluble fraction may act as a substrate for bacterial growth within the small and large bowel. In order to develop novel foods which either increase the rate of bioaccessibility (in the case of foods targeted for consumption by athletes, infants and the elderly) or decrease the bioaccessibility (in the case of food matrices which encapsulate probiotics and thus may need to remain intact throughout digestion), a deeper understanding of human digestion is required as well as the ability to predict the behavior of food matrices within the human gastrointestinal (GI) tract.

The degradation of food particles within the stomach is complex and results from both mechanical forces and chemical reactions. Peristaltic movements within the stomach compress the food bolus, which can result in fracturing of food particulates, and may facilitate erosion or shearing due to the mixing of the stomach contents. Tenderization of food particles results from the absorption of gastric juice; both acidic hydrolysis and enzymatic reactions cause leaching of nutrients from the food particle making them bioaccessible. The extent of soluble particle loss, and hence nutrient bioaccessibility, as well as the erosion of the particle are also dependent upon the food structure, preparation, particle size, meal volume and composition, viscosity, pH, and temperature.

An important factor contributing to the bioaccessibility of nutrients during gastric digestion is the structure of the food matrix. When vitamin B_{12} is encapsulated in a water-in-oil-in-water double emulsion only 4.4% of vitamin B_{12} was released after

120 minutes of gastric digestion, whereas all of the non-encapsulated vitamin B_{12} was bioaccessible (Giroux et al 2013). While it is expected that the protein content of the food matrix will have a marked effect on the extent of proteolysis, it has been shown that the fat content of foods can reduce protein digestibility (Grimshaw et al 2003); it was hypothesized that the fat encapsulated the protein molecules, restricting digestion. A study comparing the digestibility of proteins in various foods (legumes, cereals, milk products and chicken meat) has shown that the secondary structure elements of the proteins within the food played a major role in reducing protein digestibility (Carbonaro et al 2012). These same secondary structures are found in β-lactoglobulin, which has been shown to be resistant to proteolysis by both pepsin and trypsin (Guo et al 1995). In addition to the food composition and protein structure, pH can affect the efficacy of pepsin. Studies with kiwifruit have shown that even after an hour of digestion, there was very little breakdown of proteins when digested in simulated gastric fluid with pH greater than 2.5 (Lucas et al 2008).

To understand the complexities of gastric digestion and to build models which accurately describe the underlying digestive mechanisms, it is essential to determine the effects of such different factors (food structure, preparation, particle size, meal volume and composition, viscosity, pH, and temperature) on gastric digestion prior to investigating the interactions between those factors

There have been few models proposed in the literature that describe food digestibility. Current mathematical models which describe food digestibility have primarily focused on the wet mass retention ratio of the studied food (wet sample weight after digestion time divided by the initial wet sample weight) (Kong and Singh 2009b); however, the wet mass retention ratio is more suitable to describe the satiety properties of a food matrix during digestion rather than the bioaccessibility of nutrients

within a food matrix. As observed in studies with raw and roasted almonds, the wet mass retention ratio increased with digestion time as the food matrix absorbed gastric fluid, whereas the dry solid mass decreased over the digestion time (Kong and Singh 2009a). Thus the wet retention ratio does not provide information on soluble solid loss (or bioaccessibility), rather it provides information on the change in volume of the food particle. Increased particle size reduces the rate at which the food particle empties from the stomach and increases the volume of the bolus, both of which are directly related to the feeling of fullness or satiety (Marciani et al 2001).

Recently, the dry solid loss of carrot was described using the Weibull function (Kong and Singh 2011); however, this description of the dry solid loss does not adequately describe the solid loss after an extended time (time equaling 36 hours). Such empirical models, although useful for inference purposes, do not incorporate any of the mechanisms that influence digestibility. For instance, the Weibull function does not describe the process of diffusion of the gastric fluid into the food particle, which may be pH dependent. Models of the mechanisms underlying the degradation of food particles will yield a better understanding of the interaction and role of different processes in the breakdown of food particles.

It is well known that the pH of the gastric contents after a meal is not static in time, rather the pH of the gastric contents can reach approximately 5 within minutes after the ingestion of a meal, and may take up to 2-3 hours before the gastric contents reaches a pH below two (Malagelada et al 1976). In previous *in vitro* studies of carrot digestion, the pH of the simulated gastric fluid had a marked effect on the amount of soluble loss from the food matrix (Kong and Singh 2011). The rate of soluble loss from a food matrix in the stomach is therefore not static in time and cannot be predicted based on a static pH level. Here, only the effect of pH on digestion is considered as the

pH directly affects enzymatic reactions, varies over the digestive time, and has been shown to have an effect on the amount of soluble loss from the food matrix.

Given these results, the rate of diffusion of the fluid into a food particle is hypothesized to not only be dependent upon the concentration of the fluid diffusing into the food particle, but is also dependent on the pH of the fluid and the structure of the food matrix. Furthermore, these dependencies contribute to the increased rate of soluble loss and protein degradation in particles submerged in gastric fluid with low pH.

Note that the hypotheses are independent of pepsin-mediated pH and food effects on the rate of diffusion of the fluid into a food particle during gastric digestion (e.g., pepsin was not included in the simulated gastric fluid to ensure that any difference observed in the propagation of the acidic fluid between food matrices was a result of the food structure). Even though pepsin effects are excluded from this study, this does not preclude the important role of pepsin-dependent effects on the rate of diffusion of the gastric fluid into a food particle (understanding the pepsin-independent effects is a prerequisite to understanding the pepsin-dependent effects).

The aim of this work is to demonstrate the dependency of solid loss on pH and food structure by developing a dynamic, mechanistic mathematical model that describes the soluble loss of a food particle due to degradation by acidic hydrolysis in the human stomach using raw carrot and Edam cheese as model food systems. As mentioned earlier, there has yet to be a mechanistic model proposed in the current literature. Specifically, the propagation of the wetting front into the food particle, which has a major influence on the rate of nutrient release during gastric digestion, will be described. The model will be tested by fitting the model to the measured non-linear rate of soluble particle loss during digestion at various constant pH levels. Because the pH within the stomach is not static, the model will be used to predict the likely rate of

soluble particle loss during digestion in the stomach where pH decreases with time after meal ingestion. This model can be used to help understand and optimize the relationship between food structure/composition and food degradation in the human stomach, which may help in the development of novel foods with desired functionality.

3.3. Materials and Methods

3.3.1. Digestion Simulation

Raw carrots were purchased from local vegetable shops (Hamilton, New Zealand). Attention was taken to purchase carrots of similar length (17.35 ± 1.24 cm) and weight (111.83 ± 6.43 g). A cork borer was used to take cylindrical samples (diameter 5.3 mm × 21 mm length) from the core of the raw carrot, parallel to the length of the carrot. The diameter of the sample was within the range of particle sizes which enter the stomach after mastication (Mishellany-Dutour et al 2011, Peyron et al 2004), though on the larger end of the spectrum in order to improve the visualization of the simulated gastric fluid (SGF) penetration front. The length of the cylindrical samples was exaggerated to ensure that diffusion of SGF from either the top or bottom of the cylinder did not influence the diffusion of gastric fluid at the center of the cylindrical sample.

To gauge the effect of pH on diffusion rates, individual samples were placed in sterile, 50 ml polypropylene centrifuge tubes (RayLab, New Zealand) with 30 ml of SGF in a $37°C \pm 0.1°C$ shaking water bath (Daihan Scientific Co., Ltd., Korea) at 30 rpm for 5, 10, 20, and 40 minutes. Four replicates were examined at each time period. SGF was prepared without pepsin or mucin: NaCl (8.775 g/L), 2 M HCl (10 mL) and distilled water (990 mL) (Kong and Singh 2008). It has previously been shown that neither mucin nor pepsin had a significant effect on the solid loss of carrot; the lack of

proteolysis in carrots may be attributed to the fact that carrots only contain minor amounts of protein (Kong and Singh 2009b, Kong and Singh 2011). SGF without pepsin or mucin is essentially acidic water (AW), thus it is referred to as such in this work. This experiment was repeated at six different pH levels: pH 1.50, 2.00, 3.50, 4.30, 5.25 and 7.00 $\pm$ 0.01. AW was adjusted to the required pH by the addition of either HCl or NaOH. Methylene blue was added to the AW in order to visualize the AW penetration front (~2mg/450 ml of AW) (Kong and Singh 2009b). Given that the area of a methylene blue molecule is approximately 1.32 – 1.35 nm^2 (Hang and Brindley 1970) and the space between the cells of the carrot can range from 100 nm to the micrometer scale, the addition of methylene blue to the AW will have little to no effect on the diffusion rates of the AW.

Edam cheese (Fonterra, New Zealand) was purchased from a local grocery store (Hamilton, New Zealand). In order to compare the effect of the food matrix on the diffusion of AW, sampling and digestion methods for Edam cheese were identical to the methods described for carrot, with the following exceptions. Blocks of Edam were frozen at -20°C prior to sampling in order to reduce sample compaction as a result of cutting and the samples were allowed to defrost at room temperature prior to digestion simulation. Given the purpose of the experiment was to examine the AW penetration front and not the solid loss during digestion, the digestive times were 5, 10, 15 and 20 minutes. More frequent time frames were chosen for Edam to reduce the possibility of the cheese melting at the given temperature. In order to ensure that any difference in the AW propagation front between food matrices was a result of the food matrix itself, pepsin was also not included in the AW for Edam. As observed in previous studies with kiwifruit (Lucas et al 2008) and casein proteins (Guo et al 1995), one would expect some proteolysis of cheese at low pH levels although not at pH greater than 2.5 – 3.

Such proteolysis at low pH may create additional solid loss and increase the speed of the AW propagation front in cheese food matrix. However, the role of protein hydrolysis on solid loss and the speed of the SGF propagation front are beyond the scope of this work.

To halt the diffusion process, samples were removed after the respective soaking times and frozen by submergence into liquid nitrogen and stored at -80°C. Sections of approximately 4 mm were taken from the center of the cylindrical samples, using a cryostat microtome (Leica, Germany) set at -12°C, which allowed the samples to remain frozen until images were taken reducing the risk of further diffusion of AW in the samples. Images of the cross sections were obtained at 16× magnification using a high definition digital camera (Cannon PowerShot G6, Japan) attached to a microscope (Zeiss, Germany). Images were obtained on a white background (OCT compound, Sakura Fineteck, USA).

3.3.2. Mathematical Model of Moisture Transport

In the instance of sorption or desorption, the dependence of the effective diffusion coefficient (EDC) on moisture content is well established (Crank 1975) and has been shown to be relevant to cheese in the modeling work of Payne and Morison (1999) and experimental work of Guinee and Fox (1983). In each instance, the EDC increased concomitantly with an increase in moisture content. This activity is not restricted to cheese, but has been demonstrated in the absorption of water in peas (Waggoner and Parlange 1976), soybean, corn, cotton seeds (Phillips 1968), and rice (Gomi et al 1996), in the dehydration of carbohydrates (Aldous et al 1997) and the drying of gelatin and sugar solutions (Yamamoto 1999). The models which describe the dependence of the EDC on moisture content primarily use either an exponential

function (Crank 1975), sum of exponentials (Gomi et al 1996, Gomi et al 1998) or the power law (Yamamoto 1999). In this work, a standard exponential function was used:

$$D(\theta) = A\exp(b\theta) \tag{3.1}$$

where the parameters $A, b \geq 0$.

As shown in previous work (Saguy et al 2005, Syarief et al 1987), the theory of liquid transport in porous materials, such as soil, can also be applied to food structures. This theory is based on Darcy's Law for unsaturated porous media (with no gravity effects) and conservation of mass. Thus, the moisture content, θ, diffusing into a food matrix (i.e., the AW concentration), which is expressed as volume of water in a unit volume of porous media (sum of solid and pore volumes), can be described by the following diffusion equation:

$$\frac{\partial\theta}{\partial t} = \nabla(D(\theta)\nabla\theta) \tag{3.2}$$

where $D(\theta)$ is interpreted as the ratio of hydraulic conductivity to specific water capacity. Assuming diffusion along the radius of a cross section of a cylinder, this becomes

$$\frac{\partial\theta}{\partial r} = r^{-1}\frac{\partial}{\partial r}\left(D(\theta)\frac{\partial\theta}{\partial r}\right) \tag{3.3}$$

where *r* is the radial distance from the center of the cylinder. The initial and boundary conditions are respectively:

$$\theta(r, t=0) = 0 \tag{3.4a}$$

$$\theta(r = R(t), t) = 1 \tag{3.4b}$$

$$\frac{\partial\theta(r, t=0)}{\partial t} = 0. \tag{3.4c}$$

That is, initially there is no AW in the food matrix and the boundary of the food matrix, $R(t)$, which may be a function of time *t*, is fully saturated.

3.3.3. Determining Diffusion Coefficients

Images of the partially digested carrot and Edam cheese cross sections were uploaded into MATLAB (The MathWorks; www.mathworks.com) [Figure 3.1]. The center of each sample was determined by visual inspection and the initial radius was known (2.65 mm). The mean color density distribution for green, red and blue, were determined in MATLAB as a function of distance from the center of the sample. The red color density distribution provided the best indicator for the AW penetration front profile, as the mean color density of the control samples (samples that had not undergone any digestive processing) resulted in a relatively horizontal line, except at the boundary of the sample. In the red, green and blue color density profiles, the color density increased at the boundary of the sample which reflects cutting imperfections in the cork borer. However, the apparent boundary effects had less of an impact on the red color density profile.

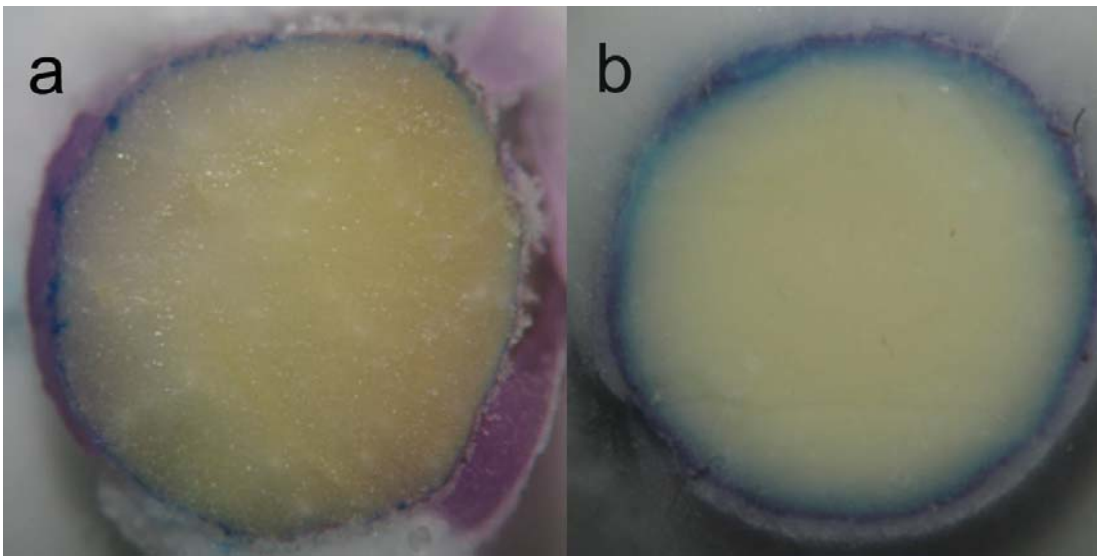

Figure 3.1 Cross section of carrot core (a) and Edam cheese (b) after 5 minutes in acidic water at pH 7 and at pH 3.5, respectively. Area in which acidic water has penetrated is shown by the presence of methylene blue (blue/purple).

Using a linear transformation, the mean color density distribution [Figure 3.2a] was transformed into a concentration profile of the AW as a function of distance from the center of the samples [Figure 3.2b]. To account for discrepancies in the red color density values of carrot samples (as carrot core color varies between carrots and within the same carrot), the value of the red color density at approximately 45 μm from the center was used to represent the value for which no AW was present. Thus, only samples in which the AW did not fully penetrate the sample were selected for data analysis. Furthermore, Edam cheese samples were chosen for analysis if 1) the AW had not fully penetrated the sample, 2) the sample maintained its cylindrical shape, and 3) fissures did not occur in the sample. Given that the boundary of the samples were not perfectly uniform, the minimum mean color density was used to represent the distance at which the concentration of AW reached its maximum. To account for the lack of uniformity at the boundary of the carrot, it was assumed that the AW concentration was 100% from the point where the AW reached its maximum concentration to the boundary of the carrot.

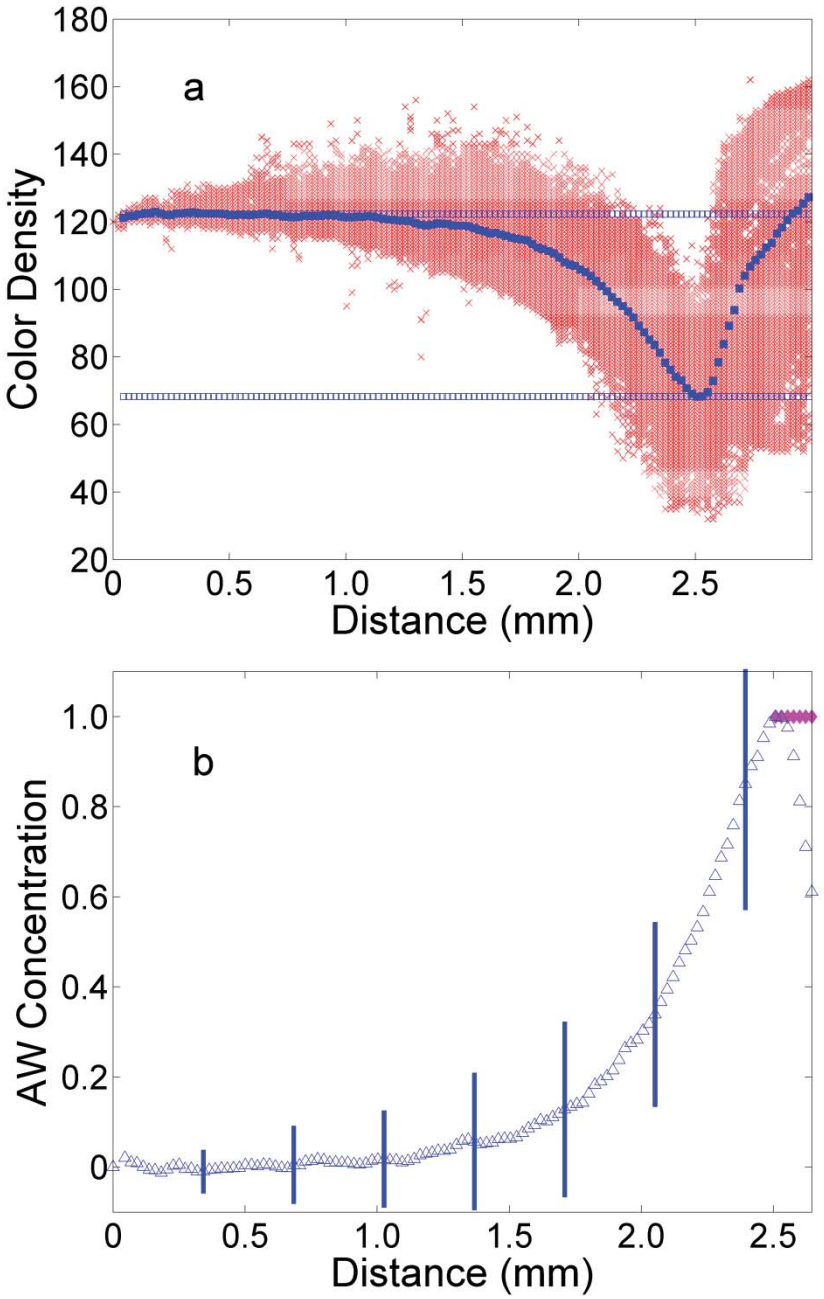

Figure 3.2 (a) Color density profile as a function of distance from the center of carrot core: raw data (red crosses), mean value (blue squares) and average maximum and minimum values (dashed lines). (b) Linear transformation of average color density value (blue triangles), standard deviation (blue bars), and smoothed edge effects (magenta diamonds).

3.3.4. Data Analysis

To determine the EDC model parameter means for the carrot samples (Eq. 3.1), the multi-response method described in Pell & Kowalski (1991) was used. In this method the trace of the matrix $\boldsymbol{Z}^{\mathbf{T}}\boldsymbol{Z}$ is minimized, were $\boldsymbol{Z}$ is the matrix of residuals of the difference between the AW penetration front profile at 5 and 10 minutes and the model. This is equivalent to minimizing the mean square error. The trace of $\boldsymbol{Z}^{\mathbf{T}}\boldsymbol{Z}$ was used as the data were of the same units and scale (Pell and Kowalski 1991). As a result of the limited number of usable Edam cheese samples, the EDC model parameter means were determined by minimizing the mean square error for individual AW penetration front profiles.

Unless otherwise specified, nonlinear regression model parameters were found by minimizing the mean square error in MATLAB (The MathWorks; www.mathworks.com). Significance tests for the relationship of pH to the distance for which the AW concentration reached 50%, $\theta_{1/2}$, were conducted using a one-way ANOVA in GenStat V13.2 (VSN International Ltd., UK). Partial differential equations were solved in MATLAB using the initial-boundary value solver pdepe.

3.4. Results and Discussion

3.4.1. Choice of Model Food Matrix

Given that the initial step in calculating the EDC requires the model food to maintain a symmetric cross section of known size, it was essential that the selected food matrices did not swell as a result of gastric fluid absorption or undergo conformational changes at a temperature of 37°C. If the food structure undergoes conformational changes, this results in a moving boundary problem which complicates the measurement of the EDC. For this study our model food was the carrot which has a relatively

isotropic structure, even though the cellular structure is heterogeneous. Additionally, it was previously shown that raw carrot is geometrically stable and does not swell under gastric fluid digestion conditions (Kong and Singh 2008, Kong and Singh 2011).

Other foods such as meat, rice and almonds were considered; however, these foods all have particular characteristics that complicate the estimation of the diffusion rates with our methods. For example, it was found that high moisture cheese would begin to melt at a temperature of 37°C, the sampling method increased the density of the samples, and in many cases caused fissures in samples which enabled diffusion of gastric fluid along the crevice path (data not shown) limiting its usefulness. The anisotropic structure of meat fibers, distribution of fat, variable moisture content, and potential differences in the cooked state all add additional complications in the sampling of meat and the estimation of diffusion rates. Furthermore, studies of beef jerky (Kong and Singh 2009b), almonds (Kong and Singh 2009a), and rice (Kong et al 2011) showed that these food structures increased in wet weight during the initial stages of digestion, which results in a moving boundary problem making the estimation of diffusion rates more complex.

3.4.2. Effect of pH on the Effective Diffusion Coefficient

Figure 3.3a,b illustrates the effect of pH on the rate of diffusion of the AW into the carrot matrix. Within 20 minutes, the AW adjusted to pH 1.5, fully penetrated the carrot core (2.65 mm), whereas the AW adjusted to pH 4.3 penetrated less than 1 mm. Several conditions were required and assumptions made, as described previously, in order to use the color density profile to describe the AW penetration front. Thus, the results presented here are based on the samples which were soaked in gastric fluid for either 5 or 10 minutes; longer time periods resulted in the full penetration of the sample with low AW pH levels.

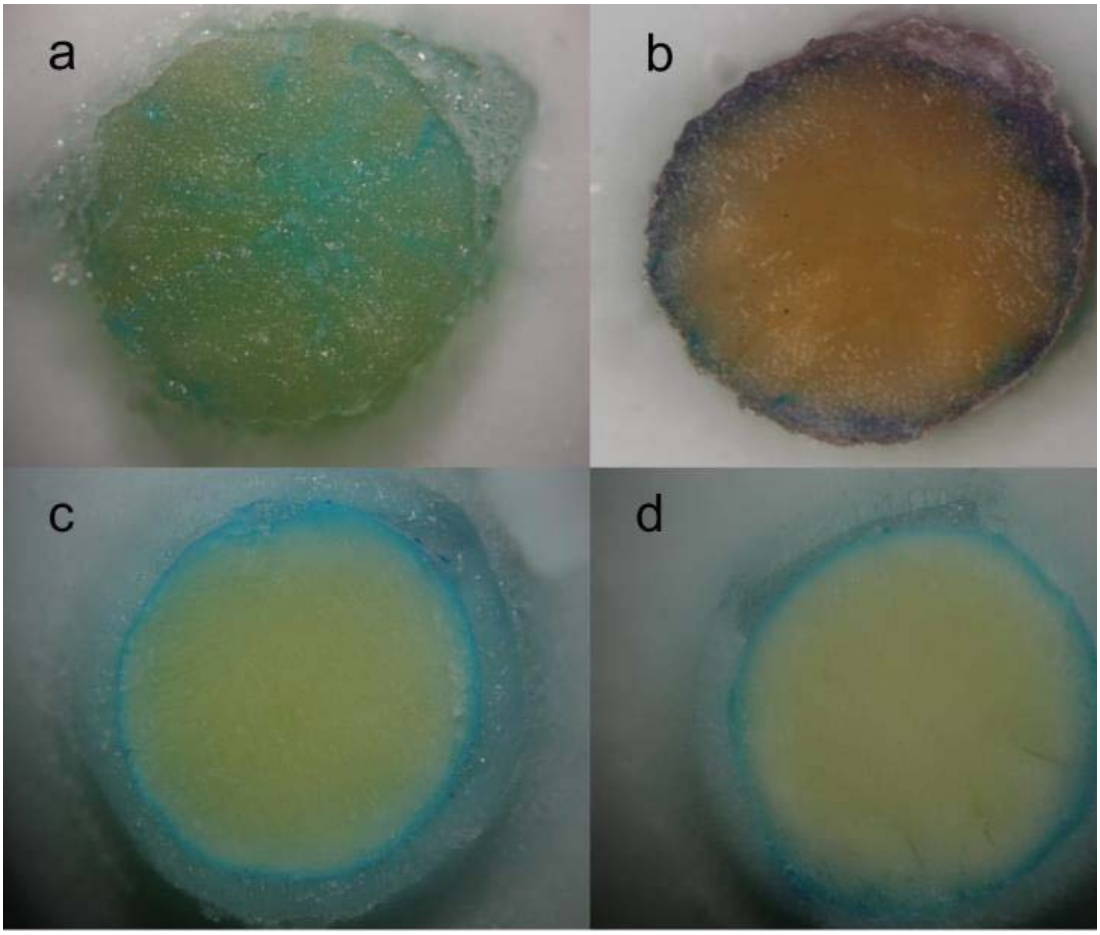

Figure 3.3 Cross section of carrot core after 20 minutes in acidic water (AW) at pH 1.51 (a) and at pH 4.3 (b). Cross section of Edam cheese after 5 minutes in AW at pH 1.51 (c) and at pH 7 (d). Area in which AW has penetrated is shown by the presence of methylene blue (blue/purple).

The AW concentration profiles were different for various pH concentrations at the same soaking time period [Figure 3.4a]. The difference in effective diffusion rates between pH decreased as the pH became less acidic. To determine the significance of the effect of pH on the AW concentration, the distance at which the AW concentration reached 50%, $\theta_{1/2}$ μm, for each pH concentration examined was considered [Figure 3.4b] after soaking in gastric fluid for 5 and 10 minutes. An exponential regression model was fit to the 10 minute data (Eq. 3.5):

$$\theta_{1/2} = 22672 \times 10^{-1[pH]} + 641.95 . \quad 3.5$$

The exponential model is biologically relevant given the definition of pH, and accounts for 83.9% of the variance in distance. A one-way ANOVA for the data after soaking for 5 minutes (not shown) and 10 minutes [Figure 3.4b] shows that the effect of pH on the distance for which the AW concentration reached 50%, $\theta_{1/2}$, is significant for low pH levels ($P<0.001$); however, there was no significant difference in the mean values for pH between 3.5 and 7.0.

The results in this study were compared with those in Kong and Singh (2009b) by determining the SGF penetration front profile for their image of a carrot soaked in SGF (pH 1.8-2.0) for 20 minutes. Contrary to visual inspection, the SGF had fully penetrated the carrot sample, in that there was a dramatic drop in red color density near the center of the carrot. While the SGF had traveled to the center of the carrot sample, the color density was not uniform and there was a higher concentration of methylene blue at the center and near the boundary of the carrot samples. This is consistent with our observations of carrot samples soaked in AW at pH 1.5 [Figure 3.3a] and pH 2.0 under identical experimental conditions.

The diffusion rates between food matrices were different [Figure 3.5]. After ten minutes of soaking, the distance at which the AW concentration reached 50% was significantly different between Edam cheese and carrot at pH 1.5 and pH 7.0 ($P < 0.001$); the distance at which the AW concentration reached 50% for carrot was approximately 3 times greater than Edam cheese at pH 1.5 and approximately 1.4 times greater than Edam cheese at pH 7.0. This may be attributed to the difference in water content, protein content and protein type between the two food matrices.

The high water content of carrot ($\approx 90\%$, or 2.2 times greater than Edam) would facilitate the diffusion of AW within the carrot. The protein content of Edam (26.4%)

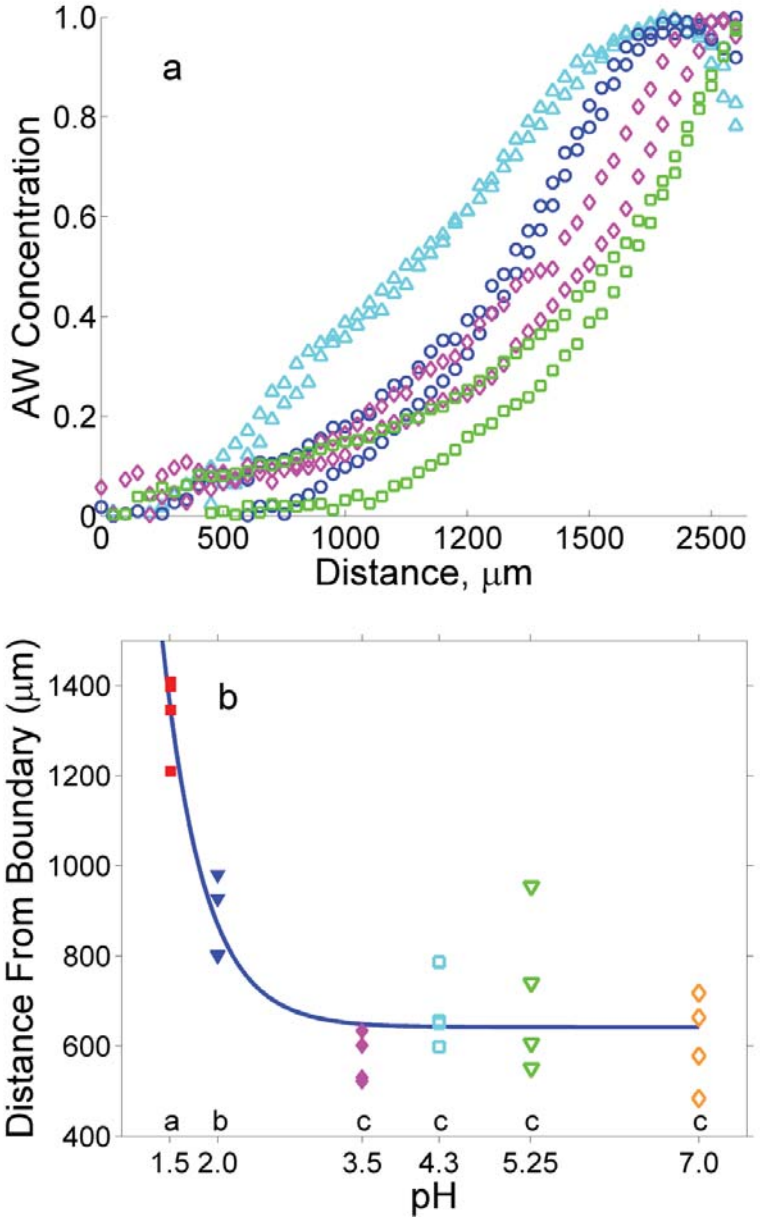

Figure 3.4 (a) AW concentration as a function of distance (μm) from the center of partially digested carrot, after 10 minutes, at pH 1.51 (blue triangle), pH 2.00 (purple circle), pH 4.30 (pink diamonds), and pH 7.00 (green squares). (b) Distance (μm) at which the AW concentration reaches 50% for carrot samples soaked in AW for 10 minutes, at pH 1.51 (solid square), 2.00 (solid triangles), 3.50 (solid diamonds), 4.30 (open square), 5.26 (open triangles) and 7.00 (open diamonds). The nonlinear regression model (Eq. 3.5) is represented by the curve. The different letters a, b, and c denote significant differences in mean values as determined by one-way ANOVA ($P < 0.001$).

may restrict the diffusion of gastric fluid as a result of coagulation of proteins. Guo (1995) demonstrated that casein coagulates at pH between 3-4, restricting the susceptibility of these proteins to proteolysis by pepsin. This coagulation of proteins, may also be the reason that cheese has been shown to provide a good conduit for probiotic delivery (Sharp et al 2008), as the coagulation of casein may hinder the gastric fluid from diffusing into the food matrix, preserving the bacteria during gastric digestion. The freezing of the Edam prior to sampling may also have resulted in cellular damage. Such damage could potentially increase the rate at which the AW penetrated the cheese, which would result in an even greater difference between carrot and Edam if the Edam had not been frozen prior to sampling. Given the number of usable samples of Edam cheese (as a result of conformational changes and fissures in the food material), a significant effect of pH on the distance at which the AW reached 50% in Edam cheese was unable to be determined.

3.4.3. Choice of Effective Diffusion Coefficient

As in the work by Davey et al (2002), the sum of exponentials equation (Gomi et al 1996, Gomi et al 1998) did not improve the fit of the AW penetration front. Additionally, Eq. 3.1 was compared to a power law function (Yamamoto 1999) and it was found that the power law function did not describe the water penetration front better than the exponential equation. Although the exponential description of the effective diffusion coefficient resulted in the best fit for the AW penetration front for both the carrot and Edam cheese [Figure 3.5], the exponential function did not adequately describe the AW concentration at the boundary of the samples. The lack of uniformity at the boundary of the carrot and Edam cheese samples, as well as the additional attached frozen AW, generated difficulties in determining the concentration of AW at the actual boundary of the samples [Figure 3.3]. As described previously, to account for

the lack of symmetry of the cut sample it was assumed that the maximum concentration of AW was the minimum value of the mean red color density near the boundary. This may provide an underestimate of the AW near the boundary of the sample. If this were the case, then the exponential equation would provide an even better description of the data. If there is a leveling off in the AW near the boundary of the sample, and this behavior is not an artifact, then the Maxwell-Stefan model (Krishna and Wesselingh 1997, Payne and Morison 1999, Verschueren et al 2007) may provide a better description of this behavior; however, this would be at the expense of having a considerably greater number of model parameters.

The fit of the model (Eq. 3.3 with Eq. 3.1) to the carrot data resulted in an R^2 value of 0.99 at both pH values, and R^2 = 0.99, 0.98 for the model fit to the cheese data at pH 1.5 and pH 7, respectively. The high R^2 values determined by comparing the model fit to the experimental data emphasizes the accuracy of the model and further demonstrates the dependence of the diffusion coefficient on the concentration of fluid diffusing into the food particle (Eq. 3.1).

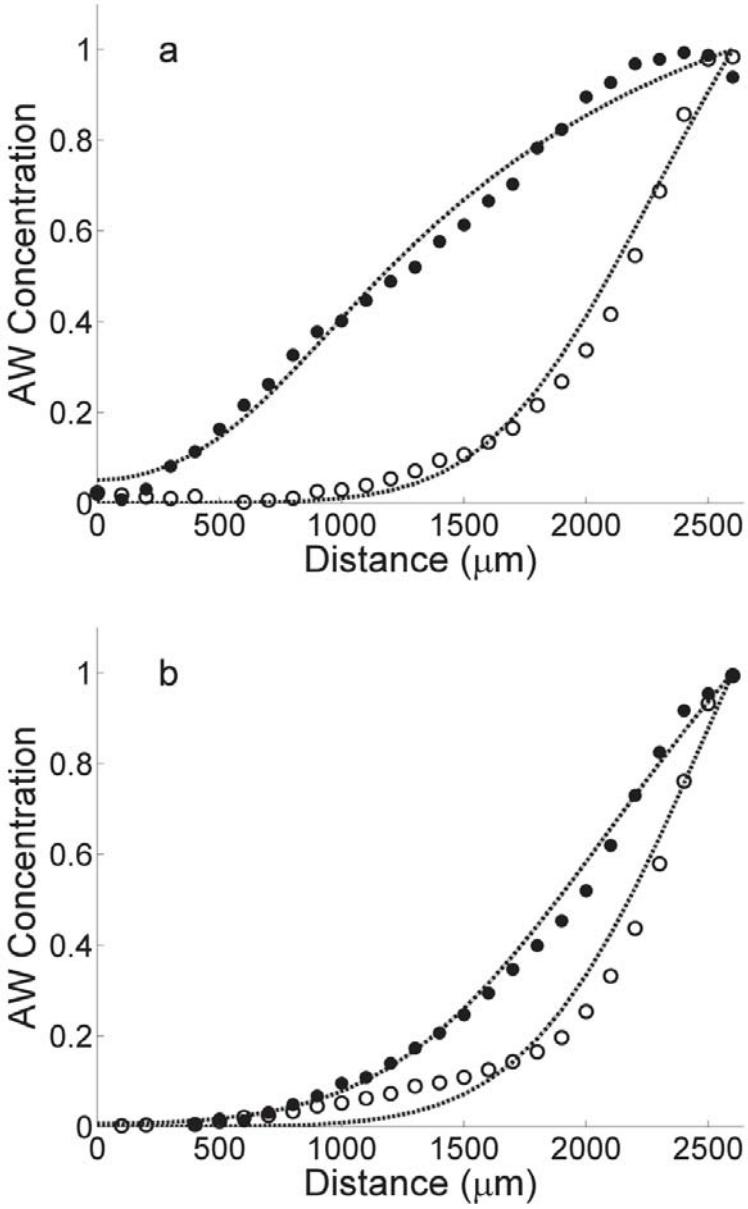

Figure 3.5 Acidic water penetration front profiles for carrot (solid circles) and Edam cheese (open circles) soaked for 10 minutes at pH 1.51 (a) and at pH 7 (b). The model fit (Eq. 3.1, 3.2, and 3.4) for individual profiles is denoted by the dotted curves.

3.4.4. Effective Diffusion Coefficient and Relation to pH in Carrot

In order to determine the distribution in the model parameters, a Markov chain Monte Carlo (MCMC) analysis on the combined AW penetration front profiles was performed (Gilks et al 1996, Shorten et al 2004). From the MCMC analysis, the relationship between pH and the coefficients of the diffusion model (Eq. 3.1) were then determined by fitting a nonlinear regression model using maximum likelihood (Eqs. 3.6 and 3.7):

$$A = -9.997 \times 10^{-10-0.2339[pH]} + 8.091 \times 10^{-10} \qquad 3.6$$

$$b = 20.55 \times 10^{-0.641[pH]} \qquad 3.7$$

where the units of A are m^2s^{-1}, and the parameter b is dimensionless [Figure 3.6].

The relationship between pH and b implies that the diffusion coefficient is dependent upon the AW concentration for pH < 3.5 and that for pH $\geq$ 3.5 the diffusion coefficient is constant. Additionally, the relationship between pH and A shows that the diffusion coefficient is dependent upon the AW concentration for pH < 3.5 and is relatively constant for pH $\geq$ 3.5.

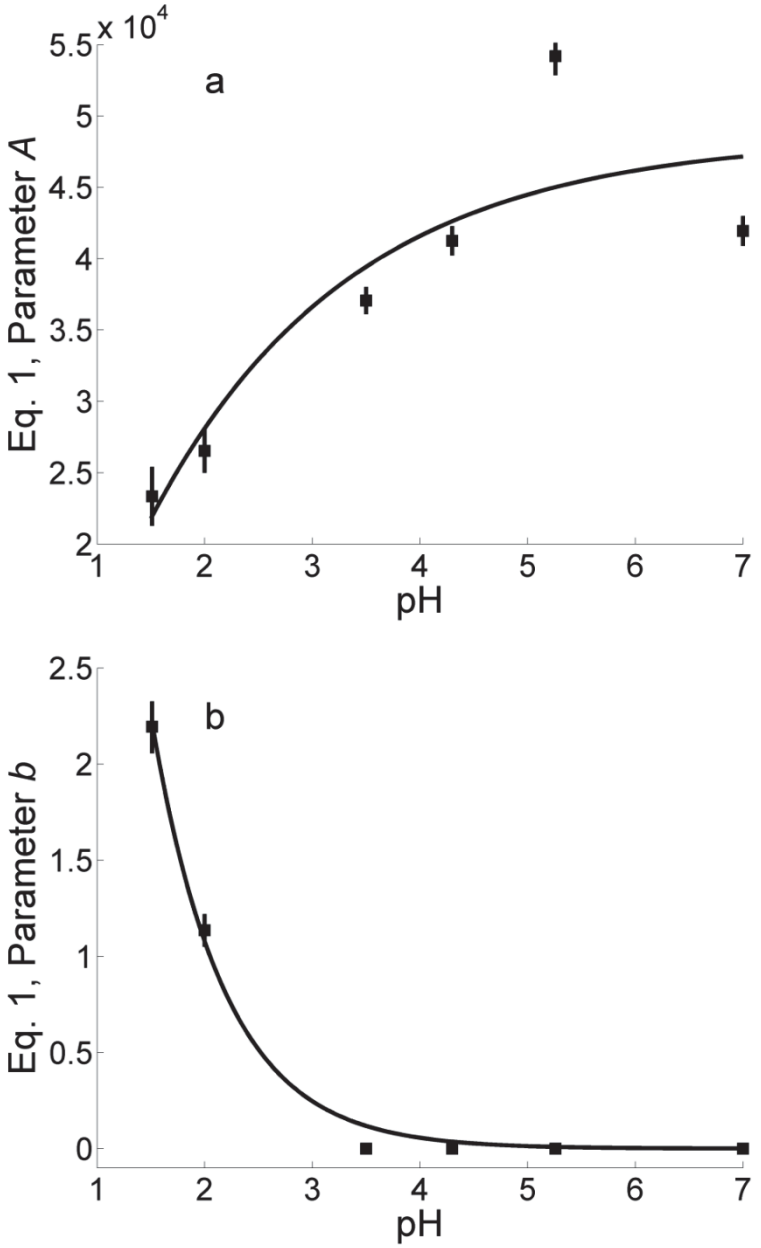

Figure 3.6 Estimated parameters *A* and *b* (squares), with standard error of the mean, for the EDC Eq. 3.1 based on least squares best fit of multi-response data. The model description (curves, Eqs. 3.6 and 3.7, respectively) of the relationship between the parameter and pH is consistent with Figure 3.4b.

3.4.5. Bioaccessibility Model

The food particle experiences acidic hydrolysis and subsequent solid loss in the region where the SGF permeates (Kong and Singh 2009b, Tydeman et al 2010). Therefore, the model proposed here assumes that the rate at which the density of the dry food particle, $\rho(r)$, changes is proportional to the AW concentration, θ, and the density at radius *r* and time *t*:

$$\frac{\partial \rho}{\partial t} = -k\theta\rho \qquad 3.8a$$

$$\rho(r, t=0) = n\rho_0 \qquad 3.8b$$

$$\frac{\partial \rho(r=0,t)}{\partial t} = \frac{\partial \rho(r=R(t),t)}{\partial t} = 0 \qquad 3.8c$$

where *k* is the rate of food degradation and the ratio of dry sample weight at time *t*, $S(t)$, to the initial dry weight of the sample, S_0 is

$$\frac{S(t)}{S_0} = \frac{2\pi L_0}{S_0}\int_0^{R(t)} r\rho dr + (1-n) \qquad 3.9$$

where L_0 is the initial length of the sample, *R*(*t*) is the radius of the sample at time *t* and *n* is the expected percentage solid loss after a long period of soaking in gastric fluid (i.e. the proportion of non-degradable food matrix).

In order to validate the model, the model, incorporating the diffusion coefficients found for the relative pH values, was compared to the work by Kong & Singh (2011). As in our work, the data reported by Kong & Singh (2011) was for raw carrot (Fanbin Kong, pers. comm.). While Kong & Singh (2011), used SGF rather than AW for their experiment, the aforementioned work and previous work have shown that the addition of pepsin and mucin did not affect the solid loss of raw carrot (Kong and Singh 2009b, Kong and Singh 2011). As shown in Figure 3.7, the above model characterizes the expected solid loss at constant pH. Thus, rather than two distinct

diffusion coefficients, as described previously by Kong & Singh (2011), this work demonstrates that the expected solid loss is dependent on the concentration of AW and the available degradable food matrix. Our observed effect of pH on the propagation of the AW wetting front explains a component of the measured solid loss at constant pH. Additionally, within the region of the carrot samples where the SGF had traversed, significant cell separation and cell rupture had occurred (Kong and Singh 2009b, Tydeman et al 2010). One may therefore interpret the decreased rate of solid loss at pH 1.8 after 1 hour of soaking in SGF (Kong and Singh 2011) as insoluble solid loss, or cellular loss, rather than soluble solid loss.

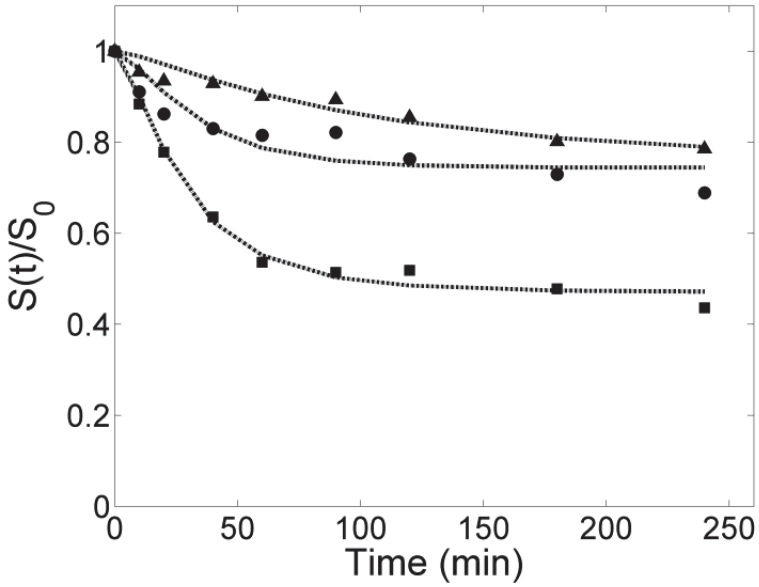

Figure 3.7 Solid loss of carrots at fixed pH of 5.3 (triangles), 3.5 (circles) and 1.8 (squares) (Kong and Singh 2011) and model fit (Eqs. 3.8 and 3.9) for the same fixed pH (curves).

The pH of the contents within the human stomach is not static. Figure 3.8 describes the change in pH from ten minutes to 4 hours after the ingestion of a meal composed of coarsely ground tenderloin steak, cooked and seasoned with salt, white

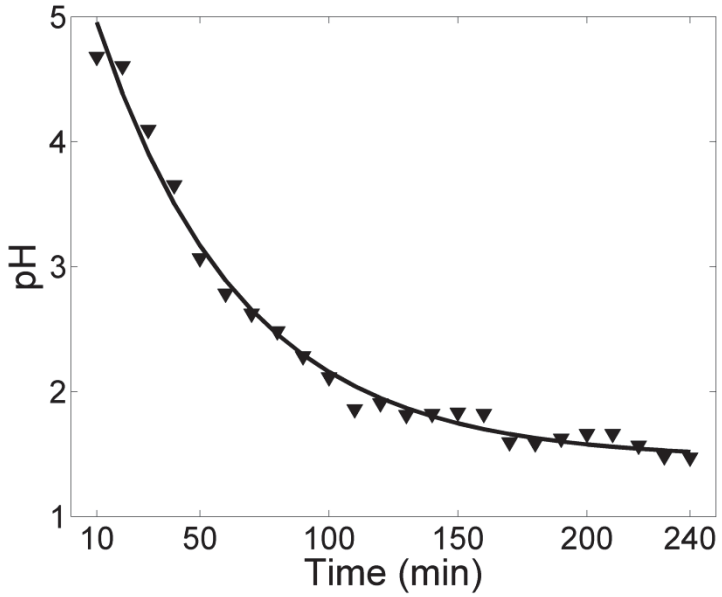

Figure 3.8 pH of human gastric contents at ten minute intervals (triangles) using data taken from Malagelada et al (1976), and best fit exponential equation (Eq.3.10, curve).

bread with butter, vanilla ice cream topped with chocolate syrup and a glass of water (Malagelada et al 1976). This change in pH, relative to time, is described in this work with an exponential function, which is biologically relevant to the data:

$$pH = 4.179\exp\left(-0.0179\,t\right)+1.4613 \qquad 3.10$$

where $t=0$ corresponds to 10 minutes after the ingestion of the meal. The type of meal ingested will have a marked effect on the pH of the stomach. For example, meals that are primarily vegetarian or vegan will be less acidic than meals which include meat. Therefore, Eq. 3.8 may not be suitable to describe all possible meal combinations. Additionally, this equation assumes that the pH of the gastric contents is uniform throughout the stomach.

Taking into consideration the change in gastric pH over time one would expect that the rate of solid loss of the carrot core would be slower initially, when pH is high, and then increase as the pH decreases. Figure 3.9 shows the solid loss of carrot core,

relative to the initial weight of a dry carrot core, at pH 1.8 as shown previously in Kong and Singh (2011) as well as our model prediction for the dynamic pH in Figure 3.8. It was assumed that $\rho_0 = 5.07 \times 10^{-12}$ g μm^{-3} (Selman et al 1983) and $n = 0.54$ in the model (Eqs. 3.8-3.9). This simulation demonstrates that the rate of solid loss is initially slower and increases as the gastric pH decreases.

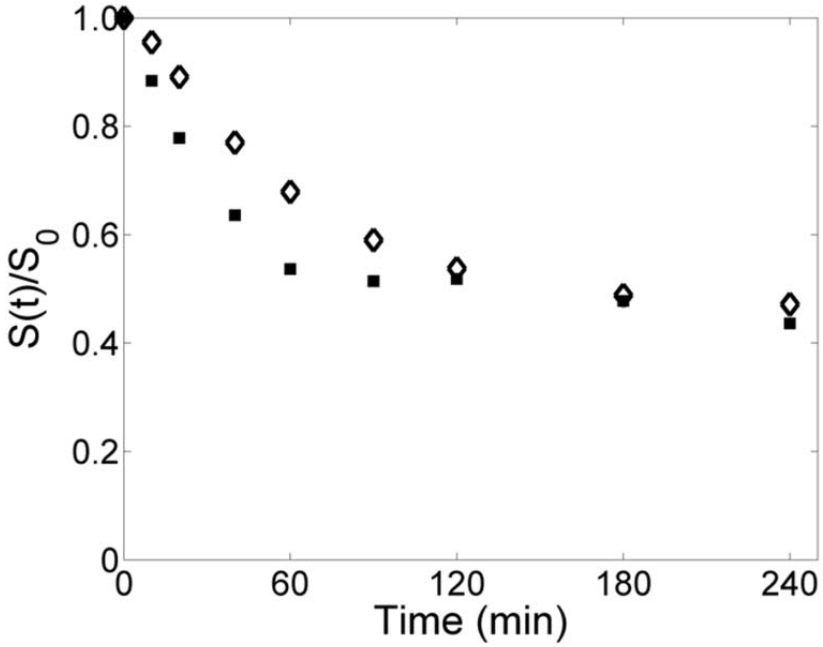

Figure 3.9 Carrot core solid loss at fixed pH of 1.8 (squares) (Kong and Singh 2011) and predicted carrot core solid loss determined by the variation of gastric pH over time in Figure 3.8 (diamonds).

3.5. Concluding Remarks

The effect of pH on the acidic hydrolysis of food solids within the human stomach is of importance as it is one of the factors regulating satiety and the release of nutrients into the stomach for absorption in the small bowel. Additionally, acidic hydrolysis within the stomach damages the cell surface of indigestible starch and fiber

which allows access for bacterial enzymes, and the growth of bacterial biofilms on the plant surface later in the small and large bowel. This work has shown that the diffusion of gastric fluid into a food particle is pH dependent, and will depend upon the food structure as demonstrated by the different penetration front profiles between raw carrot core and Edam cheese. Other factors no doubt play a role in the diffusion of gastric fluid into a food particle.

Additional studies are required to determine the exact relationship between pH and the efficacy of different enzymes in the gastric fluid. Such studies must use foods with low fat, as the fat content may hinder proteolysis within the stomach. Given that fat is primarily digested in the small bowel, additional studies determining the effects of fat content on gastric digestion would also be of great value.

The model here may be used to investigate the effects of pH on food structures, which may help to improve the functionality of novel foods. Future work may extend this model to include enzymatic reactions, change in temperature of the food bolus during the digestive period, and mechanical forces such as the fluid dynamics and peristaltic contractions which have a significant effect on the erosion and fragmentation of food particles. However, additional experimental work is required for such models to be constructed.

Chapter 4 Monoculture Parameters Successfully Predict Coculture Growth Kinetics of *Bacteroides thetaiotaomicron* and Two *Bifidobacterium* Strains

4.1. Abstract

Microorganisms rarely live in isolation, but are most often found in a consortium. This provides the potential for cross-feeding and nutrient competition among the microbial species, both of which make it challenging to predict growth kinetics in coculture because the number of interactions increases factorially with the number of bacteria considered. In this paper a previously developed mathematical model to describe substrate consumption and subsequent microbial growth and metabolite production for bacteria grown in monoculture was modified. The model was used to characterize substrate utilization kinetics of 18 *Bifidobacterium* strains. Some bifidobacterial strains demonstrated preferential degradation of oligofructose in that the bacterium completely metabolized sugars with low degree of polymerization (DP) (DP ≤ 3 or 4) before metabolizing sugars of higher DP, or vice versa. Thus, the model was extended to describe the preferential degradation of substrate. In addition, the model was adapted to describe the competition between *Bacteroides thetaiotaomicron* LMG 11262 and *Bifidobacterium longum* LMG 11047 or *Bifidobacterium breve* Yakult for inulin as well as cross-feeding of breakdown products from the extracellular hydrolysis

of inulin by *B. thetaiotaomicron* LMG 11262. This study demonstrated that coculture growth kinetics could be predicted based on the respective monoculture growth kinetics. Using growth kinetics from monoculture experiments to predict coculture dynamics complements data obtained from *in vitro* experiments and may reduce the number of *in vitro* experiments required to parameterize multi-culture models.

4.2. Introduction

Commensal intestinal bacteria have been found to have a substantial impact on not only intestinal health, but the overall health of the host. The primary SCFA produced by the commensal bacteria are butyrate, acetate and propionate. Butyrate provides an energy source for the intestinal epithelial cells, improves the mucosal integrity of the intestinal wall, and regulates gene expression and cell growth (Macfarlane and Cummings 1991, Nepelska et al 2012). The role of SCFA in human health is not restricted to the intestinal tract. Acetate is utilized as an energy source by the heart, brain and skeletal muscles (Macfarlane and Cummings 1991). Propionate enhances satiety by regulating hormones responsible for stomach emptying and appetite and is associated with the inhibition of cholesterol, triglyceride and fatty acid synthesis in the liver (Hosseini et al 2011); the effects suggest that propionate may play a significant role in obesity in humans. SCFA production is a result of bacterial fermentation of food that has not been digested and absorbed in the small bowel.

Commensal intestinal bacteria are primarily saccharolytic and metabolize resistant starch and indigestible non-starch oligosaccharides and polysaccharides. Some bacteria are able to utilize proteins and lipids that escape digestion or absorption in the small bowel; however the amount of protein that reaches the large bowel is only one-fifth that of carbohydrates (3-9 g/day verses 8-40 g/day, respectively) (Macfarlane and

Cummings 1991). It has been reported that less than ~0.001% of the commensal bacteria are capable of metabolizing the 5-10% of the bile acids which escape re-absorption in the distal ileum (0.3-0.6 g/day) (Begley et al 2006, Jones et al 2004, Ridlon et al 2006). The high proportions of carbohydrates which enter the large bowel, as compared to proteins and lipids, has led to an enteric colonic bacterial population more suited to metabolizing resistant starch and non-starch polysaccharides.

Given that the commensal bacteria readily metabolize dietary fibers, products such as inulin and oligofructose are commonly used food ingredients in "functional foods". Neither inulin nor oligofructose are hydrolyzed in the stomach or absorbed in the small bowel, yet they are completely fermented by the commensal bacteria in the large bowel (Cherbut 2002, Ramnani et al 2010). *In vivo* studies have shown that inulin and oligofructose have a bifidogenic effect, or increase the number of certain *Bifidobacterium* species, and in many cases there is also an increase of *Lactobacillus* (Bouhnik et al 1999, Costabile et al 2010, Gibson et al 1995, Meyer and Stasse-wolthuis 2009, Ramnani et al 2010). Given the bifidogenic effect of fructans, *Bifidobacteria* are often combined with fructans as a synbiotic because of their beneficial effects to the host; however, *in vitro* studies have shown that many *Bifidobacteria* are unable to break down and metabolize sugars with a degree of polymerization (DP) greater than 8 (Falony et al 2009b, Rossi et al 2005). Given that bacteria do not live in isolation, but are often found as mixed species biofilms (Macfarlane and Macfarlane 2006), the bifidogenic effect of fructan prebiotics may be a result of microbial cross-feeding (Falony et al 2009a).

Only a few coculture experiments that specifically characterized bacterial cross-feeding and nutrient competition have been reported (Falony et al 2006, Falony et al 2009a) and often do not report the bacterial growth, metabolites and substrate

degradation associated with each strain during coculture (Belenguer et al 2006, Chassard and Bernalier-Donadille 2006, Degnan and Macfarlane 1995, Duncan et al 2004). These data are essential to determine bacterial interactions and the parameter values for macroscopic mathematical models of interacting microbial populations. Furthermore, there are currently few mathematical models that describe either bacterial cross-feeding or nutrient competition.

Wintermute and Silver (2010) proposed a simple dynamic model to describe the level of cooperation between two auxotrophic *Escherichia coli* mutants. This model was a slight simplification of a model described by Bull and Harcombe (2009), in that the model did not allow for the growth of the individual species in the absence of cross-feeding or cooperation. However, neither model was suitable for explicitly describing and understanding the nature of the interactions between microbial populations because they did not incorporate the mechanisms that influence those interactions.

At present there are a few published models that have extended the microbial population model of Baranyi and Roberts (1994) to include the effects of mechanistic processes, such as metabolite production and subsequent pH changes that may limit microbial growth (Janssen et al 2006, Poschet et al 2005, Van Impe et al 2005). These models did not incorporate substrate limitations, which is a key factor in mono- and coculture microbial growth. A dynamic, mechanistic model has been proposed to demonstrate bacterial growth (determined by optical density) and the subsequent butyrate production as a result of lactate utilization (Muñoz-Tamayo et al 2011), however this model did not incorporate either the bacterium that produced the lactate or the substrate hydrolyzed by the lactate-producing bacterium.

This work is motivated by the hypothesis that a mathematical model of microbial growth can be used to predict coculture growth kinetics based on monoculture

growth kinetics. Here, the aim is to develop a model that draws upon the previously proposed dynamic, mechanistic mathematical model of Amaretti et al (2007) to describe the mechanisms for substrate consumption and subsequent microbial growth and metabolite production for bacteria grown in monoculture. This model was extended to describe the preferential degradation of oligofructose for monoculture microbial growth. Finally, the model was adapted to describe competition between two bacterial species for a particular substrate as well as cross-feeding resulting from the breakdown products of extracellular carbohydrate hydrolysis by one of the bacterial species. This competitive/cross-feeding model incorporates the primary metabolites produced by both bacterial species. This model was used to explore and predict the growth dynamics between *Bacteroides thetaiotaomicron* LMG 11262 and *Bifidobacterium longum* MG 11047 and *B. thetaiotaomicron* LMG 11262 and *Bifidobacterium breve* Yakult as compared to experimental coculture data.

4.3. Materials and Methods

4.3.1. Monoculture and Coculture Bacterial Data

The experimental work reported by Falony and colleagues provided the data required to estimate the model parameters for monocultures. The data were obtained from the graphical representation using automatic image capturing software. The degradation of fructose, oligofructose (OraftiP95; BENEO-Orafti NV, Tienen, Belgium) and inulin (OraftiHP; BENEO-Orafti) in monoculture by *B. thetaiotaomicron* LMG 11262 (Falony 2009, Falony et al 2009a) and 10 *Bifidobacterium* species constituting 18 strains was investigated by Falony et al (2009b). These authors then extended their work by exploring the competitiveness of various *Bifidobacterium* species in coculture with *B. thetaiotaomicron* LMG 11262 where inulin (OraftiHP) was included as the

carbohydrate substrate (Falony et al 2009a). All substrate quantities reported in the aforementioned work were in fructose equivalents (FE).

All fermentations were conducted in 2-1 Biostat B-DCU fermenters (Sartorius AG, Göttingen, Germany) containing 1.5 l of medium for colon bacteria, developed by Van der Meulen et al (2006b) supplemented with 50 mM FE of either fructose, oligofructose or inulin as the energy source. The average DP of oligofructose was 4 and the average DP of inulin was greater than 23, which implies this would be approximately 12.5 mM of oligofructose and 2 mM of inulin. Continuous sparging of the medium with a mixture of 10% CO_2 and 90% N_2 (Air Liquide, Paris, France), ensured anaerobic conditions. Fermentation temperature and pH were kept constant at 37°C and pH of 6.3, which was controlled automatically online (MFCS/win 2.1; Satorius). A gentle, continues stirring of 100 rpm was also controlled online to keep the medium homogenous (Falony et al 2009a, Falony et al 2009b).

4.3.2. Mechanistic Model for Bacterial Growth in Monoculture

To determine the model parameters, the mechanistic model described by Amaretti et al (2007) was both simplified and modified. First-order kinetics was substituted for the Monod equation used in Amaretti et al (2007) due to the low concentrations of substrates, S (mM FE), used in the experimental work (Falony et al 2009a, Falony et al 2009b). Thus, in the equations below, η (h mM FE)$^{-1}$ represents the maximum specific growth rate divided by the Monod constant. Additionally, metabolites such as acetate, lactate, formate or succinate were assumed to be produced at a rate proportional to the rate of substrate degraded by the bacterial population; hence, metabolites are produced as a result of microbial growth and maintenance. The model is

$$\frac{dS_T}{dt} = -\frac{\eta}{Y_{X/S}} 10^B S_T - m10^B \quad 4.1a$$

$$\frac{dB}{dt} = \frac{1}{\ln(10)}(\eta S_T - k_d) \quad 4.1b$$

$$\frac{dP_i}{dt} = -k_i \frac{dS_T}{dt} \quad 4.1c$$

where $B = \log_{10} X$ [where X is the bacterial population density (CFU/ml)], $Y_{X/S}$ (CFU/ml (mM FE)$^{-1}$) is the yield of bacteria X from substrate S_T (mM FE), m $\left(\text{mM FE (h CFU/ml)}^{-1}\right)$ is the rate that the bacteria utilize the fructose equivalents for cell maintenance, k_d (log(CFU/ml) h^{-1}) is the cellular death rate (or equivalently the rate of reduction of bacteria due to either cell lysis or quiescence/unculturablility), and k_i (mM (mM FE)$^{-1}$) characterizes the rate of production of the i^{th} metabolite, P_i (mM), from substrate utilization.

This system of equations assumes that the bacteria can completely metabolize the substrate; however, in the case of oligofructose and inulin, many of *Bifidobacterium* species are unable to degrade long chain polysaccharides (De Vuyst and Leroy 2011, Falony et al 2009b). To account for the inability of some bacterial species to fully degrade the model substrate, the total substrate $S_T(t) = S_U + S(t)$ was defined to be the sum of undegradable $\left(S_U = (1-a)S_T(0)\right)$ and degradable $\left(S(0) = aS_T(0)\right)$ fractions, where a is the fraction of the substrate that the bacterium is capable of utilizing within the 48-hour experimental period and $S_T(0)$ is the total initial concentration of substrate.

Based on our definition of the total substrate,

$$\frac{dS_T}{dt} = \frac{dS_U}{dt} + \frac{dS}{dt}.$$

However, the undegradable portion, S_U, does not change over time. Thus, $dS_U/dt = 0$ and Eq. 4.1a-c becomes:

$$\frac{dS}{dt} = -\frac{\eta}{Y_{X/S}} 10^B S - m10^B;\ S(0) = aS_T(0) \quad 4.2a$$

$$\frac{dB}{dt} = \frac{1}{\ln(10)}(\eta S - k_d) \quad 4.2b$$

$$\frac{dP_i}{dt} = -k_i \frac{dS}{dt} \quad 4.2c$$

$$S_T(t) = S_U + S(t) \quad 4.2d$$

The model was fit to the multi-response data (bacteria, substrate and metabolite concentrations) using nonlinear regression (Bates and Watts 2007). In the fitting procedure, bacterial population measurements were $\log_{10}$ transformed to ensure that the model residuals were homoscedastic (i.e., the variance of the variables is homogeneous). The residual matrix $\mathbf{Z}=\mathbf{Y}-\mathbf{H}(\boldsymbol{\Theta})$ was formed using the n×m observation matrix $\mathbf{Y}$ (i.e., the experimental data, including the $\log_{10}$ transformed bacterial population values) and the n×m response matrix $\mathbf{H}(\boldsymbol{\Theta})$ (i.e., model values) defined by either Eq. 4.2, Eq. 4.3 or Eq. 4.5 (where n is the number of times that response variables were measured, m is the number of measured response variables and $\boldsymbol{\Theta}$ is the vector of unknown model parameters: $Y_{X/S}$, η, m, k_d and k_i with $i = 1 \text{or } 2$). The variances of the deviations in measurements within response variables were assumed to be constant and independent, but variances in measurement deviations were allowed to be different between response variables. Based on this assumption, the product of the diagonal of the square matrix $\mathbf{Z}^\mathbf{T}\mathbf{Z}$ was minimized**,** where the i^{th} entry in the diagonal of $\mathbf{Z}^\mathbf{T}\mathbf{Z}$ is the sum of the squared residuals for the i^{th} differential equation. Different assumptions about the measurement deviations result in different fitting criterions (Bates and Watts 2007). For example, if the variance in measurement deviation is the same between

response variables then the appropriate fitting criterion would be to minimize the sum of the diagonal of the square matrix $\mathbf{Z^TZ}$. This procedure ensures that the estimated model parameters are independent of the scale of measurement (Pell and Kowalski 1991) and ad-hoc transformations of the data to ensure that the variance in the measurement deviations in the response variables are similar (Amaretti et al 2007) are not required. Improper assumptions about the measurement deviations (i.e. that they are the same for each response variable) can result in biased parameter estimates and invalid inference. This is important because the bacterial population as measured by viable counts (CFU/ml) on a $\log_{10}$ scale varied between 5 and 11, whereas the concentrations of nutrients and metabolites produced varied between 0 and 120 (mM).

All differential equations were solved using ode15s in MATLAB (The MathWorks; www.mathworks.com). To determine the standard errors in the model parameters, a Markov chain Monte Carlo (MCMC) analysis was performed (Gilks et al 1996, Shorten et al 2004) in MATLAB.

4.4. Results and Discussion

4.4.1. Model Fit to Monoculture Data

Eqs. 4.2a-d adequately described the degradation of inulin and subsequent growth of bacteria and production of metabolites for all 18 bifidobacterial strains and *B. thetaiotaomicron* LMG 11262 reported by Falony (2009) and Falony et al (2009b) [Figure 4.1]. The residuals between the model fit and the experimental data were normally distributed with standard deviations for inulin consumption, bacterial growth and acetate production of 1.35 mM FE, 0.17 log(CFU/ml) and 2.31 mM, respectively. The cumulative R^2 values (all 19 strains) for the model fit to inulin consumption,

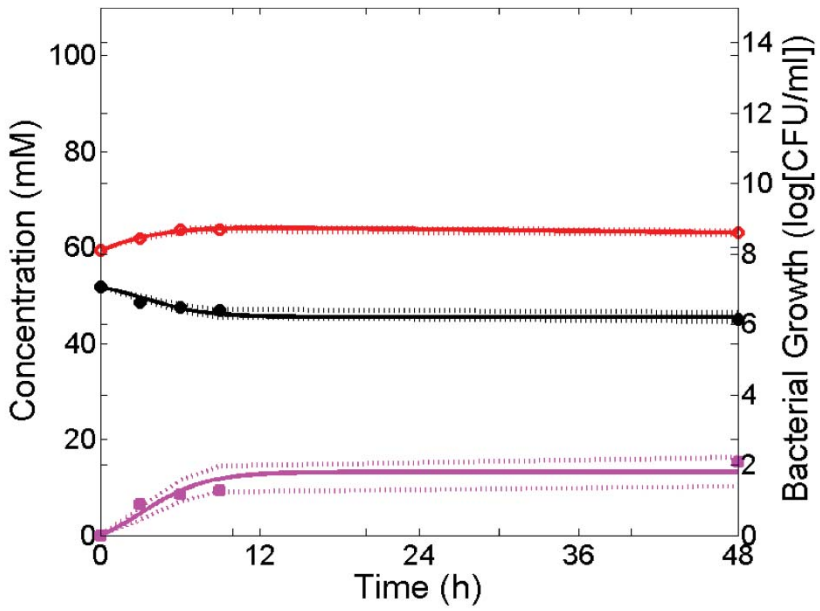

Figure 4.1 Model fit (Eqs. 4.2a-d) (solid lines) to *Bifidobacterium catenulatum* LMG 1043 growth (red circles) from inulin hydrolysis (black solid circles) and subsequent acetate (magenta solid squares) and lactate (cyan open squares) production (Falony et al 2009b). Ninety-five percent confidence intervals are denoted by dotted lines.

bacterial growth and acetate production were 0.98, 0.96, and 0.94 respectively, demonstrating the goodness of fit for the model to the data.

The model estimates the percentage of inulin utilized by the bacterial strain within 48 hours. Based on the experimental data (Falony et al 2009b), it appeared that OraftiHP contained inulin with a DP ranging from 1 to 65. Most of the bifidobacteria strains degraded the inulin fractions simultaneously or preferentially, starting with inulin fractions with low DP before utilizing fractions of higher DP. Thus, this model provides the upper limit of the DP that the bacterial strain can degrade provided the distribution of the particular DPs are known.

The model (Eqs. 4.2a-d) also adequately described the bifidobacterial growth, substrate degradation and metabolite production when bifidobacteria were grown with

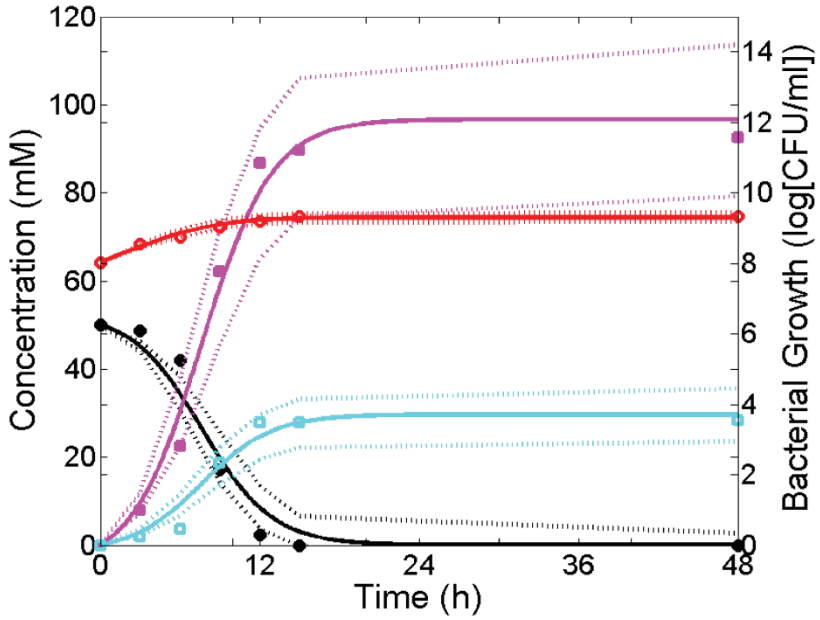

Figure 4.2 Model fit (Eqs. 4.2a-d) (solid lines) to *Bifidobacterium adolescentis* LMG 10733 growth (red circles) fructose hydrolysis (black solid circles) and subsequent acetate (magenta solid squares) and lactate (cyan open squares) production (Falony et al 2009b). Ninety-five percent confidence intervals are denoted by dotted lines.

fructose as the substrate. The residuals between the model fit and the experimental data were normally distributed with standard deviations for fructose consumption, bacterial growth, acetate production and secondary metabolite production of 2.56 mM F, 0.73 log(CFU/ml), 3.29 mM and 1.72 mM, respectively. The cumulative R^2 values (bifidobacteria only) for the model fit to fructose consumption, bacterial growth, acetate production and secondary metabolite production were 0.99, 0.70, 0.99 and 0.99 respectively. In our model fit [Figure 4.2] only two of the metabolites were accounted for (acetate and formate or lactate), however the model can be extended to describe other measureable extracellular metabolites produced by the bacterium (data not shown).

The model could not describe the dramatic drop in bacterial counts between 9 and 15 hours as seen with both *Bifidobacterium bifidum* strains when grown with fructose [Figure 4.3a,b]; however the model predicted bacterial counts at the end of the experimental time (48 hours) that were consistent with the experimental data.

The model did not account for the high yield and growth rate from 0-9 hours when *B. gallicum* LMG 11596 [Figure 4.4a] and *B. angulatum* LMG 11039 were grown with fructose as the substrate. For these two strains very little substrate was depleted in the 9 hours of growth, which suggests that the actual number of initial bacteria may have been higher than what was reported by the authors (Falony et al 2009b). When the initial counts were increased by 1 log(CFU/ml), the model described the growth kinetics of both of these strains [Data shown for *B. gallicum* LMG 11596 only, Figure 4.4b.]. The standard deviation of the residuals after removing the four bacterial strains mentioned above were 2.80 mM fructose, 0.21 log(CFU/ml) bacteria, 3.58 mM acetate, and 1.81 mM secondary metabolite. The cumulative R^2 values (14 strains) were 0.99, 0.95, 0.99 and 0.99 for the fructose utilization, bacterial growth, acetate production and secondary metabolite production, respectively, demonstrating the goodness of fit of the model to the experimental data.

The model (Eqs. 4.2a-d) was also capable of describing bacterial growth kinetics where oligofructose was the substrate [Figure 4.5], except under circumstances where the substrate was degraded preferentially. The residuals between the model fit and the experimental data for the 13 strains that did not degrade the substrate preferentially were normally distributed with standard deviations for oligofructose consumption, bacterial growth, acetate production and secondary metabolite production of 3.49 mM FE, 0.18 log(CFU/ml), 3.87 mM and 2.15 mM, respectively. The cumulative respective R^2 values were 0.98, 0.96, 0.99 and 0.98.

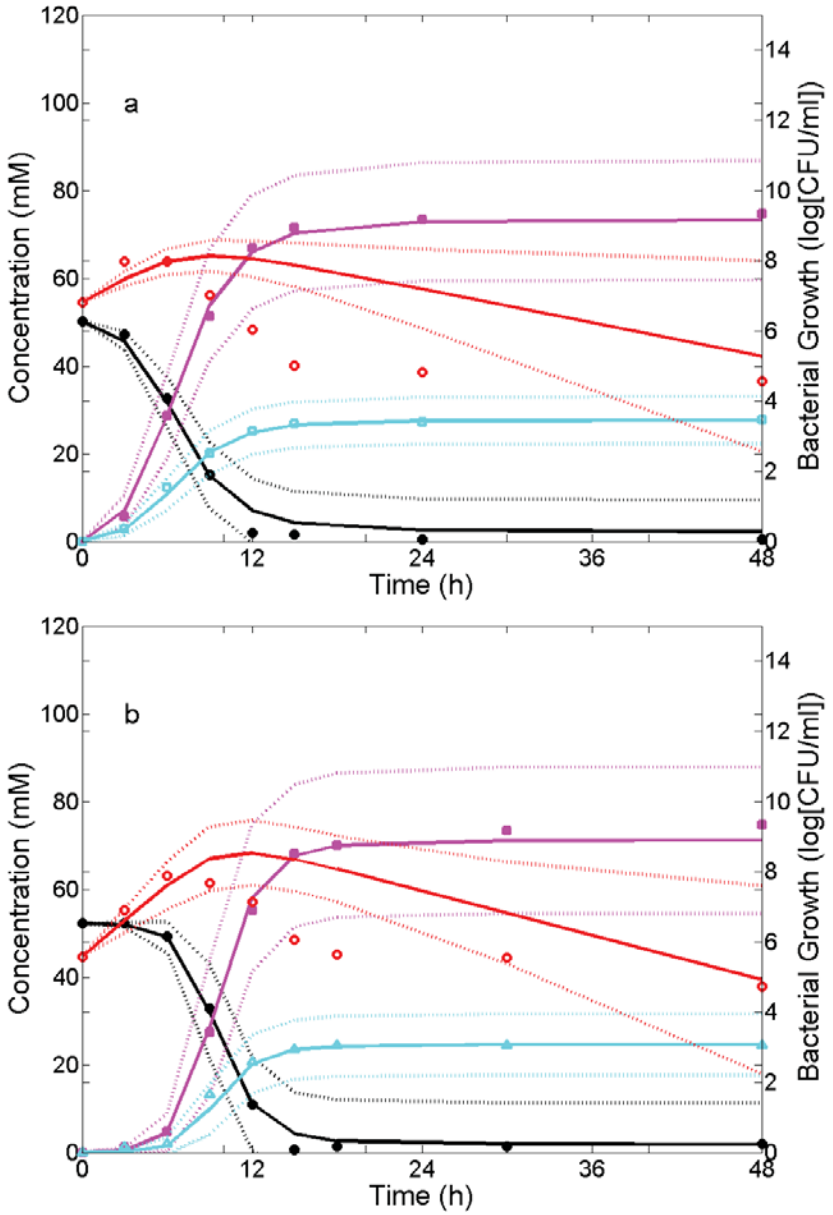

Figure 4.3 Model fit (Eqs. 4.2a-d) (solid lines) to bacterial growth (red circles) from fructose hydrolysis (black solid circles) and subsequent acetate (magenta solid squares) and lactate (cyan open squares) or formate (cyan open triangles) production. The bacteria represented here are (a) *Bifidobacterium bifidum* DSM 20082 and (b) *B. bifidum* LMG 11583, showing that the model cannot account for the dramatic drop in bacteria from time 9-18 hours yet can still account for the bacteria counts at the end for the 48 hour experimental period. Data found in Falony et al (2009b). Ninety-five percent confidence intervals are denoted by dotted lines.

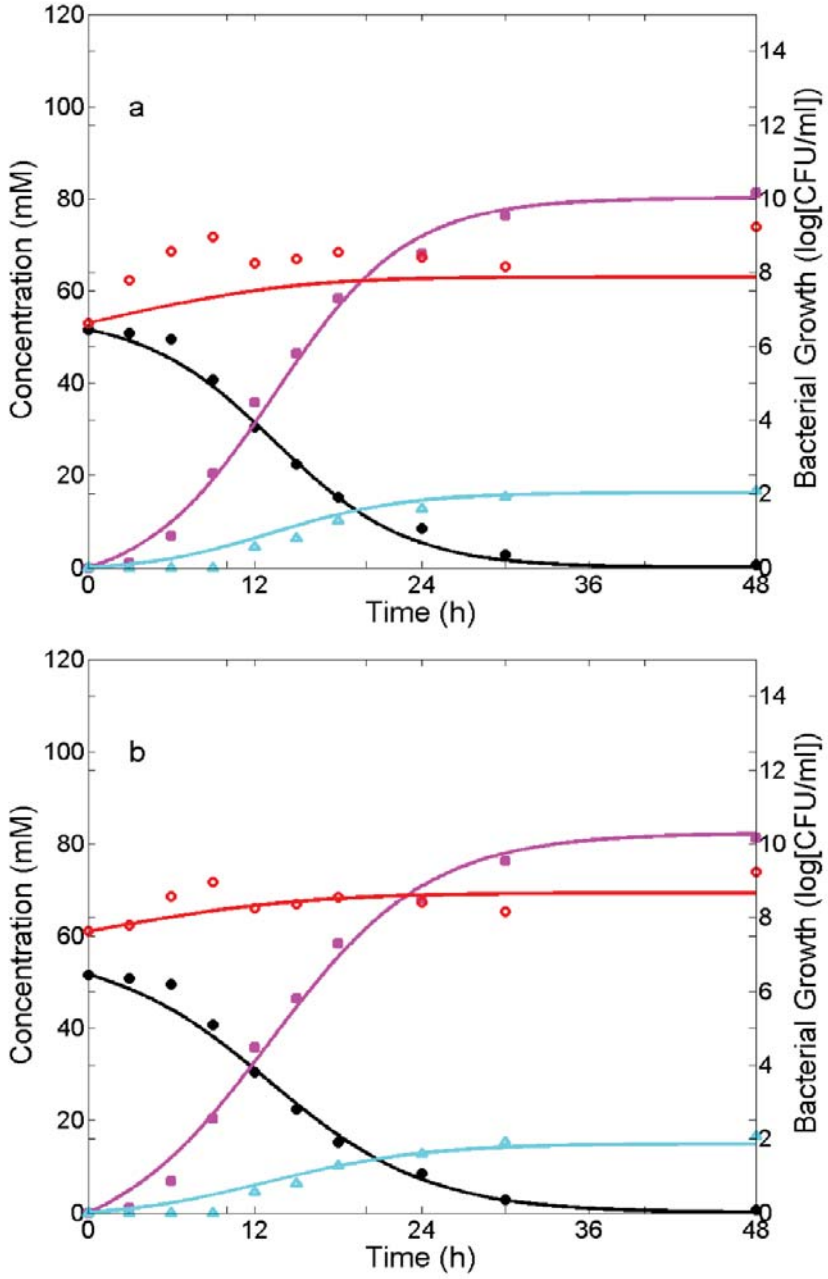

Figure 4.4 Model fit (Eqs. 4.2a-d) (solid lines) to *Bifidobacterium gallacum* LMG 11596 growth (red circles) from fructose hydrolysis (black solid circles) and subsequent acetate (magenta solid squares) and formate (cyan open triangles) production. (a) The model cannot account for the high yield during the initial 9 hours of the experiment (Falony et al 2009b), however an increase of the initial concentration of *B. gallacum* LMG 11596 by 1 log(CFU ml^{-1}) results in a good fit (b). Ninety-five percent confidence intervals are denoted by dotted lines.

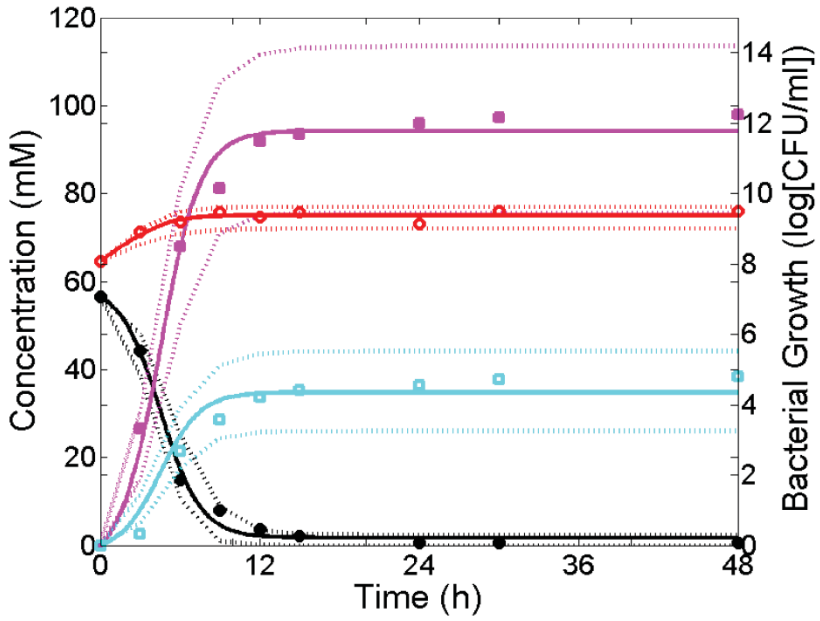

Figure 4.5 Model fit (Eqs. 4.2a-d) (solid lines) to *Bifidobacterium catenulatum* LMG 1043 growth (red circles) from oligofructose hydrolysis (black solid circles) and subsequent acetate (magenta solid squares) and lactate (cyan open squares) productions (Falony et al 2009b). Ninety-five percent confidence intervals are denoted by dotted lines.

When bacteria degrade oligofructose preferentially the model must be adjusted to describe the sequence of substrate utilization as shown in Eq. 4.3a-d:

$$\frac{dS_\alpha}{dt} = -\frac{\eta_\alpha}{Y_{X/S\alpha}} 10^B S_\alpha - m10^B \tag{4.3a}$$

$$\frac{dS_\beta}{dt} = \left(-\frac{\eta_P}{Y_{X/S\beta}} 10^B S_\beta - m10^B \right) H(c - S_\alpha) \tag{4.3b}$$

$$\frac{dB}{dt} = \frac{1}{\ln(10)} \left(\eta_\alpha S_\alpha + \eta_\beta S_\beta - k_d \right) \tag{4.3c}$$

$$\frac{dP_{\{\alpha,\beta\}}}{dt} = \sum_{i=\alpha,\beta} -k_i \frac{dS_i}{dt}. \tag{4.3d}$$

Here α and β represent the primary and secondary oligosaccharides or fermentation metabolites, respectively, and $H(c - S_\alpha)$ is the Heaviside function, where $H(c - S_\alpha) = 0$ if the concentration of the primary metabolite is greater than or equal to *c*, otherwise $H(c - S_\alpha) = 1$. As before, to account for the inability of some bacterial species to fully degrade the model substrate, the total substrate $S_T(t) = S_U + S(t)$ was defined to be the sum of undegradable $\left(S_U = (1 - a_\alpha - a_\beta)S_T(0)\right)$ and degradable $\left(S_\alpha(0) + S_\beta(0) = (a_\alpha + a_\beta)S_T(0)\right)$ fractions, where a_α and a_β are the fraction of the substrate that is degraded as a primary and secondary nutrient source, respectively, within the 48 hour experimental period and $S_T(0)$ is the total initial concentration of substrate.

The residuals between the model fit (Eq. 4.3a-d) and the experimental data for the five strains were normally distributed with standard deviations for oligofructose consumption, bacterial growth, acetate production and secondary metabolite production of 3.19 mM FE, 0.26 log(CFU/ml), 4.54 mM and 2.15 mM, respectively. The cumulative respective R^2 values were 0.98, 0.95, 0.98 and 0.97. In this analysis the strain *Bifidobacterium adolescentis* LMG 10734 was also included even though it appears to breakdown oligofructose in more than two stages. However, as seen in Figure 4.6 and by the R^2 values, which include this strain, Eqs. 4.3a-d adequately described the experimental data.

Energetically, acetate is the most favorable fermentation product during fructose, oligosaccharide and inulin degradation by bifidobacteria. According to the fructose 6-phoshate phosphoketolase (F6PPK) pathway when two fructose molecules are metabolized, half of the carbon atoms from the fructose will contribute to the formation of 3 acetate molecules and the remaining carbon atoms will contribute to the

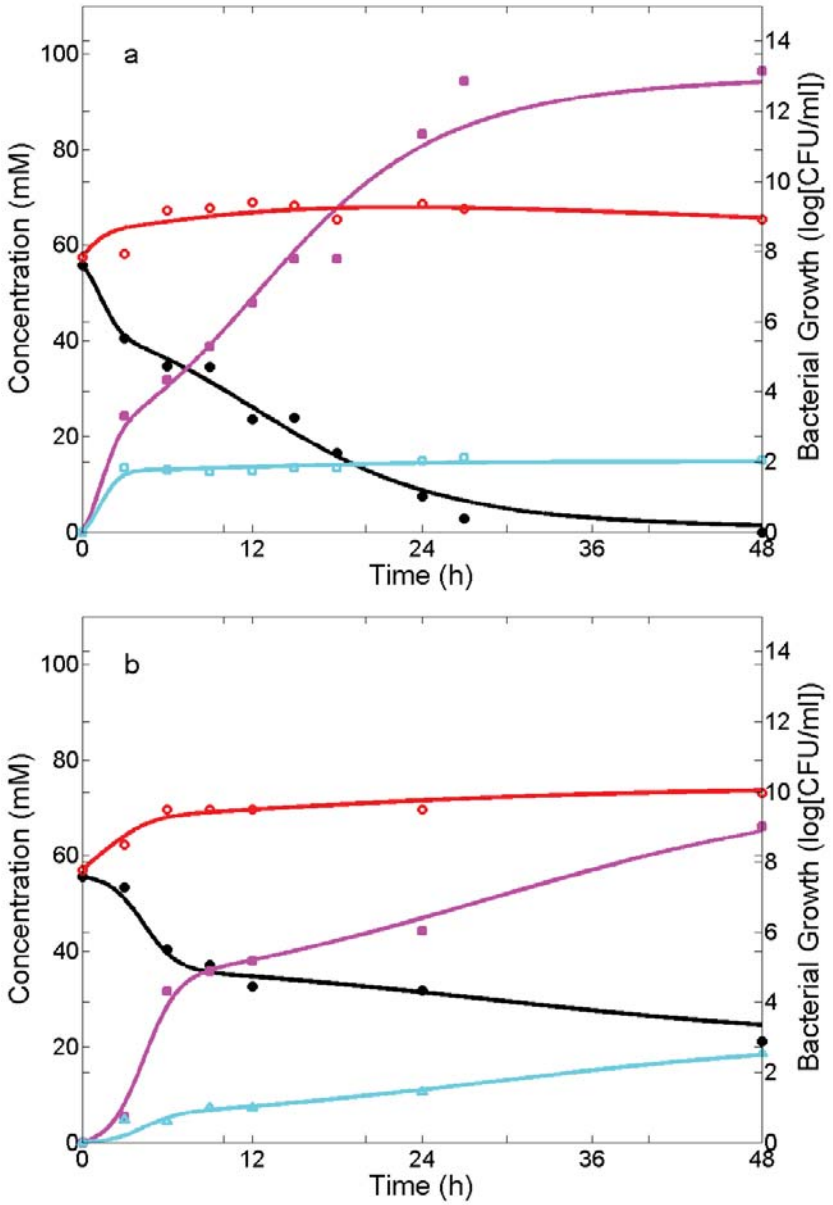

Figure 4.6 Preferential degradation of oligosaccharide (black solid circles) by bacteria (red open circles) and subsequent production of acetate (magenta solid squares) and formate (cyan open triangles) or lactate (cyan open squares) (Falony et al 2009b). Best fit of Eqs. 4.3a-d are represented by solid lines. (a) The model (Eqs. 4.3a-d) adequately depicts growth kinetics of *Bifidobacterium adolescentis* LMG 10734 even though this bacterium degrades oligofructose preferentially in more than two stages (DP 2 & 3, then DP 4, followed by remaining sugars). (b) Preferential degradation of oligosaccharide from saccharides with DP from 1-3, then DP 4 by *B. breve* LMG 13194.

formation of pyruvate which is then reduced to either 1) lactate or 2) formate, acetate and ethanol (Sela et al 2010, Van der Meulen et al 2006a). During monoculture experiments with bifidobacteria, two contrasting metabolite production rates for acetate were noted as well as two contrasting metabolite production profiles; these differences appear to be dependent on the utilization of either the preferred or secondary carbohydrate substrates. In the five strains that showed preferential degradation, acetate and lactate were produced from the utilization of the primary carbohydrates. When the bacteria began to utilize the secondary carbohydrates the conversion of pyruvate to lactate ceased which resulted in the production of formate and an increased production of acetate. The conversion rate of oligofructose to acetate was approximately 1.32 times greater when the bacteria were metabolizing the secondary carbohydrates than when metabolizing the primary carbohydrates. The reduction of pyruvate to lactate does not yield ATP, whereas the reduction of pyruvate to formate, acetate and ethanol results in an additional ATP as well as NAD^+ (Sela et al 2010, Van der Meulen et al 2006a). In addition to a change in the metabolite profiles, there was little to no growth of bacteria during the time that the bacteria metabolized the secondary carbohydrates, implying that the additional ATP is not used for bacterial growth. Lowered growth rates and low substrate concentrations have been associated with this switch from lactate production to acetate, formate and ethanol production (De Vuyst and Leroy 2011, Falony et al 2006, Van der Meulen et al 2006b).

In every monoculture experiment with bifidobacteria, whether grown with fructose, oligofructose or inulin as the substrate, as well as for the monoculture of *B. thetaiotaomicron* LMG 11262 grown with inulin as the substrate, the maintenance term, *m*, was not significantly different from zero ($P<0.001$). Thus, Eq. 4.2a may be simplified to:

$$\frac{dS}{dt} = -\frac{\eta}{Y_{X/S}} 10^{B} S \,. \qquad 4.4$$

Amaretti et al (2007) also found that the maintenance term was not significantly different from zero for the growth of *Bifidobacterium adolescentis* MB 239 on glucose, galactose, lactose, and galactooligosaccharides. A maintenance term not significantly different from zero suggests that under low substrate concentration the majority of the bacteria are actively growing and dividing, quiescent or unculturable.

4.4.2. Classification of Bifidobacteria Strains Based on the Model Parameters

Previous studies have suggested that bifidobacterial strains can be separated into at least 4 clusters that are able to be differentiated on the basis of inulin-type fructans degradation (Falony et al 2009b). Principal component and cluster analysis separated strains into:

- Cluster A) bifidobacteria unable to degrade polysaccharides with a DP > 2. Strains included in this category included *B. bifidum* DSM 20082 and *B. breve* LMG 11040;
- Cluster B) bifidobacteria able to degrade oligofructose, DP $\leq$ 8, but not inulin and, in most cases, the strains showed a preferential degradation pattern. Strains included in this category included *B. breve* LMG 13194 and *B. longum* LMG 13196;
- Cluster C) bifidobacteria strains with the ability to partially degrade inulin, the DP varying between strains with a maximum DP $\cong$ 20 (De Vuyst and Leroy 2011), and in a non-preferential DP degradation pattern. Strains included in this category included *B. adolescentis* LMG 10502 and *B. longum* LMG 11570; and

- Cluster D) two bifidobacterial strains that were able to degrade inulin much like those in Cluster C, however they were not able to determine if there was a preferential degradation pattern from the oligofructose and fructose experiments. Strains included in this category included *B. longum* LMG 11047 and *B. thermophilum* LMG 11574 (Falony et al 2009b).

For bifidobacteria grown with inulin as the substrate, an analysis was undertaken to see whether the parameters, $Y_{X/S}$, η and a were significantly different between the clusters A-D as determined by Falony et al (2009b). One-way ANOVA (GenStat V13.2, VSN International Ltd., UK) showed that the fraction of inulin used (a) was significantly different between clusters ($P < 0.001$); however there was no significant difference in either the yield ($Y_{X/S}$) or η (the maximum specific rate divided by the Monod constant) between clusters.

After further assessment, the data suggests there may be subcategories within the previously described clusters. For instance, it appears that *B. adolescentis* LMG 10502 may degrade inulin and oligofructose extracellularly, which was evident by the increase of monosaccharides in the growth medium when *B. adolescentis* LMG 10502 was grown with oligofructose. This may also be the case for *B. longum* LMG 11570 and *B. adolescentis* LMG 10733. All three of these bacteria are classified in Cluster C. Additionally, it appears that the preferential degradation profile is not restricted to bacteria that degrade only mono- and oligofructose (Cluster B) and may be divided into two types: bacteria such as *B. angulatum* LMG 11039, which prefer polysaccharides with a DP greater than 1 (and less than approximately 20) to monosaccharides, or bacteria such as *B. breve* LMG 13194 which prefer to degrade short chain to long chain oligosaccharides. Thus, the phenotypes could be further divided into sub-clusters

according to their patterns of substrate utilization. Given that our model was formulated to describe primary and secondary preferential degradation, it is capable of describing both types of preferential degradation, along with the resulting metabolites.

4.4.3. Mechanistic Model for Coculture Bacterial Growth

Here microbial cross-feeding was assumed to occur as a result of the buildup of monosaccharides from the extracellular breakdown of polysaccharides by one of the bacterial populations, as observed in the works of Falony et al (2009a) and Van der Meulen et al (2006b). One of the bacteria can use both long (L) and short chain (S) polysaccharides whereas the other cross-feeding bacterium can only use short chain polysaccharides:

$$\frac{dS_L}{dt} = -(1 + r_M)(Bac1S_L) \tag{4.5a}$$

$$\frac{dS_S}{dt} = (Bac1S_S) + (Bac2S_S) - r_M(Bac1S_L) \tag{4.5b}$$

$$\frac{dB_1}{dt} = \frac{1}{\ln(10)}(\eta_1(S_L + S_S) - k_{d,1}) \tag{4.5c}$$

$$\frac{dB_2}{dt} = \frac{1}{\ln(10)}(\eta_2(S_S) - k_{d,2}) \tag{4.5d}$$

$$\frac{dP_i}{dt} = -k_{1,i}(Bac1S_L + Bac1S_S) - k_{2,i}(Bac2S_S). \tag{4.5e}$$

A detailed description of the model parameters is listed in Table 4.1. In the work presented here, it was assumed that short chain polysaccharides comprise of sugars with DP ranging from 1 to approximately 20, the maximum DP reported to be utilized by *Bifidobacterium* (Falony et al 2009b).

Bacteroides thetaiotaomicron and *Bifidobacterium longum* have been reported to be among the most prevalent bacterial species associated with food particles (Macfarlane and Macfarlane 2006) with *B. thetaiotaomicron* being one of the more

Table 4.1 Parameter description and equations to for the coculture/cross-feeding model.

Parameter	**Description**	**Equation**
S_L	Concentration of long chain (LC) polysaccharides (mM FE)	
S_S	Concentration of short chain (SC) polysaccharides (mM FE)	
r_M	Rate at which LC's are converted to monomers/fragments	
$Bac\{j\}S_{\{L,S\}}$	Rate of either LC or SC polysaccharide degradation (mM FE h^{-1}) by either the monomer/fragment producing bacteria $(j=1)$ or the cross-feeding bacteria $(j=2)$	$-\frac{\eta_j}{Y_{X/S,j}}10^{Bj}S_{\{L,S\}}-m_j10^{Bj}$
η_j	Maximum utilization rate divided by Monod constant for j^{th} bacterium (h^{-1} FE^{-1})	
$k_{d,j}$	Cellular death rate for j^{th} bacterium (log(CFU/ml) h^{-1})	
$k_{j,i}$	Conversion constant (mM (mM FE)$^{-1}$) of the substrate (mM FE) to the i^{th} metabolite, P_i (mM), by either the monomer/fragment producing bacteria $(j=1)$ or cross-feeding bacteria $(j=2)$	

versatile polysaccharide fermenting bacteria (Degnan and Macfarlane 1995). Falony and colleagues (2009a) have shown that *B. longum* LMG 11047 has the capacity to partially degrade inulin and thus competes with *B. thetaiotaomicron* LMG 11262 for polysaccharides with a maximum DP around 20.

Thus, to test the coculture model, the parameters determined from the best fit of Eqs. 4.1a-d. to the monoculture data of *B. longum* LMG 11047 [Figure 4.7a] and *B. thetaiotaomicron* LMG 11262 [Figure 4.7b] grown with inulin as the substrate were used (Falony 2009, Falony et al 2009b). It was assumed that $S_S(0) = aS$ and $S_L(0) = (1-a)S$, where a is the fraction of the inulin concentration, S (mM FE), that the cross-feeding bacteria were capable of degrading in monoculture. There was no noticeable amount of formate in the monoculture of *B. longum* LMG 11047 when grown with inulin so the parameter for the rate of production of formate was determined from a best fit of Eqs. 4.2a-d to the growth of *B. longum* LMG 11047 in monoculture on oligofructose. This required a transformation of the parameter value to account for the change in metabolite profiles from oligofructose to inulin (less lactate, more formate and acetate). The conversion rate of inulin to formate, $k_{form,In}$, was calculated as $k_{form,In} = k_{form,Oligo}(Y_{In}/Y_{Oligo})$ where $k_{form,Oligo}$ is the conversion rate of oligofructose to formate, Y_{Oligo} and Y_{In} are the yield of bacteria from oligofructose and inulin metabolism, respectively, as determined from the best fit of Eqs. 4.2a-d to the growth of *B. longum* LMG 11047 in monoculture.

The production of formate in the coculture environment would imply that *B. longum* LMG 11047 out competed *B. thetaiotaomicron* LMG 11262 for both the monosaccharides and oligosaccharides, as formate is not a metabolic end product of *B. thetaiotaomicron* LMG 11262. Additionally, the higher formate concentration (as compared to *B. longum* LMG 11047 in monoculture) implies that inulin degradation by

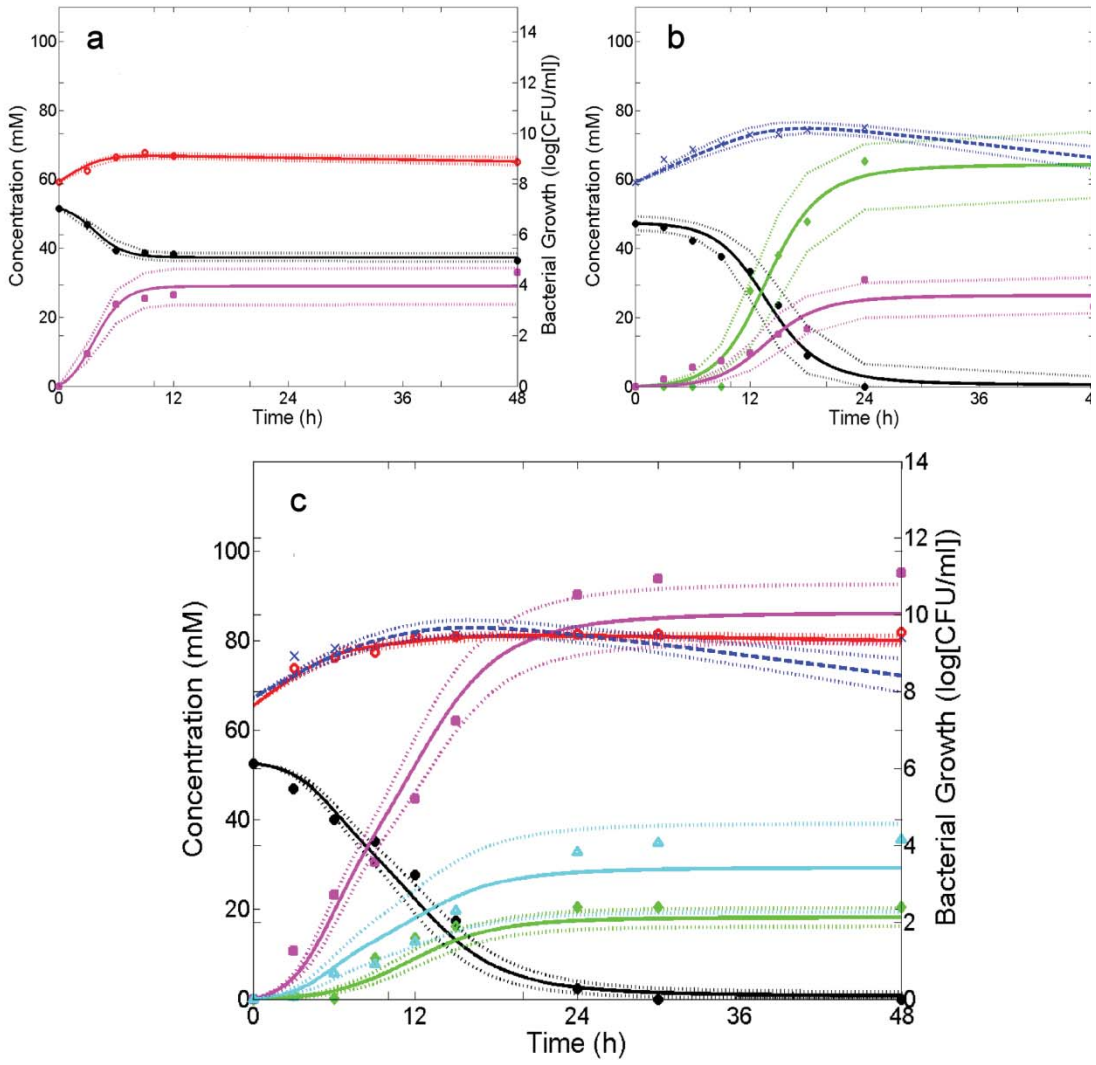

Figure 4.7 Growth kinetics of (a) *Bifidobacterium longum* LMG 11047 (red open circles) and (b) *Bacteroides thetaiotaomicron* LMG 11262 (blue crosses) in monoculture and the two strains in (c) coculture: inulin (black solid circles), acetate (magenta squares), succinate (green diamonds), and formate (cyan triangles) (Falony 2009, Falony et al 2009a, Falony et al 2009b). Solid lines represent the (a,b) model best fit of Eqs. 4.1a-c to the monoculture data (a,b) and the model prediction (Eqs. 4.5a-e) to the coculture data using parameter values derived from monoculture data prediction (c). Dotted lines represent the 95% confidence intervals. Note that the error associated with formate (c) may be considerably larger given the calculation of $k_{form,In} = k_{form,Oligo}\left(Y_{In}/Y_{Oligo}\right)$, where Y_{In} and Y_{Oligo} were determined from the best fit values and $k_{form,Oligo}$ from the MCMC.

B. thetaiotaomicron LMG 11262 may produce oligofructose in addition to monosaccharides. Figure 4.7a,b demonstrates the fit of Eqs. 4.2a-d to the growth of *B. longum* LMG 11047 and *B. thetaiotaomicron* LMG 11262 when grown with inulin in monoculture (Falony et al 2009a). As seen in Figure 4.7c, even though Eqs. 4.5a-e were based on parameters derived from monoculture data, the model successfully described the competitive dynamics between *B. longum* LMG 11047 and *B. thetaiotaomicron* LMG 11262 growing in coculture in terms of the amounts of substrate utilized, bacterial growth and metabolite produced. The predicted values for acetate after 24 hours were within the 95% confidence intervals of the monoculture parameter values.

Given that there are more monosaccharides available from the hydrolysis of the inulin by *B. thetaiotaomicron* LMG 11262, more than trace amounts of lactate (4.3 ± 0.1 mM at 30 hrs) would be expected to be reported (Falony et al 2009a). The lack of lactate may be associated with the increase in other metabolites such as acetate (predicted value 86 mM and experimental value 95 mM at 48 hrs) or formate (predicted value 31mM and experimental value 35 mM at 48 hrs). Such a shift in metabolite production has been noted in previous studies with *Bifidobacterium* (De Vuyst and Leroy 2011, Van der Meulen et al 2006a) and was discussed earlier. As noted earlier, the shift in metabolite profiles has been associated with lowered growth rates and lower substrate concentrations. This was found to be the case in the coculture environment. The reduced growth rate obtained in monoculture (with inulin as compared to fructose) for *B. longum* LMG 11047 was used and given the competition for substrate, there was reduced substrate concentration availability per bacterial species. The parameter value for the bacterial death rate for the *Bacteroides* strain in monoculture that was used to predict the coculture growth of the *Bacteroides* strain resulted in a lower predicted value

at 48 hours than the experimental data; however, the experimental value was within the 95% confidence interval of the predicted value.

4.4.4. Sensitivity of Coculture Model Results to Growth Parameters Based on Monoculture Data

Even though *B. longum* LMG 11047 is capable of utilizing long chain polysaccharides, many *Bifidobacterium* species do not metabolize inulin, and only metabolize monosaccharides or oligosaccharides with a $DP \leq 8$. For instance *B. breve* Yakult, a common probiotic, has been shown to utilize only monosaccharides, yet *in vivo* and *in vitro* studies have shown that there is an increase in overall bifidobacterial numbers with the addition of inulin into the diet (Bouhnik et al 1999, Chen et al 2013, Costabile et al 2010, Gibson et al 1995, Ramnani et al 2010). To further validate our model and to help elucidate the mechanisms behind the increased growth of *Bifidobacterium* when inulin is added to the diet, the parameters found from the best fit of Eqs. 4.2a-d monoculture of *B. breve* Yakult were used in conjunction with Eqs. 4.5a-e to predict the growth of *B. breve* Yakult with *B. thetaiotaomicron* LMG 11262 in coculture with inulin. Given that *B. breve* Yakult only utilizes monosaccharides, it was expected that *B. breve* Yakult would grow purely from the hydrolytic breakdown products produced from extracellular degradation of polysaccharides by *B. thetaiotaomicron* LMG 11262. Hence, the parameter values obtained from fitting Eqs. 4.2a-d to the monoculture data when *B. breve* Yakult was grown with fructose as the metabolite were used. As seen in Figure 4.8a, the parameter values from monoculture did not adequately describe the degradation of inulin by *B. breve* Yakult and *B. thetaiotaomicron* LMG 11262 in coculture. It appears that when *B. thetaiotaomicron* LMG 11262 was grown in coculture with *B. breve* Yakult, the value of η for *B. thetaiotaomicron* LMG 11262 may be lower than when grown in monoculture.

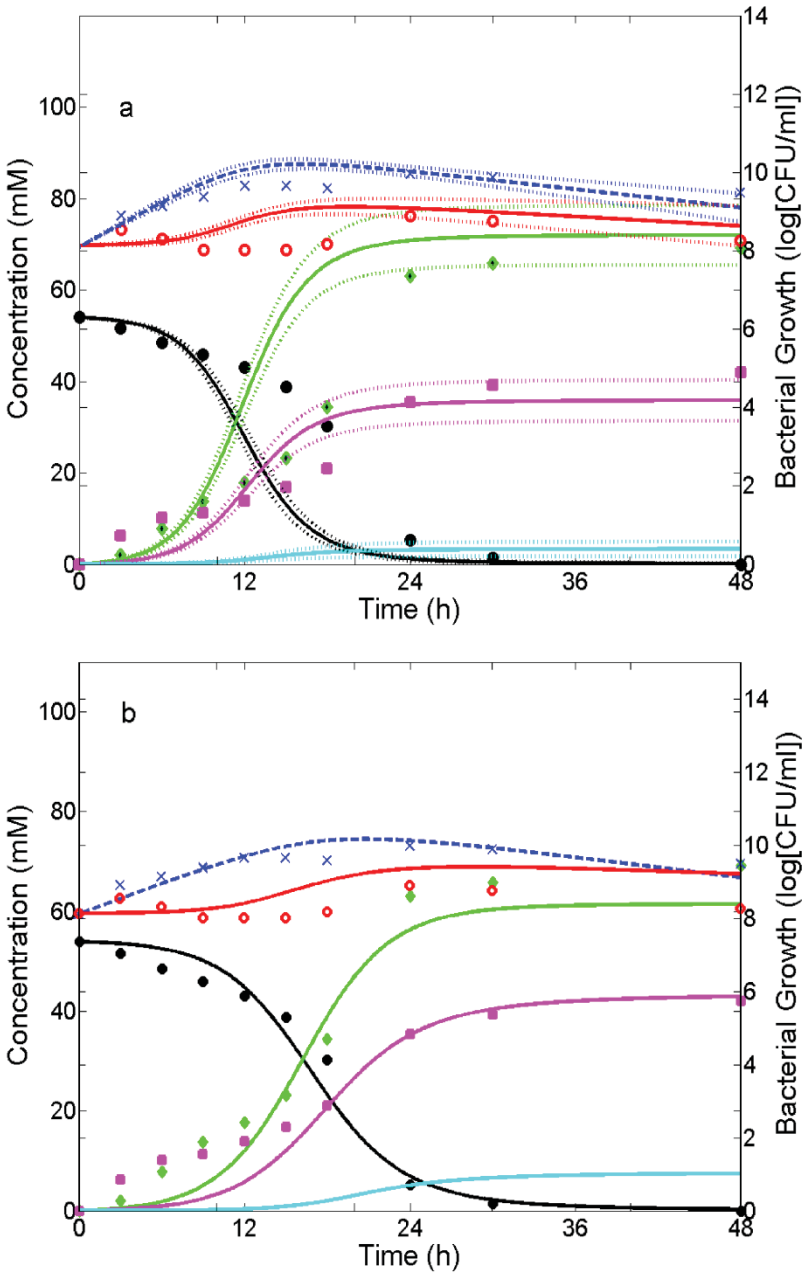

Figure 4.8 Coculture growth kinetics of *Bifidobacterium breve* Yakult (red circles) and *Bacteroides thetaiotaomicron* LMG 11262 (blue crosses): inulin (black solid circles), acetate (magenta squares), succinate (green diamonds), and formate (cyan) (Falony et al 2009a). Solid lines represent the model prediction (Eqs. 4.5a-e) to the coculture data using parameter values derived from monoculture data prediction (a) and model prediction (Eqs. 4.5a-e) with a decrease in the specific growth rate of *B. thetaiotaomicron* LMG 11262 (b). Dotted lines represent the 95% confidence intervals (a).

The parameter η is defined as the maximum specific growth rate divided by the Monod constant, so a decrease in η implies a decrease in the specific growth rate for *B. thetaiotaomicron* LMG 11262 in coculture with *B. breve* Yakult. It is well accepted that there is variability in microbial growth between experiments and the effect of a decrease in the growth rate of *B. thetaiotaomicron* LMG 11262 on the coculture dynamics was examined. Figure 4.8b shows that a decrease from $\eta = 0.011 \text{ to } \eta = 0.008$, which is 3.1 standard deviations from the mean, results in a reasonable prediction of the coculture dynamics (cumulative $R^2 = 0.97$). This difference in growth rate may be within the expected variability of experimental results. Additional experiments are necessary to determine the variability in growth rate. Alternatively, there is a possibility that *B. breve* Yakult produces a bacteriocin or another inhibitory metabolite, that was not measured in the experimental design nor accounted for in our model that may reduce the specific growth rate of *B. thetaiotaomicron* LMG 11262. A number of bifidobacteria have been shown to produce bacteriocins (Kanmani et al 2013, Muñoz-Quezada et al 2013); however there is no reference of antimicrobial activity by *B. breve* Yakult in the literature. Previous *in vitro* and *in vivo* studies with pectic-oligosaccharides, oligofructose, and inulin have shown an increase in bifidobacteria growth and a decrease in or restricted growth of *Bacteroides* (Chen et al 2013, Gibson et al 1995). Unfortunately, these studies only reported total counts of *Bacteroides* and *Bifidobacterium*; knowing the particular species or strains whose numbers increased or decreased would provide additional insight into the effects of prebiotics and may encourage the use of particular strains of *Bifidobacterium* as prebiotics or synbiotics. Regardless of the mechanism influencing the decrease in the specific growth rate of *B. thetaiotaomicron* LMG 11262, the decrease in growth of *B. thetaiotaomicron* LMG 11262 provides an advantage to the *B. breve* Yakult in that it is able to compete for the

monosaccharides that are released as a result of long chain polysaccharides hydrolysis by *B. thetaiotaomicron* LMG 11262.

4.5. Concluding Comments

This work has shown that a modified version of the model proposed by Amaretti et al (2007) (Eqs. 4.2a-d) is capable of accurately describing the microbial growth and metabolite production by 18 different *Bifidobacterium* strains and *B. thetaiotaomicron* LMG 11262 as a result of the metabolism of either inulin or fructose. Additionally, the model can be used to describe the growth kinetics of *Bifidobacterium* when grown with oligofructose as long as the bacterium degrades the carbohydrate fractions simultaneously. In the case when the bacteria preferentially degrade oligofructose fractions (either in the order of fractions with low DP to high DP, or vice versa), an additional model was proposed (Eqs. 4.3a-d). These models have shown that metabolite production is proportional to substrate utilization and that very little of the substrate was used for bacterial maintenance, which may imply that many of the bacteria were in a quiescent state as a result of low nutrient availability.

Most importantly, this work demonstrated that microbial cross-feeding and competition, as a result of the release of partially degraded polysaccharides from extracellular degradation of inulin, can be predicted using parameter values determined from monoculture experiments. This is a significant finding in that it may reduce the number of *in vitro* experiments necessary to model multi-culture bacterial dynamics. There is a substantial lack of published work that reports the growth kinetics of bacteria in coculture over time. Additional *in vitro* experiments with a variety of bacteria and/or microbiota are essential to determine in which cases and with which bacterial species the model is valid.

The release of partially degraded polysaccharides is only one form of microbial cross-feeding. Some bacterial species are capable of utilizing metabolites produced by another species for growth (Duncan et al 2004, Falony et al 2006). In some cases, microbial cross-feeding is a combination of the use of metabolites and partially degraded substrates which accumulate from extracellular hydrolysis (Belenguer et al 2006, Falony et al 2006). Thus, the model proposed here (Eqs. 4.5a-e) is only one pathway for which bacteria cross-feed. In future research, the model described here could be extended to incorporate the other forms of microbial cross-feeding.

Chapter 5 Anisotropic Nutrient Transport in Three Dimensional Single Species Bacterial Biofilms

5.1. Abstract

The ability of a biofilm to grow and function is critically dependent on the nutrient availability, and this in turn is dependent on the structure of the biofilm. This relationship is therefore an important factor influencing biofilm maturation. Nutrient transport in bacterial biofilms is complex; however, mathematical models that describe the transport of particles within biofilms have made three simplifying assumptions: the effective diffusion coefficient (EDC) is constant, the EDC is that of water, and/or the EDC is isotropic. Using a Monte Carlo simulation, the EDC was determined, both parallel to and perpendicular to the substratum, within 131 real, single species, three-dimensional biofilms that were constructed from confocal laser scanning microscopy images. Our study showed that diffusion within bacterial biofilms was anisotropic and depth dependent. The heterogeneous distribution of bacteria varied between and within species, reducing the rate of diffusion of particles via steric hindrance. In biofilms with low porosity, the EDCs for nutrient transport perpendicular to the substratum were significantly lower than the EDCs for nutrient transport parallel to the substratum. Here, a reaction–diffusion model to describe the nutrient concentration within a bacterial biofilm that accounts for the depth dependence of the EDC is proposed.

5.2. Introduction

Intestinal bacteria play an essential role in human health. Commensal bacteria within the large bowel have been found to affect host function by producing short chain fatty acids (Albrecht et al 1996, Macfarlane and Macfarlane 2007, Younes et al 2001), synthesizing vitamins (Albrecht et al 1996, Burgess et al 2009, Conly et al 1994, Glancey et al 2007, Madhu et al 2009), modulating the immune system (Borruel et al 2002, Furrie et al 2005, Macfarlane et al 2009, Saulnier et al 2009) and inhibiting the colonization of the intestinal tract by potentially pathogenic bacteria (Coconnier et al 1993, De Ruyter et al 1996, Lievin et al 2000). These benefits are a result of bacterial fermentation of food particles which escape digestion in the small bowel (Bernalier-Donadille 2010, Cummings et al 1987, Cummings and MacFarlane 1997, Eyssen 1973, Hamilton et al 2007, Macfarlane and Cummings 1991, Macfarlane et al 1992, Ridlon et al 2006, Thomas et al 2001).

Biofilms are ubiquitous in nature, and were first reported associated with food particles in human fecal matter by Macfarlane et al (1997). Even though only 5% of the bacterial population in these samples were reported to be biofilms, the evidence of high levels of acetate within the proximal colon, which is readily produced by heterogeneous bacterial biofilms (Leitch et al 2007, Macfarlane and Macfarlane 2006, Macfarlane and Dillon 2007), implies that either biofilms are abundant the human proximal colon or that biofilm formation facilitates substantial acetate production. [For an extensive reviews on bacterial biofilms in the human bowel, see Flint et al (2012) and Van Wey et al (2011).]

Biofilms are distinguished from adherent cells by the evidence of a slime coating the bacterial consortia. This slime or extracellular polymeric substances (EPS) can be comprised of polysaccharides, proteins, DNA and lipids that are associated primarily

through ionic interactions (Gristina 1987). Ninety to ninety-nine percent of the biofilm water content lies within this slime or EPS (Flemming et al 2005) providing a network for the transport of nutrients into the biofilm. The extracellular space within the biofilm also accounts for 4-98% of the biofilm volume (Libicki et al 1988, Wood et al 2002) and is not uniformly distributed because of the complex spatial distribution of the bacteria within the biofilm (Bridier et al 2010). The effect of the biofilm structure on nutrient transport has been investigated theoretically using two-dimensional transmission electron microscopy micrograph images of biofilm structures (Wood et al 2002), but not within real three-dimensional bacterial biofilms.

Existing experimental methods, such as pulse field gradient nuclear magnetic resonance with confocal laser scanning microscopy (CLSM) (McLean et al 2008) or without CLSM (Beuling et al 1998, Renslow et al 2010), microelectrodes (Beyenal and Lewandowski 2002, Rasmussen and Lewandowski 1998), fluorescence return after photobleaching (FRAP) (Bryers and Drummond 1998, Waharte et al 2010), and fluorescence correlation spectroscopy (FCS) (Briandet et al 2008), have been used to calculate the effective diffusion coefficient (EDC) parallel to the substratum in biofilms. Such studies have shown that the EDC can vary at different locations within the biofilm (Beyenal and Lewandowski 2002, Bryers and Drummond 1998, Renslow et al 2010, Yang and Lewandowski 1995) and have resulted in EDCs that range from 5% to 95% of that in water (Beuling et al 1998, Wood and Whitaker 2000).

Although information on transport parallel to the substratum is useful, three-dimensional modeling simulations and *in situ* experimental studies have shown that transport of nutrients perpendicular to the substratum is critically relevant to biofilm function. In the case of low velocity flow in the bulk liquid environment (De Beer et al 1996), or when the chemical is only produced or consumed by the bacteria within the

biofilm (Picioreanu et al 2004), the concentration gradient is normal to the substratum; however, in the latter case, this may depend upon the biofilm morphology since multidimensional gradients may occur in biofilms which are highly porous and channeled. Furthermore, in multi-species biofilms the concentration gradient may be multidimensional if the chemical facilitates microbial cross feeding (i.e. is produced by and utilized by different bacteria within the biofilm) (Picioreanu et al 2004). Thus there is a need for estimating the EDC in biofilms both parallel to and perpendicular to the substratum.

Despite the evidence that nutrient transport is multidimensional, to date, mathematical models have made three simplifying assumptions with regards to the transport of particles within a biofilm: 1) the EDC is constant (Alpkvist and Klapper 2007, Chang et al 2003, Hermanowicz 2001, Rahman et al 2009, Rajagopalan et al 1997, Xavier et al 2004); 2) the EDC is that of water (Alpkvist and Klapper 2007, Kreft et al 2001, Rajagopalan et al 1997, Xavier et al 2004); and 3) the EDC is isotropic (the same in directions parallel and perpendicular to the substratum) (Alpkvist and Klapper 2007, Chang et al 2003, Rahman et al 2009, Xavier et al 2004). There is one journal article which characterizes the relationship between nutrient transport perpendicular to the substratum and distance from the substratum; however, this linear description does not consider the behavior near to, or far from, the substratum (Beyenal and Lewandowski 2002). There are a multitude of models describing the relationship between either biofilm porosity (volume fraction of the biofilm that is liquid) or biofilm density and nutrient diffusion within the biofilm (Beuling et al 2000, Fan et al 1990, Ho and Ju 1988, Horn and Morgenroth 2006, Kapellos et al 2007, Libicki et al 1988, Maxwell 1892, Mota et al 2002, Wang and Zhang 2010, Wood et al 2002). Some are heuristic fits to data, whereas others are derived using theoretical arguments based on

simplified biofilm geometry. It is not clear which of these models is most suitable for describing the effect of biofilm structure on nutrient transport within the biofilm.

Many models partition the biofilm into two distinct components where one component is comprised of biomass (bacteria and EPS) and the other of water (Alpkvist and Klapper 2007, Hermanowicz 2001, Wanner et al 2006, Wood and Whitaker 2000). The biofilm can then be considered a porous media. The biomass within the biofilm reduces the rate of diffusion of particulates parallel to the substratum via steric hindrance (De Beer et al 1997, Guiot et al 2002). However, the distribution of biomass may be heterogeneous (Bridier et al 2010) and the diffusion parallel to the substratum may be different to the diffusion perpendicular to the substratum. For example, if the biomass is compact with multiple column like structures growing perpendicular to the substratum (Bridier et al 2010, Danese et al 2000), the expectation would be that the columns of bacteria would hinder the transport of particles parallel to the substratum to a greater degree than perpendicular to the substratum. Thus the hypothesis of this work is that the EDC in biofilms is anisotropic, with a level of anisotropy that is dependent on the biofilm structure. The tortuosity factor, τ, is used to describe the resistive properties of solutes in porous media and is defined here by the homogenized diffusion equation (Shorten and Sneyd 2009),

$$\frac{\partial C}{\partial t} = \tau D \nabla^2 C = D_{\text{eff}} \nabla^2 C \qquad 5.1$$

where C is the concentration of nutrient within the biofilm at time, t, D is the nutrient diffusion coefficient in water, and D_{eff} is the EDC, which is a function of the biofilm structure.

The purpose of this study is four fold: 1) to utilize an alternative method for determining EDCs within real three-dimensional bacterial biofilms; 2) to determine whether or not the EDC within bacterial biofilms is isotropic or anisotropic; 3) to

ascertain the relationship between the porosity of the biofilm and the EDC; and 4) to construct a model of nutrient transport within a bacterial biofilm growing on a nutrient-providing substratum.

5.3. Materials and Methods

5.3.1. Biofilm Structures

Two-dimensional CLSM images of 131 distinct, single species biofilms (*Salmonella enterica*, *Pseudomonas aeruginosa*, *Escherichia coli*, *Enterococcus faecalis*, *Staphylococcus aureus*, and *Listeria monocytogenes*), formed on polystyrene 96-well microtiter plates as described previously (Bridier et al 2010), were acquired. For a complete list of the bacterial strains, please refer to Appendix A. Twenty-four hour biofilms were labeled with Syto9 (Invitrogen, France), a cell permeant green fluorescent nucleic acids dye. For one strain of each species, biofilms were also labeled with Alexa Fluor 633 conjugated to Concanavalin A (ConA; Molecular Probes, Invitrogen Corporation) by adding 10 µl of a solution at 1 mg/ml directly to the wells. This fluorescent lectin specifically binds α-mannopyranosyl and α-glucopyranosyl and thus enables the visualization of some polysaccharides of the biofilm matrix (Chen et al 2007). Biofilms were scanned at 400 Hz using a 40× with a 0.8 N.A. (Leica HCX Apo) water immersion objective lens with a 488 nm argon laser set at 25% intensity. Emitted fluorescence was recorded within the range of 500-600 nm in order to visualize Syto9 fluorescence and from 650 nm to 750 nm for ConA. The CLSM images had a width of 119 µm, length of 119 µm (512×512 pixels) and were taken at a depth of 1 µm intervals for Syto9 alone and had a width and length of 375 µm and were taken a depth of 1 µm for Syto9 and ConA mix. Total biofilm depth varied from 10 µm to 65 µm. Within each bacterial species, there were ten different strains and a minimum of two biofilms were

grown for each strain. Although the biofilms used in this study are potentially pathogenic, they reflect the diversity of biofilm structure and the various degree of porosity within biofilms found in a range of environments.

The three-dimensional renderings of bacterial biofilms were constructed by stacking the two-dimensional CLSM slides in MATLAB (The MathWorks; www.mathworks.com). In order to accurately determine the biofilm structure from the CLSM slides, the background shades were segmented from those of the relevant structural information (foreground shades) using the Otsu method. This method finds the threshold shade intensity, $0 \le k^* \le L-1$ where L is the maximum level of shade intensity (i.e. $L = 256$ for 8-bit images), that maximizes the weighted between-class variance of the shade intensity histogram using the entire stack of CLSM images (Yerly et al 2007). Thus, using the zeroth- and first-order cumulative moments of this histogram, the weighted between class variance, $\sigma_B^2(k)$, is defined as

$$\sigma_B^2(k) = \frac{[\mu_T \omega(k) - \mu(k)]^2}{\omega(k)[1-\omega(k)]} \qquad 5.2a$$

where the zeroth- and first order cumulative moments of the histogram are defined, respectively, as

$$\omega(k) = \sum_0^k p_i \qquad 5.2b$$

$$\mu(k) = \sum_0^k i p_i \qquad 5.2c$$

and the total mean level of shade intensity is defined as

$$\mu_T = \mu(L-1) = \sum_0^{L-1} i p_i \,. \qquad 5.2d$$

Thus, according to the Otsu method, the optimal threshold shade intensity, k^*, is given as (Yerly et al 2007)

$$\sigma_B^2(k^*) = \max_{0 \le k \le L-1} \left(\sigma_B^2(k)\right). \qquad 5.2e$$

The Otsu method is the optimal method for determining whether a particular voxel is obstacle free based on a CLSM image. This segmentation method is species independent and satisfies visual inspection even in images with biofilm coverage levels near 1.2% (Yerly et al 2007).

5.3.2. Modeling Diffusion

To estimate the EDC within the aforementioned biofilms a Monte Carlo random walk of a particle diffusing through the biofilm was simulated (Ölveczky and Verkman 1998, Saxton 1987, Saxton 1994). In this technique, the tracer moved along a uniform, cubic mesh where both the obstacles (bacteria) and the obstacle free (water and EPS) zones were specified. When the tracer moved to a point on the mesh that was defined as an obstacle (i.e. a bacterium) the tracer remained in the original position at the boundary of the obstacle (this represents particle reflection from the surface of the biofilm). If Ω is defined to be the set of all points which represent obstacles on the domain, then a random walk, $\vec{\mathbf{x}}(t) = \langle x_1(t), x_2(t), x_3(t) \rangle$, on that domain is given by,

$$\vec{\mathbf{x}}_{j+1} = \vec{\mathbf{x}}_j + \eta_j \sqrt{6D\Delta t} \qquad 5.3$$

$$t_{j+1} = t_j + \Delta t$$

$$\vec{\mathbf{x}}_{j+1}(t_{j+1}) = \begin{cases} \vec{\mathbf{x}}_{j+1} & \text{if} \quad \vec{\mathbf{x}}_{j+1} \notin \Omega \\ \vec{\mathbf{x}}_j & \text{if} \quad \vec{\mathbf{x}}_{j+1} \in \Omega \end{cases}$$

where $\boldsymbol{\eta}_j$ is a unit vector in one of the six Cartesian axis directions, Δt is the time step, and $\Delta x = \sqrt{6D\Delta t}$ is the mesh size. The definition of the mesh size results from the fact that the mean square displacement, $\langle r^2(t) \rangle$, of a particle diffusing in *n* dimensions is given by

$$\left\langle r^2(t)\right\rangle = 2nDt \tag{5.4}$$

thus

$$\left\langle r_i^2(\Delta t)\right\rangle = 2nD\Delta t$$

or

$$\left\langle r_i(\Delta t)\right\rangle = \sqrt{2nD\Delta t}\ .$$

An ensemble of tracer paths, beginning at a random position, $\vec{\mathbf{x}}(0) \notin \Omega$, was used to calculate the mean-squared displacement and the tortuosity, τ, respectively.

$$\left\langle r_i^2(t)\right\rangle = \left\langle \left\| x_i(t) - x_i(0) \right\|^2 \right\rangle \tag{5.5}$$

$$\tau_i = \frac{D_i^{\mathbf{eff}}}{D} = \lim_{t\to\infty} \frac{\left\langle r_i^2(t)\right\rangle}{2Dt} \tag{5.6}$$

This definition of tortuosity is also referred to as relative diffusivity in (Hinson and Kocher 1996, Horn and Morgenroth 2006).

To calculate the mean-squared displacement, the Monte Carlo simulated random walk was repeated 1000 times for all 131 biofilms. For each simulated walk, the tracer took 10^7 steps with a step size (i.e. mesh size) of 0.25 μm. The average of the tortuosity factors in the *x* and *y* directions were used to determine the tortuosity factor parallel to the substratum. In addition to calculating the tortuosity factor for each biofilm, the porosity at every 1μm of depth within each biofilm and the average porosity over the entire biofilm were calculated.

5.4. Results and Discussion

5.4.1. Anisotropic Diffusion

For particles moving parallel to the substratum our method provided values that are in agreement with the tortuosity factors found using Maxwell's equation for

impermeable cells (Eq. 5.7) [Figure 5.1a] (Hinson and Kocher 1996, Wood and Whitaker 1999) :

$$\tau_M(\varepsilon) = \frac{2\varepsilon}{3-\varepsilon} \qquad 5.7$$

where ε is the porosity of the biofilm. However, our results provide evidence that Maxwell's equation does not adequately depict the tortuosity factor for particles that move perpendicular to the substratum [Figure 5.1b].

Direct comparison to experimental findings is limited, as there have been few studies for which porosity was directly calculated, and these studies have not used bacterial biofilms (Axelsson and Persson 1988, Chresand et al 1988, Ho and Ju 1988). Nonetheless, these studies also found that Maxwell's equation adequately described the relationship between porosity and tortuosity [Table 5.1, Figure 5.1c] when a particle diffuses parallel to the substratum.

The tortuosity factors perpendicular to the substratum were significantly lower than those parallel to the substratum in biofilms with low porosity; thus, providing evidence that diffusion within bacterial biofilms is anisotropic [Figure 5.1b]. These observations are of significance and imply that the transport of nutrients into biofilms by diffusion is slower than previously reported (Kreft et al 2001, Rajagopalan et al 1997, Xavier et al 2004). The ability for a biofilm to grow and function is critically dependent on the nutrient availability, and this in turn is dependent on the structure of the biofilm. This relationship is therefore an important factor influencing biofilm maturation.

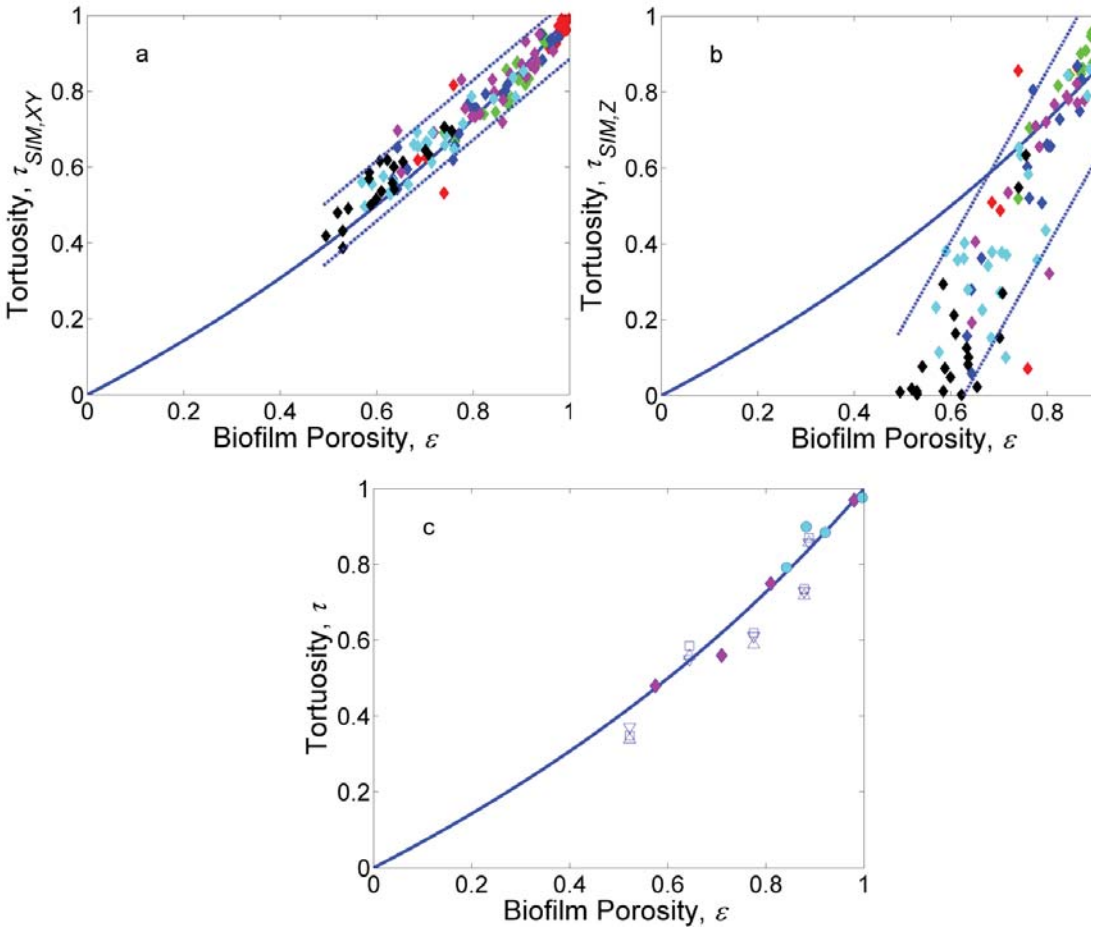

Figure 5.1 Model simulations of tortuosity *E. coli* (blue diamond), *E. faecalis* (black diamond), *L. monocytogenes* (green diamond), *P. aeruginosa* (magenta diamond), *S. aureus* (cyan diamond), and *S. enterica* (red diamond). Average tortuosity values parallel to the substratum, $\tau_{SIM,XY}$, (a) and perpendicular to the substratum, $\tau_{SIM,Z}$, (b) versus porosity, ε, of the biofilm. Maxwell's equation (solid line), Eq. 5.7, and 95% confidence intervals (dotted lines) based on linear regression. (c) Experimental data of tortuosity verses porosity from the literature. Reprinted with permission from *Biotechnology and Bioengineering.*

Table 5.1 Summary of experimental data used in Figure 5.1c Reprinted with permission from Biotechnology and Bioengineering.

Type of Cell	**Solute**	ε	τ	**Source**	**Symbol**
Mammalian cells	Lactate	0.575	0.480	(Chresand et al 1988) [a]	
		0.710	0.560		
		0.810	0.750		
		0.980	0.970		
Penicillium chrysogenum	Oxygen	0.996	0.977	(Ho and Ju 1988)	
		0.921	0.885		
		0.882	0.900		
		0.842	0.792		
Saccharomyces cerevisiae	Lactose	0.888	0.858	(Axelsson and Persson 1988)[a,b]	
		0.878	0.718		
		0.775	0.589		
		0.644	0.559		
		0.522	0.339		
	Glucose	0.888	0.857		
		0.878	0.729		
		0.775	0.611		
		0.644	0.550		
		0.522	0.371		
	Galactose	0.888	0.870		
		0.878	0.735		
		0.775	0.620		
		0.644	0.585		
		0.522	0.349		

(*a*) Indicates data that has been interpolated from a graphical source. (*b*) Values reported here differ from those reported by (Wood et al 2002) as they calculated the ratio of effective diffusion coefficient and the diffusion coefficient within alginate gels rather than in pure water.

5.4.2. Relationship between Diffusion and Volume Fraction of Bacteria

The lack of agreement between the simulated tortuosity values perpendicular to the substratum, $\tau_{SIM,Z}$, and those calculated by Maxwell's equation was hypothesized to be attributed to the complexity of the distribution of bacteria within the biofilms. The volume fraction of bacteria, $1-\varepsilon(z)$, was found to vary within a biofilm and be a function of the distance, z (μm), from the substratum [Figure 5.2]. This non-linear distribution of bacteria, which is consistent with previous studies (Lewandowski 2000, Venugopalan et al 2005, Zhang and Bishop 1994), creates a bottle neck effect which

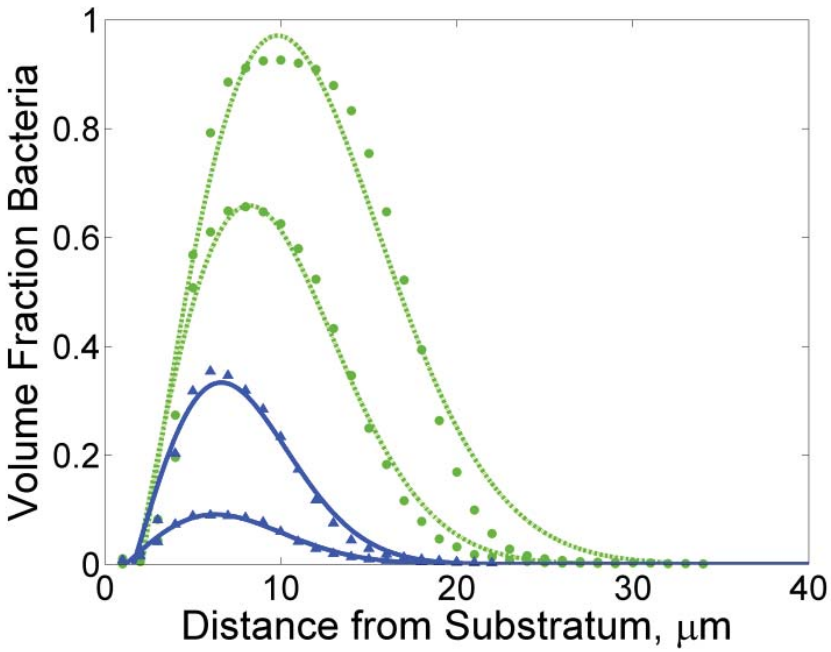

Figure 5.2 Volume fraction of bacteria, $1-\varepsilon(z)$, within an *E. coli* biofilm as a function of depth (μm) calculated using raw data (diamonds and circles) and by Eq. 5.8 (curves). Strain A (solid blue) and Strain B (dotted green) demonstrate both the intra-species and intra-strain variation of volume fraction of bacteria. Reprinted with permission from *Biotechnology and Bioengineering.*

restricts the diffusion of particles perpendicular to the substratum. Surprisingly, this nonlinear distribution was also found in biofilms with column like structures, which had an effect on nutrient transport perpendicular to the substratum that was contrary to our initial conjecture.

The porosity, ε, as a function of depth z (μm) from the substratum can be approximated by

$$\varepsilon(z) = 1 - a(z-b)\exp\left(-c(z-b)^2\right) \qquad 5.8$$

and the bacterial distribution of each strain can be approximated by $1-\varepsilon(z)$ when grown on a polystyrene microtiter plate [Figure 5.2]. The minimum porosity within the biofilm and the depth at which the minimum porosity occurred varied both within and between species and strains [Figure 5.2].

The model parameters a, b, c in Eq. 5.8 were estimated for each biofilm using non-linear least squares. These parameters were then associated with a random effects model:

$$y_{ijk} = \mu + b_i + s_{ij} + e_{ijk} \qquad 5.9$$

where μ is a fixed overall mean, b_i is a species effect (for species i), s_{ij} is the effect for the j^{th} strain, and e_{ijk} is the residual effect (for the k^{th} replicate). The random effects model for the parameters in Eq. 5.8 is summarized in Table 5.2, it is important to note the effects of the coefficients in Eq. 5.8 on the porosity and distribution of bacteria within a biofilm. Differentiating Eq. 5.8 and setting the derivative equal to zero, the depth at which the biofilm reaches its minimum porosity (or maximum volume fraction of bacteria) and the minimum porosity are, respectively:

$$z = b + \sqrt{(2c)^{-1}} \qquad 5.10$$

$$\varepsilon = 1 - a\sqrt{(2c)^{-1}}\exp(-0.5). \quad 5.11$$

Hence, the depth at which the biofilm reaches its minimum porosity is dependent upon the values of *b* and *c*, and the minimum porosity is dependent upon the values of *a* and *c.* Additionally, *c* describes the distribution of the bacteria within the biofilm, i.e. the level of localization of the biofilm in space. Given that the variation between species at all levels is significant for both *a* and *b* [Table 5.2], it is clear that the variability between species, within species and between strains with regards to the minimum porosity and the depth at which the minimum porosity occurs is substantial. While

Table 5.2 Random effects model for the coefficients *a*, *b* and *c* from Eq. 5.8; the tortuosity values determined by the Monte Carlo random walk for diffusion parallel to the substratum, $\tau_{SIM,XY}$, and perpendicular to the substratum, $\tau_{SIM,Z}$; and tortuosity values calculated using Eq. 5.13 with the raw data for porosity, $\tau_{Z,RAW}$, and the estimated values for porosity using Eq. 5.8, $\tau_{Z,EST}$. Reprinted with permission from *Biotechnology and Bioengineering.*

Values	**Mean (All Data)**	**Between Species Variance**	**Within Species (Between Strains) Variance**	**Within Strain Variance**
a	0.1165	0.0036	0.0033	0.0013
b	-1.5506	1.5579	1.6274	6.6297
c	0.0102	5.7072×10^{-7}	1.64×10^{-5}	1.95×10^{-5}
$\tau_{SIM,XY}$	0.7547	0.0142	0.0057	0.0061
$\tau_{SIM,Z}$	0.6340	0.0779	0.0234	0.0245
$\tau_{Z,RAW}$	0.6517	0.0627	0.0218	0.0179
$\tau_{Z,EST}$	0.6167	0.0666	0.0237	0.0175

variation between species, within species and between strains is small for the coefficient *c*, a slight change in *c* will have a dramatic effect on the graph of Eq. 5.8. By adding 0.005 to the mean value of *c* (keeping *a* and *b* constant) a biofilm which has a distribution consistent with strain A (higher), Figure 5.2, will be transformed to that of strain B (lower), Figure 5.2. Thus, the differences in the distribution of bacteria within the biofilm, and the biofilm porosity, can be characterized by the parameters *a*, *b*, and *c* in Eq. 5.8. Given the considerable intra- and inter-species variation (Bridier et al 2010) [Table 5.2], erroneous conclusions may arise when using mean values in modeling either the biofilm porosity or the distribution of bacteria within a single species biofilm. Additionally, biofilms are typically composed of multiple microbial species as well as various strains within the same species, and thus average values for single-species bacterial biofilms may not accurately describe heterogeneous biofilms.

To take into consideration the change in porosity at different depths within the biofilm, homogenization theory was used to calculate the average tortuosity factor of a particle diffusing parallel to, τ_{XY}, and perpendicular to, τ_Z, the substratum, respectively:

$$\tau_{XY} = \frac{D_{XY}^{\mathbf{eff}}}{D} = \frac{1}{L}\int_0^L \tau_M\left(\varepsilon(z)\right)dz \qquad 5.12$$

$$\tau_Z = \frac{D_Z^{\mathbf{eff}}}{D} = L\Big/\int_0^L \frac{1}{\tau_M\left(\varepsilon(z)\right)}dz \qquad 5.13$$

where *L* is total depth of the biofilm in μm (Goel et al 2006, Keener and Sneyd 1998, Shorten and Sneyd 2009, Suslina 2005). Raw data values for $\varepsilon(z)$ [Figure 5.3a] and the best fit equation in the form of Eq. 5.8 [Figure 5.3b] were used to generate a parity plot of the tortuosity values obtained from our simulation, $\tau_{SIM,Z}$, and the tortuosity values calculated by Eq. 5.13 [Figure 5.3]. The change in porosity (as a function of depth),

$\varepsilon(z)$, rather than the average biofilm porosity, ε, has a significant impact on nutrient diffusivity perpendicular to the substratum. Additionally, Eqs. 5.12 and 5.13 provide accurate estimations for the tortuosity values when nutrient transport is parallel to or perpendicular to the substratum, respectively. However, when using Eq. 5.8 as the function of porosity rather than the raw data, Eq. 5.13 fails to provide reasonable estimates for the tortuosity values when the porosity nears zero.

The values for the random effects model pertaining to the tortuosity values were determined for A) simulated values, B) values as determined by Eq. 5.13 using raw data for porosity $(\tau_{Z,RAW})$, and C) values as determined by Eq. 5.13 using Eq. 5.8 for porosity $(\tau_{Z,EST})$ [Table 5.2]. The mean tortuosity value parallel to the substratum is significantly greater than the mean tortuosity value perpendicular to the substratum (≈19%). The variance between species was approximately 5.5 times greater for the tortuosity values perpendicular to the substratum than those parallel to the substratum, and approximately 4 times greater for both the within species variance and within strain variance. In both cases, the within species variance and the within strain variance were similar. Values for tortuosity calculated by Eq. 5.13 resulted in an overestimate of the mean (+0.0177) when used in conjunction with the raw data and an underestimate (-0.0173) when used in conjunction with Eq. 5.8. However, this difference was not significant ($P < 0.05$). With regard to the variance between species, within species and within strains, both $\tau_{Z,RAW}$ and $\tau_{Z,EST}$ provide similar values which were in agreement with those calculated for the simulated tortuosity values, $\tau_{SIM,Z}$.

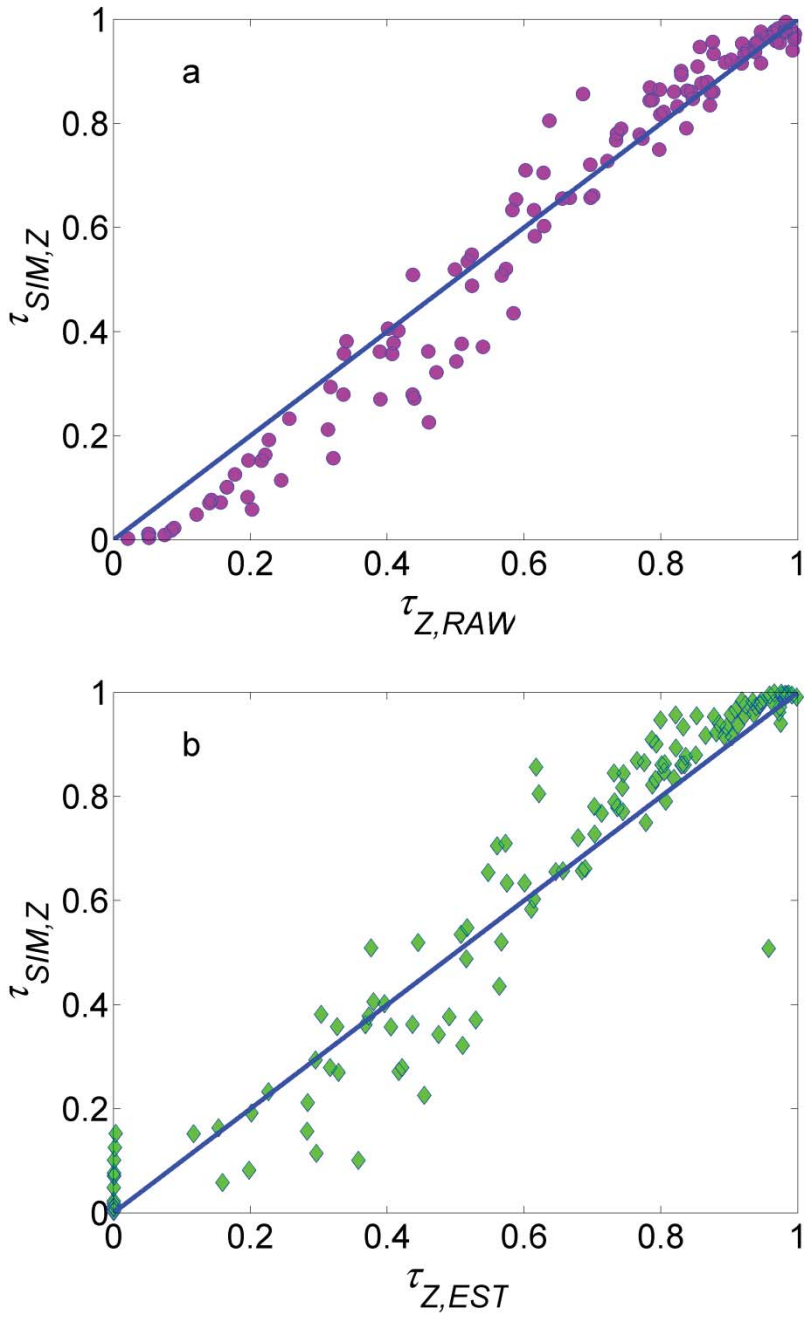

Figure 5.3 Parity plot of simulated tortuosity factor, $\tau_{SIM,Z}$, and the average tortuosity factor, τ_M, as calculated using Eq. 5.13, of a particulate diffusion perpendicular to the substratum using (a) raw data $\left(\tau_{Z,RAW}\right)$ and (b) estimated porosity values from Eq. 5.8, $\left(\tau_{Z,EST}\right)$. Reprinted with permission from *Biotechnology and Bioengineering.*

5.4.3. The Effects of Extracellular Polymeric Substances on Diffusion

EPS within bacterial biofilms is multifunctional. For instance, components of the EPS have been recognized to provide structural stability and differentiation (Danese et al 2000, Flemming et al 2007), aid in surface binding or coaggregation (Koo et al 2010, Marvasi et al 2010, Vu et al 2009), and provide or store nutrients to be utilized in times of nutrient deficiency (Wang et al 2007, Wolfaardt et al 1999).

Given the various roles of EPS one would expect the EPS to hinder diffusion in much the same way as the bacteria; hence, hindrance would depend on the porosity of the EPS, the diameter of the channels within the EPS, the size of the molecule being transported, and the distribution of the EPS. To further our knowledge in this area, six biofilms were constructed and examined, as described in our methods, which were stained for both bacteria and EPS. For a complete list of the bacterial strains, please refer to Appendix A.

The measurable volume fraction of EPS was calculated as a function of depth, and found that the EPS distribution can also be described by Eq. 5.8 [Figure 5.4a]. This distribution is in agreement with other reports (Staudt et al 2004, Venugopalan et al 2005). Mean ratios of bacteria to EPS can vary between species as well as over time (Staudt et al 2004, Venugopalan et al 2005); thus the volume fraction of EPS within a biofilm is not necessarily correlated to the volume fraction of bacteria. Estimates of EPS bio-volume have been reported to be between 10% and 90% of the total organic matter (Nielsen and Jahn 1999). In the 6 biofilms studied here, the measurable EPS ranged from 13.4% to 28.1% of the total biomass.

The EDCs were calculated, with and without the inclusion of EPS. Given our method for determining the EDCs, the inclusion of EPS essentially decreases the overall porosity of the biofilm. As expected, it was found that diffusion was still anisotropic;

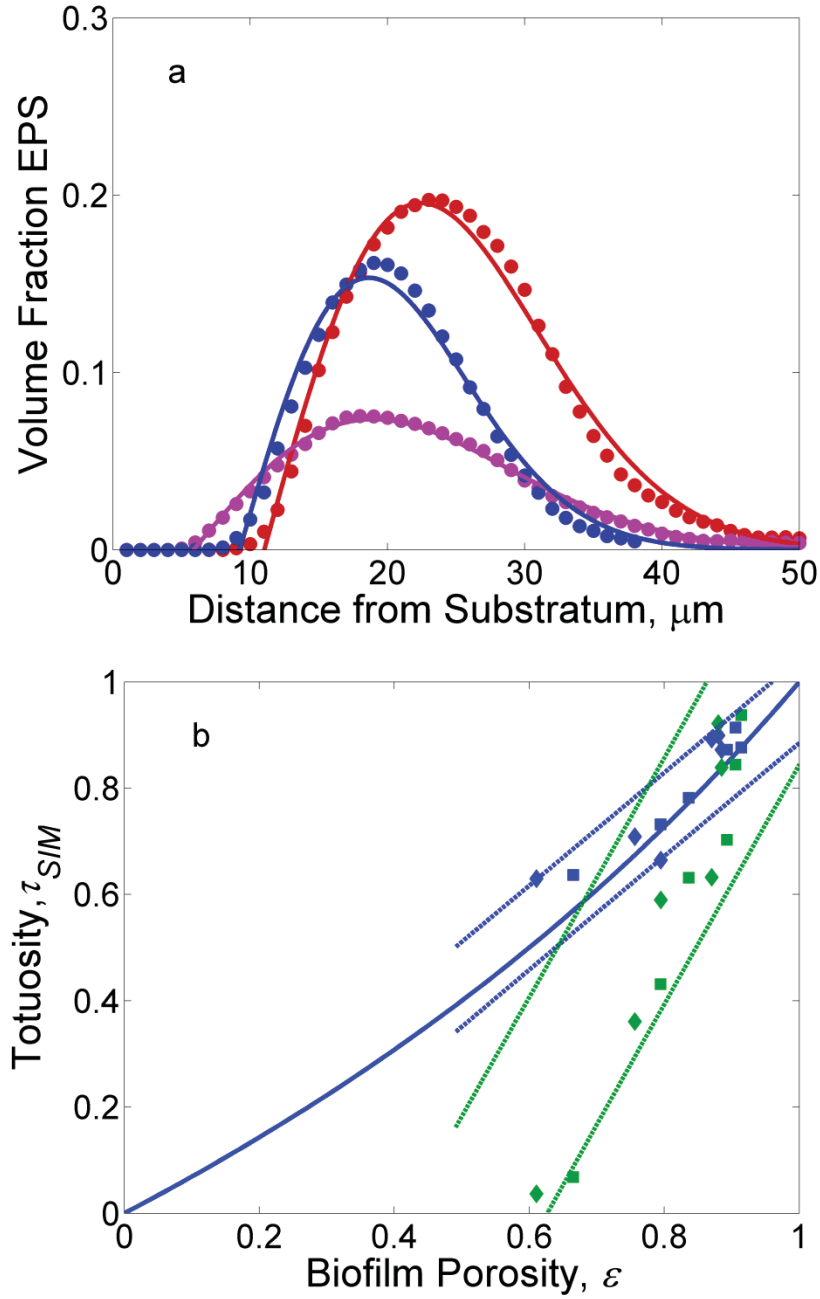

Figure 5.4 (a) Volume fraction of EPS within *E. faecalis* (blue), *P. aeruginosa* (magenta), and *S. enterica* (red) biofilms as a function of depth (μm) calculated using raw data (diamonds) and by Eq. 5.8 (solid curves). (b) Average tortuosity values parallel (blue) and perpendicular (green) to the substratum, with (diamonds) and without EPS (squares), versus porosity, ε, of the biofilm along with Maxwell's equation, Eq. 5.7 (solid line). Ninety-five percent confidence intervals (dotted lines) calculated from original 131 data points using linear regression. Reprinted with permission from *Biotechnology and Bioengineering.*

tortuosity factors for particles moving parallel to the substratum could be described by Maxwell's equation, and tortuosity factors for particles moving perpendicular to the substratum deviated from Maxwell's equation [Figure 5.4b]. Additionally, Eqs. 5.12 and 5.13 held for calculating the average tortuosity factor (data not shown).

To verify the reliability of our method to calculate EDCs, the results were compared to those of others (Oubekka et al 2011). Oubekka and colleagues calculated the EDC of BODIPY fluorescence in *Staphylococcus aureus* biofilm using FRAP. Their results corresponded to a mean tortuosity value of 0.4659 ± 0.175 for a particle moving parallel to the substratum. Using the same biofilm as Oubekka and colleagues, which was stained for both EPS and bacteria, our methods resulted in a tortuosity value of 0.709 for a particle moving parallel to the substratum and 0.361 for a particle moving perpendicular to the substratum. Our estimate is within 95% confidence levels of those calculated by Oubekka and colleagues.

The difference between the calculations found in this study and those reported by Oubekka and colleagues may potentially be attributed to the fact that ConA does not stain for all components of the EPS, and thus the calculation of the volume fraction of EPS in this study was an underestimate. Current mechanisms used to either visualize EPS in images or to separate EPS from bacterial biofilms have proven to be inefficient. EPS staining using lectin-staining combined with various imaging techniques have been used to estimate the EPS volume fraction (Boessmann et al 2003, Staudt et al 2004, Venugopalan et al 2005); however, lectin only binds to particular polysaccharides and these polysaccharides may only account for a portion, and in some cases a minor portion, of the total EPS (Flemming et al 2007, Laspidou and Rittmann 2002). Physical methods to extract EPS from intact biofilms have proven to be partially effective as these methods remove only 3-68% of the total EPS or the methods result in cell lysis

which interferes with the analysis of the EPS composition (Cao et al 2004, Nielsen and Jahn 1999). Thus, at this time there is no method which will accurately quantify the volume fraction of a biofilm which is EPS and the method used here is expected to provide an upper bound on tortuosity.

5.4.4. Reaction-Diffusion Model

This study has shown that the biomass distribution has a significant impact on the transport of nutrients within a biofilm. At the local level, Maxwell's equation is sufficient to describe the tortuosity factor, thus diffusion of nutrients in any direction within a rectangular biofilm can be described by the following diffusion equation and boundary conditions, respectively:

$$\frac{\partial C(x,y,z,t)}{\partial t} = \nabla \cdot \left[D\tau_M \left(\varepsilon(x,y,z) \right) \nabla C \right] \tag{5.14}$$

$$C(x,y,z=L_z,t) = C_0$$

$$\frac{\partial C(x,y,z=0,t)}{\partial z} = -F$$

$$C(x=0,y,z,t) = C(x=L_x,y,z,t) = C(x,y=0,z,t) = C(x,y=L_y,z,t) = C_0$$

where $C(x,y,z,t)$ is the concentration of nutrients attached to a substratum at time *t*, $\varepsilon(x,y,z)$ is the local porosity, L_z (μm) is the biofilm height, L_x (μm) is the biofilm depth, L_y (μm) is the biofilm width, C_0 is the concentration of nutrients at the biofilm-bulk fluid interface, and *F* is the flux of nutrients at the biofilm-substratum interface. For nutrient utilization by the biofilm, Eq. 5.14 becomes:

$$\frac{\partial C(x,y,z,t)}{\partial t} = \nabla \cdot \left[D\tau_M \nabla C \right] - r\left(1-\varepsilon(x,y,z)\right) B_{\max} \left(\frac{C}{C+K} \right) \tag{5.15}$$

where r is the rate of nutrient utilization by the biofilm, $B_{\max}$ is the maximum mass of bacteria per volume, and K is the nutrient concentration giving one-half the maximum rate of nutrient utilization (or the Monod saturation constant).

The biofilms studied in this work have a porosity that is dependent on distance from the substratum $\varepsilon(x,y,z)=\varepsilon(z)$. By using Eqs. 5.12 and 5.13 (homogenization) it follows that Eq. 5.15 becomes the anisotropic diffusion equation:

$$\frac{\partial C(x,y,z,t)}{\partial t} = D\tau_{XY}\frac{\partial^2 C}{\partial x^2} + D\tau_{XY}\frac{\partial^2 C}{\partial y^2} + D\tau_{Z}\frac{\partial^2 C}{\partial z^2} - r(1-\varepsilon(x,y,z))B_{\max}\left(\frac{C}{C+K}\right) \qquad 5.16$$

.

This model assumes the following:

1. Nutrients are transferred by diffusion, which obeys Fick's law only and react (or are utilized) by the bacteria.
2. Nutrient transfer is three dimensional.
3. There is only one limiting nutrient and the rate of nutrient utilization is described by the Monod equation and is dependent upon the volume fraction of biomass, $1-\varepsilon(z)$, within the biofilm.
4. Biofilm growth can either be on an impermeable substratum ($F=0$) or on a nutrient-providing substratum ($F>0$).
5. Hydrodynamic interactions between the particles and the biofilm are not included in the model.

It has been shown that convection may occur in bacterial biofilms (Stoodley et al 1994), however, the effect of convection is related to the fluid flow in the bulk liquid (De Beer et al 1996). While mixing of contents may occur in the cecum and ascending colon, very little to no mixing of the digesta occurs in the descending and transverse colon due to the viscosity of the digesta (Lentle et al 2005, Lentle and Janssen 2008, Lentle and Janssen 2010, Macfarlane and Macfarlane 2007). For simplicity, the distal

and transverse colon can be considered similar to a plug flow reactor (Kamerman and Wilkinson 2002, Muñoz-Tamayo et al 2010) where the digesta travels through the "tube" at a rate of 5.79×10^{-6} – 8.68×10^{-6} ms^{-1}. Since fluid flow in the bulk fluid must exceed 0.04 ms^{-1} to enhance nutrient transport (De Beer et al 1996), fluid flow in the large bowel would have little to no effect on the fluid dynamics within the biofilm. Additionally, this model can be easily modified to incorporate multiple rate-limiting substrates by the inclusion of multiple-Monod expressions for the reaction component of Eqs. 5.15 and 5.16 (Wanner et al 2006).

The incorporation of non-constant diffusion coefficients, which describe the anisotropic behavior, and the recognition that the bacteria will utilize nutrients from both the surrounding fluid and the substratum is where our model differs from existing models. Most models describe the uptake of nutrients by bacterial biofilms with a combination of diffusion and a Monod equation for reaction, however these models assume an impermeable substratum, except in the case of solid state fermentation (Rajagopalan et al 1997), as well as a constant diffusion coefficient (Alpkvist and Klapper 2007, Chang et al 2003, Janakiraman et al 2009, Kreft et al 2001, Picioreanu et al 2004, Rahman et al 2009, Wang and Zhang 2010, Xavier et al 2004). Eberl et al (2001) described the diffusion coefficient for biomass transport in terms of density; however their model is based on an educated guess rather than experimental values (Eberl et al 2001). Models of intestinal bacteria have incorporated nutrient uptake in order to describe bacterial growth rather than biofilm dynamics (Ishikawa et al 2011, Kamerman and Wilkinson 2002, Muñoz-Tamayo et al 2010, Wilkinson 2002). These models do not consider the change in nutrient concentration within a biofilm, as it is assumed that the bacteria are planktonic (free floating) and thus rely on nutrients from the bulk fluid rather than a substratum.

5.4.5. Model Simulation

In an attempt to mimic a bacterial biofilm attached to a fermentable food particle within the human large bowel, the parameters used in the model simulation [Figure 5.5a] represent experimental values currently available in the literature [Table 5.3]. Additionally, the initial concentration in the bulk fluid reflects the amount of glucose which enters the cecum. In the case of a biofilm attached to an impermeable substratum, the concentration of nutrients will decrease to low values at the substratum, which is consistent with the lack of viable cells observed near the substratum of biofilms grown on polystyrene plates [Figure 5.2]. However, if the bacterial biofilm is attached to a nutrient providing substratum, there will be increased growth, i.e. volume fraction of bacteria, near both the substratum-biofilm interface and the bulk fluid-biofilm interface (Macfarlane and Macfarlane 2006). This uptake of nutrients at the substratum-biofilm interface and bulk fluid-biofilm interface, causes nutrient gradients to develop so that a nutrient deficiency occurs near the center of the biofilm rather than near the substratum [Figure 5.5a]. This is consistent with the observed increase in void space at the center of biofilms growing on a food particle in human fecal matter [Figure 5.5b].

Further validation of the model was done by fitting Eq. 5.15 to concentration profiles of oxygen in artificial biofilms, grown in spherical beads, measured using microelectrodes at 30°C (Beuling et al 2000). As shown in Figure 5.6, our model is consistent with the reported oxygen concentration profiles of artificial biofilms with 1.6%, 3.6%, 7.8% and 15.5% volume fraction of bacteria. To fit our model to the data in Beuling (2000) it was assumed that the diffusion of oxygen in water at 30°C was 2.92×10^3 μm^3 s^{-1} (Wiesmann et al 1994), B_{max} was as described in Table 5.3, the distribution of bacteria was uniform as reported previously (Beuling et al 2000) and the Laplacian operator in Eq. 5.15 was transformed to spherical coordinates. Given that K is the

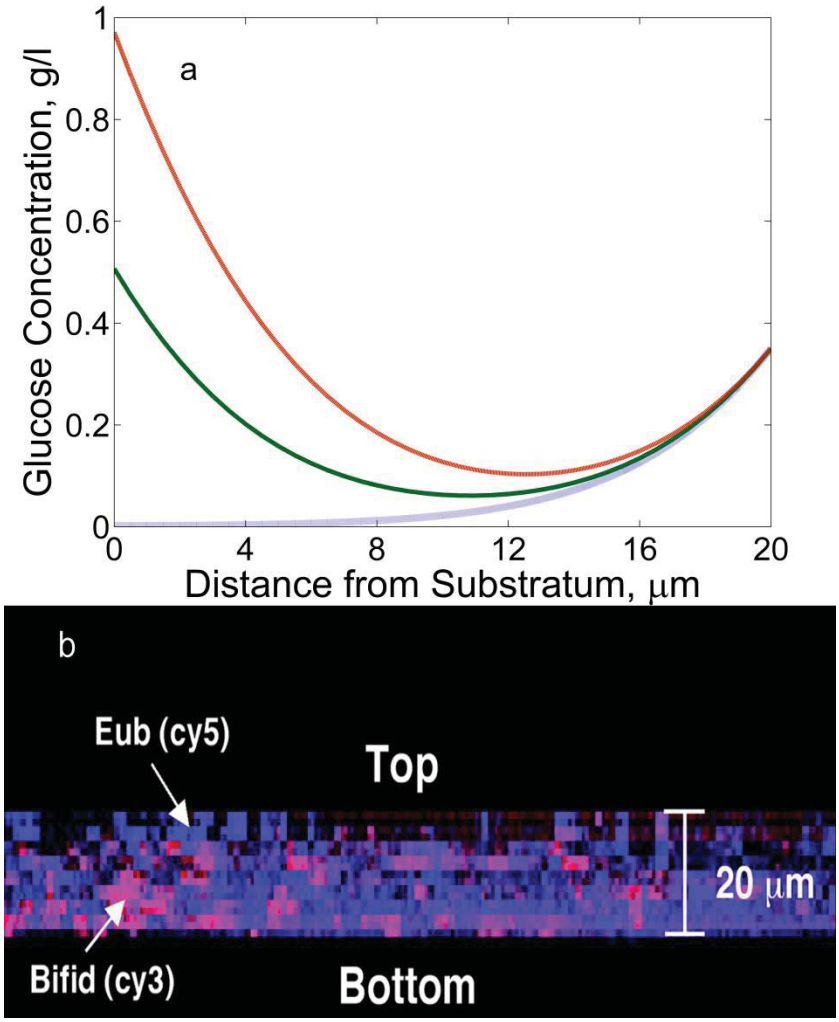

Figure 5.5 (a) Concentration of glucose (g l^{-1}) as a function of distance from the substratum (μm) attached to a non-permeable substratum (blue dotted), low value nutrient (green so*lid*) and high value nutrient (red dashed*)*. (b) Confocal z-sections of a biofilm attached to a fermentable food particle from human fecal matter. Total eubacteria (Eub) and bifidobacteria (Bifd) stained with Cy5 (blue) and Cy3 (red) labeled probes, respectively (Macfarlane and Macfarlane 2006). Used with permission from American Society for Microbiology. Reprinted with permission from *Biotechnology and Bioengineering.*

concentration of oxygen for which the utilization rate will reach half maximum, and that *K* is independent of the volume fraction of the biofilm that is bacteria, *K* was assumed to be the same for all four biofilms. While one would expect the oxygen utilization rate, *r*,

Table 5.3 Parameters used for modeling the concentration of nutrients as a function of distance [Figure 5.5a]. Reprinted with permission from *Biotechnology and Bioengineering.*

Variable	**Value**	**Units**	**References**
D	7.03×10^{2}	$\mu m^2 s^{-1}$	(Mitchell et al 1991) (at 37° C)
a	0.20158	None	This work.
b	-1.3045	None	This work.
c	0.014222	None	This work.
r	0.167	g glucose g dry biomass^{-1} s^{-1}	(Mlobeli et al 1998)
$B_{\max}$	307.69	g dry biomass l^{-1}	Estimated [a]
K	0.3	g l^{-1}	(Mitchell et al 1991)
$C(0,18)$	0.35	g l^{-1}	(Tony Bird, Pers. Comm.)
$\partial C_{LN}(t,0)/\partial z$	50	g l$^{-1}\mu m^{-1}$	Estimate
$\partial C_{HN}(t,0)/\partial z$	80	g l$^{-1}\mu m^{-1}$	Estimate

* $\tau_M(\varepsilon(z))$ is defined by the composition of Eq. 5.7 with Eq. 5.8. (*a*) 2×10^{-13} g/ dry bacterial cell; 1 cell = 0.65 μm^3. (*b*) Value from (Mlobeli 1996) was extrapolated from Fig. 13.

to be the same for all four biofilms, the oxygen utilization rate was allowed to be biofilm specific. The parameters K and r were estimated using non-linear least-squares. A value of 4.51×10^{-4} mol oxygen·m^{-3} for K was found as well as oxygen utilization rates of 1.75×10^{-5}, 4.51×10^{-5}, 3.20×10^{-5} and 3.23×10^{-5} mol oxygen·g biomass^{-1} s^{-1} for

the biofilms with 1.6%, 3.6%, 7.8% and 15.5% volume fraction bacteria, respectively. Although the utilization rates were similar in all four biofilms, the differences between the values reported here is likely a result of either a difference in the percentage of viable cells within the biofilms or an error in the calculation of the percentage of bacterial cells within the biofilms.

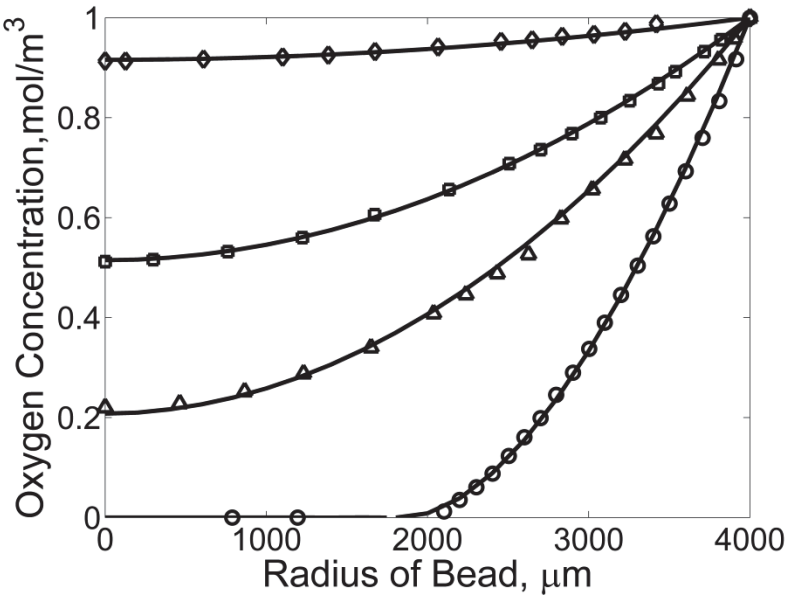

Figure 5.6 Oxygen concentration (mol m^{-3}) in artificial biofilms grown in spherical beads with cell volume fraction of 1.6% (diamond), 3.6% (square), 7.8% (triangle) and 15.5% (circle) as a function of the radius (μm) of the bead (Beuling et al 2000) with corresponding model fitting curves. Reprinted with permission from Biotechnology and Bioengineering.

5.5. Concluding Comments

Our method to calculate the EDC within bacterial biofilms provides a repeatable indirect estimate while being non-destructive to the biofilm. Our method provides tortuosity values within 95% confidence intervals as determined experimentally using

FRAP. The accuracy of our method will likely improve once there is a technique to accurately image the entire biomass volume fraction.

Our method has shown that the diffusivity of nutrients within bacterial biofilms is anisotropic and that the diffusion coefficient perpendicular to the substratum is significantly smaller than the diffusion coefficient parallel to the substratum. It was suggested by Hinson and Kocher (1996) that the diffusivity within a biofilm is lowered by the EPS rather than by steric hindrance by bacteria even though biofilms are assumed to be 99% water, of which 90-99% has been reported to be extracellular (Flemming et al 2005). Our results partially support this view, in that hindrance to nutrient transport is affected by the concentration of EPS. However, hindrance by bacteria cannot be discounted as the EPS is strain dependent and in some strains may account for as little as 10% of the total biomass. Our results indicate that both EPS and bacteria hinder nutrient transport within biofilms.

In light of these findings, a modified reaction-diffusion model to describe nutrient concentrations within bacterial biofilms that is consistent with experimental observations of oxygen transport in biofilms was proposed. While this model was chosen to describe nutrient transport within three-dimensional biofilms attached to a fermentable food particle within the human large bowel, this model is not limited to this particular application. For instance, this model may be easily modified to be utilized in solid-state fermentation models, models describing antibiotic transport within biofilms attached to medical devices or the transport of disinfectants within biofilms attached to food processing equipment.

Chapter 6 Key Contributions and Recommended Future Research

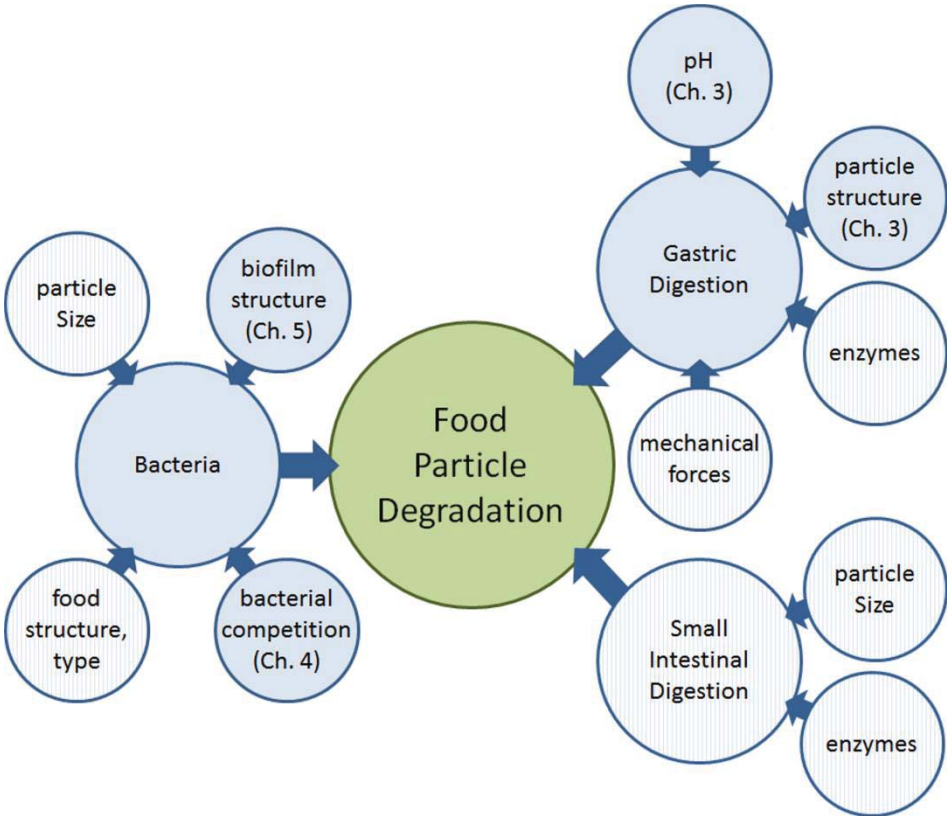

As our knowledge of food/bacteria/host interactions increases, it is becoming clear that there is enormous potential for this knowledge to contribute to the development of functional foods. To maximize the potential health benefits from functional foods, it is essential that we develop a deeper understanding of (1) how gastric digestion alters the food matrix; (2) how to predict the proportion of the food matrix which remains after digestion in the stomach and small bowel, as well as the composition of the remaining food matrix; (3) how diet impacts bacterial attachment to the digesta; (4) how diet impacts the bacterial colonization of the large bowel; and (5)

how bacteria work in a consortium to degrade food particles within the small and large bowel.

This thesis presents a number of new mathematical models which describe some of the key components of food/bacteria/host interaction in order to elucidate some of the essential physiological factors involved in nutrient bioavailability. Primarily, this thesis focused on modeling the interaction between the commensal bacteria (i.e. cross-feeding and nutrient competition) as well as the commensal bacteria/food interaction in the human large bowel. The effects of gastric pH and food matrix composition on the digestion of food within the human stomach were also considered in this thesis in order to better understand the food/bacteria and food/host interactions.

An essential aspect of food/host interactions is the ability to predict the bioaccessibility of nutrients as a result of acidic hydrolysis. Additionally, the gastric digestion aspect of this thesis provides a better understanding of how bacteria metabolize non-digested food components (food/bacteria interactions) in that bacterial extracellular enzymes may release nutrients from the food matrix in a manner similar to the way nutrients are released from a food matrix by acidic hydrolysis. In addition, the interaction between the commensal bacteria and food particles in the human large bowel is dependent on the food particle size and composition, which in turn are dependent on digestion in the stomach as the preferred substrates for bacterial fermentation are food particles which escape digestion in the small bowel.

The human stomach is a dynamic and complex system. Currently, there is a significant lack in modeling the degradation of food particles within the stomach. As mentioned in Chapter 3, in order to understand the complexities of gastric digestion and to build models which accurately describe the underlying digestive mechanisms, it is essential to determine the effects of different factors (food structure, preparation,

particle size, meal volume and composition, viscosity, pH, and temperature) on gastric digestion prior to investigating the interactions between those factors.

In Chapter 3, the focus was on the effect of pH, and acidic hydrolysis, as the pH directly affects enzymatic reactions, varies over the digestive time, and has been shown to have a significant effect on the amount of soluble loss from the food matrix. Thus, the effect of pH is foundational to the other mechanisms by which food is digested within the stomach.

In order to investigate the effect of pH, it was necessary to determine the effective diffusion coefficient (EDC) within the model foods (Edam and raw carrot core). To calculate the EDC, an objective method for measuring the propagation front of fluid into porous media was described. This is the first study to apply the method described in Chapter 3 to food digestion studies. The previous study which calculated a diffusion coefficient for simulated gastric fluid in carrot (Kong and Singh 2011) assumed that the EDC was constant, yet determined two values for the EDC (per pH value) depending on the digestion time. This was a surprising claim as it is well established that the EDC is dependent upon the moisture concentration in porous media. The method used here, further demonstrated the necessity of incorporating the concentration of the simulated gastric fluid (SGF) in determining the EDC of SGF diffusing into food matrices during gastric digestion.

In Chapter 3, a novel mechanistic, mathematical model was developed to predict solid particle loss of carrot as a result of acidic hydrolysis at constant pH. Rather than using an empirical model (Kong and Singh 2011), this model describes the solid loss in terms of the change in density of the food particle as soluble nutrients are released from the food matrix. This is consistent with digestive studies, where a “halo” effect occurs

as the cells and other components of the food matrix are damaged as a result of acidic hydrolysis, and nutrients are released (Kong and Singh 2009b, Tydeman et al 2010).

To provide a more realistic degradation profile, the model incorporated the expected change in pH during the gastric digestive period. Here a prediction of the likely rate of soluble particle loss of carrot during digestion is provided, which demonstrates that the particle loss is slower at the beginning of the digestion period as a result of high pH and an increase in solid loss occurs as the pH lowers.

The model presented here can be modified to predict the solid loss of other foods; however in order to utilize this model additional experiments are required to determine the specific pH dependency of the coefficients of the EDC parameters. Essentially, the parameter values of the exponential equation used to describe the EDC are found empirically due to necessity. Additional studies are required to determine the exact components of the food structure that dictate the parameters of the EDC function. Ideally, future work will modify the EDC function to incorporate food composition effects. It is quite possible that the pH dependency may be consistent between foods that are structurally similar. Foods such as carrot and parsnip have a high concentration of water and similar cellular structure, fat content, and protein content. Such foods may have a similar relationship between the pH and the EDC function.

Advances in modeling necessitate that the relationship between pH and the efficacy of gastric enzymes, such as pepsin, be determined. Of course, this also requires a clear understanding of the specific protein structures that are susceptible to proteolysis by pepsin. Further experiments are required to specifically consider the different components of the food matrix (protein, fat, polysaccharides, etc.) and reveal how the different components of the food structure affect the efficacy of both acidic hydrolysis and proteolysis. This is of particular necessity as the use of emulsions in food products

increases. Lipid and water emulsions may be quite complex, with the inclusion of a variety of other components: proteins, polysaccharides, sugars, salts, etc. As noted by Singh and Ye (2013) interactions between the gastric fluid and the emulsions may cause conformational changes which not only affects the structure integrity of the emulsion (especially at low pH) but may have a marked effect on the digestibility and bioaccessibility of the emulsion components. Further studies of emulsions at low pH are necessary to understand how the gastric environment affects the structural integrity of emulsions.

The model presented in this thesis depicting particle degradation can be considered a foundational model as it considers a fundamental aspect of gastric digestion (acidic hydrolysis) which also affects the efficacy of enzymatic reactions. A more complete model would extend this model to incorporate enzymatic reactions, erosion from contact between food particles and fragmentation as a result of peristaltic contractions. Of course, erosion and fragmentation will also be related to the food matrix composition.

Many foods matrices contain components which are unable to be digested in the stomach or the small bowel. For instance dietary fibers, such as non-starch polysaccharides and resistant starch, transit from the gastric region through the small intestinal tract and into the colon having only undergone conformational changes as a result of mastication and gastric digestion. These food components are then readily available for fermentation by the commensal bacteria.

Chapter 4 focused on another very important aspect of human digestion and health: the relationship between food particles and the human commensal intestinal bacteria. In this chapter a modified version of the model proposed by Amaretti et al (2007) was used to characterize growth kinetics (substrate degradation and the

subsequent growth of bacteria and production of metabolites) of 18 bifidobacterial strains when growth with inulin, oligofructose and fructose as substrates. Upon analysis, it was shown that the model can be further simplified to omit the maintenance term when the ratio of substrate concentration to bacterial inoculum is low. Further experiments are required to determine whether this is the case when bacteria are grown in a nutrient rich environment.

The aforementioned model was extended to account for preferential degradation of substrate by the bacterium, which was observed by various strains of *Bifidobacterium* when grown with oligofructose as the substrate (Falony et al 2009b). According to a review of the literature, the model proposed here is the first model to describe preferential degradation of a substrate. This is an important contribution as this model confirms that degradation of oligofructose results in different values for the bacterial yield, specific growth rate, and metabolite production rates depending on whether the degree of polymerization (DP) of the polysaccharide is preferred or less preferred. Thus, in the formulation of functional foods or prebiotics, the type of polysaccharides used will have a significant impact on the competitiveness of particular bacterium as well as the metabolites produced by the bacterium. Such effects need to be carefully considered to ensure that the formulation of a functional food has the desired functionality (i.e. increase growth rate of targeted bacterium, or increased production of a particular short chain fatty acid).

Understanding the mechanisms which cause the change in metabolite production will also play a key role in improving functional foods. At this time, there is only the observation that the type of metabolite produced depends upon the DP of the polysaccharide; however there must be a specific mechanism that triggers the reduction of pyruvate to either lactate or formate, acetate and ethanol. A correlation between the

specific growth rate of the bacterium and the observed change in metabolite production has been mentioned in the literature; however it is doubtful that a lowered growth rate is the trigger. More than likely, the lowered growth rate and yield is a result of more energy required to degrade the non-preferred substrate and less energy available to be expended on growth and cell division. This would also explain the change in metabolite production, since the reduction of pyruvate to formate, acetate and ethanol results in additional ATP which would be necessary for the bacterium to degrade the non-preferred substrate.

In addition to the models described above, a novel, mechanistic model was developed to describe the competition between *Bacteroides thetaiotaomicron* LMG 11262 and *Bifidobacterium longum* LMG 11047 and *B. thetaiotaomicron* LMG 11262 and *Bifidobacterium breve* Yakult for a substrate (inulin). This competition model includes the potential for microbial cross-feeding as a result of released nutrient fragments from extracellular degradation of the substrate.

This is the first microbial competition model of its kind, as the proposed mathematical model provides a complete picture of the growth kinetics of two competing/cross-feeding bacteria. Previously proposed models were either empirical models (provided no insight into the mechanisms driving competition or cross-feeding) or neglected important aspects of the coculture dynamics (e.g., the competing or nutrient providing bacterium, or the primary substrate).

The most significant result in Chapter 4 was that the competitive/cross-feeding model adequately predicted co-culture dynamics using parameter values determined from monoculture experiments. This finding means that significantly less bacterial growth experiments are necessary to predict coculture growth kinetics (polysaccharide degradation and the subsequent bacterial growth and metabolite production).

At this time, the competitive/cross-feeding model has been validated for *B. thetaiotaomicron* LMG 11262 grown with either *B. longum* LMG 11047 or *B. breve* Yakult. Additional experiments are necessary to validate the model for a variety of commensal bacteria. Future work would also include an extension of this model to incorporate other types of microbial cross feeding. Little work would be required to modify the competition/cross-feeding model presented here to include the consumption (by the secondary bacterium) of a metabolite produced by the primary bacterium. This model could also be extended to describe the instances where the secondary bacterium can only metabolize the primary substrate in the presence of and concurrently with a particular metabolite. Preferential degradation by either bacterium could also be incorporated into this model. In order to validate such extensions, it is essential for additional experiments, both mono- and coculture, to be conducted where the bacterial growth, substrate concentration, and metabolite concentrations are measured at frequent time intervals as seen in the work of Falony et al (2009a).

As mentioned in the introduction, Chapter 4 is a macroscopic view of bacterial growth as a result of substrate metabolism. In Chapter 5 a microscopic view was taken. Here the transport of nutrients within a bacterial biofilm was investigated. Within bacterial biofilms, nutrient gradients occur as the diffusing nutrients are utilized by the bacteria. The nutrient concentration has a marked effect on the structure of the biofilm, as bacteria will grow where the nutrients are highest.

In order to characterize the transport of nutrients within bacterial biofilms, a repeatable, indirect method to estimate of the EDC was used. This method results in EDC values (for nutrients moving parallel to the substratum) that are within the 95% confidence intervals of those determined experimentally using FRAP.

The method described in this thesis to calculate the biofilm porosity is a significant improvement to methods described previously, as the use of CLSM images is not destructive to the biofilm. The analysis of biofilms reconstructed from CLSM images revealed that the volume fraction of bacteria varies within a biofilm and is a function of the distance from the substratum. The bacterial distribution had a profound effect on the nutrient transport within bacterial biofilms. The non-linear distribution of bacteria creates a bottle neck effect which restricts the diffusion of particles perpendicular to the substratum. Surprisingly, this nonlinear distribution was also found in biofilms with column like structures, which had an effect on nutrient transport perpendicular to the substratum that was contrary to our initial conjecture. Nutrient transport perpendicular to the substratum was found to be significantly slower than transport parallel to the substratum in biofilms with low porosity.

Examination of the relationship of the biofilm porosity to the EDC calculated for 131 biofilms demonstrated that Maxwell's equation provides a reliable estimate for the EDC (as a function of biofilm porosity) when considering transport of nutrients parallel to the substratum. Maxwell's equation may also be used to estimate the EDC of a nutrient diffusing perpendicular to the substratum; however in order to do so, one must use the harmonic mean of the tortuosity (ratio of EDC to the diffusion coefficient in water) over the depth of the biofilm. This method considers the depth dependency of the bacterial distribution which is essential for calculating the EDC perpendicular to the substratum in biofilms with low porosity. Additionally, the evidence that the distribution of the bacteria has a significant effect on value of the EDC means that future experimental methods must measure the EDC perpendicular to the substratum rather than parallel, which has been the convention.

The method described in Chapter 5 to determine the fraction of the biofilm which is composed of bacteria was also used to determine the fraction of the biofilm which was composed of EPS. While the method is sound, it is dependent upon the reliability and accuracy of the method for staining the EPS before CLSM images are taken. As mentioned in Section 5.4.3, the current methods for staining the EPS are not accurate as the stain only targets specific components of the EPS. Thus, the volume fractions of EPS presented here are likely to be underestimates, which implies that the EDC values may be even lower than reported here. However, it is important to note that the relationship between the porosity and tortuosity will not change. Future work must include additional methods for visualizing the structural components of the EPS, to ensure that all components of the EPS that may hinder nutrient transport are accounted for in CLSM images.

A modified reaction-diffusion model which incorporated the porosity and distribution of the bacteria was proposed in Chapter 5. The inclusion of the bacterial population improves the description of the change of concentration of nutrients within the biofilm. The model was validated by comparing the oxygen concentration within artificial biofilms with known porosity. As demonstrated in Figure 5.6 (Section 5.4.5), the proposed reaction-diffusion model fit to the oxygen concentration profiles is remarkably accurate.

Within the human gastrointestinal tract, bacterial biofilms are typically found attached to a nutrient providing substratum (a food particle which escaped digestion in the stomach and small bowel or the mucosa of the intestinal wall) and thus nutrients are derived from both the substratum and the bulk fluid. Therefore, there will be increased growth, i.e. volume fraction of bacteria, near both the substratum-biofilm interface and the bulk fluid-biofilm interface (Macfarlane and Macfarlane 2006). This uptake of

nutrients, at the substratum-biofilm interface and bulk fluid-biofilm interface, causes nutrient gradients to develop so that a nutrient deficiency occurs near the center of the biofilm rather than near the substratum. This is clearly described by the simulation of the proposed reaction-diffusion model, which assumed that the concentration of nutrients originates from both the substratum and the bulk fluid. Additionally, these results are consistent with the observed increase in void space at the center of biofilms growing on a food particle in human fecal matter (Macfarlane and Macfarlane 2006).

The work presented in Chapter 5 clearly demonstrates the necessity of incorporating the volume fraction of bacteria in determining the rate of change in the concentration of the nutrients within the biofilm: both in terms of diffusion and reaction.

Presently, the specific processes involved in the structural formation and detachment of commensal enteric bacterial biofilms attached to food particles have yet to be ascertained. However, it is likely that both quorum sensing and nutrient availability will have a significant influence on both the structural formation and detachment of bacterial biofilms attached to digesta.

While this thesis clearly provides advances in the modeling and understanding of the dynamics of bacteria associated with food particles in the human bowel, there is still much work to be done. For instance, this thesis has not improved the mathematical models describing bacterial attachment. Bacterial attachment is a very complex process. While the DLVO, LW-AB and XDLVO models describe aspects of the physicochemical properties of bacterial attachment, they do not, however, incorporate biological factors. The lack of inclusion of biological factors in the above models may contribute to the discrepancy between model predictions and experimental observations. A critical analysis of the agreement of XDLVO and LW-AB theories with experiments may give valuable insights into the environments for which these theories are

applicable. Given the complexity of the various environments in which bacteria grow and the environmental specific attachment methods employed by bacteria, a universal model may not be feasible or appropriate. Of course a prerequisite to the further development of mathematical models is a better understanding of the mechanisms used by the commensal intestinal bacteria to attach to various food particles.

One of the key distinguishing differences between biofilms in the GI tract and biofilms found in various other environments is the fact that the biofilms in the GI tract adhere to a nutrient providing substratum. The metabolism of complex dietary plant cell wall components occurs as a result of enzymatic reactions. Given that the hydrolysis of polysaccharides by some bacterial populations results in the release of polysaccharide fragments which can be utilized by closely associated bacteria, in this case hydrolysis must occur extracellularly. It may be that copious amounts of enzymes are released and diffuse into the food matrix, releasing insoluble cell components. If this is the case, then the food degradation model described in Chapter 2 may be relevant to the metabolism of food particles by bacteria in the large bowel. Further studies are needed.

The life-cycle of a bacterial biofilm attached to a food particle in the human intestinal tract entails (1) irreversible attachment, (2) accumulation and growth, and (3) detachment. Detachment is dependent upon nutrient availability. Thus in addition, to understanding the mechanisms of enzymatic hydrolysis by the commensal bacteria, studies which measure the change in the food matrix and characterize food degradation as a result of enzymatic hydrolysis are essential.

To summarize, this thesis has provided a number of novel mathematical models which pertain to food/host for food/microbial interactions. However, there are three main contributions that should be highlighted. Nutrient transport within bacterial biofilms has been historically assumed to be isotropic. The work in this thesis has not

only provided evidence that nutrient transport within biofilms is anisotropic, but the mathematical model incorporating the bacterial distribution has clearly demonstrated that the bacterial distribution has a significant effect on nutrient transport. As mentioned earlier, mathematical models can provide information that otherwise may be difficult, expensive or even impossible to determine *in vivo*. This thesis also provides a mathematical model which can predict soluble solid loss as a result of acidic hydrolysis at various pH values, which provides a more accurate description of the *in vivo* environment. Lastly, a mathematical model which predicts the co-culture dynamics of commensal bacteria has been proposed. This model provides a better understanding of food/microbial interactions. In particular, this model will provide information on the time it takes the bacterial population to degrade different food components, the quantities of metabolites produced by the competing/cross-feeding bacteria, and the expected bacterial concentrations which result from the degradation of the substrate.

On a final note, while the models described here have been applied to particular environments, it is important to realize that these models are not restricted to any one environment. For instance the model used to describe the propagation of the acidic water during gastric digestion (Eqs. 3.1 and 3.2; Section 3.3.2) can also be applied to describe the sodium chloride concentration in cheese during the brining process (Van Wey et al Submitted-b). The non-preferential degradation, preferential degradation and competing/cross-feeding models proposed in Chapter 4 (Eqs. 4.2, 4.3 and 4.5; Sections 4.3.2, 4.4.1 and 4.4.3) have been validated for commensal intestinal bacteria; however, the models may be applicable to bacteria associated with water treatment systems, river beds, and food processing plants. And finally, the reaction diffusion model (Eq. 5.15; Section 5.4.4) proposed in Chapter 5 can be applied to any rate limiting substance (whether it be sugars, oxygen, or nitrogen) in any environment where biofilms form.

REFERENCES

Albrecht T, Almond J, Alfa M, Alton GG, Aly R, Asher D *et al* (1996). In: Baron S (ed). *Medical Microbiology*, 4th edn. The University of Texas Medical Branch at Galveston: Galveston.

Aldous BJ, Franks F, Greer AL (1997). Diffusion of water within an amorphous carbohydrate. *J Mater Sci* **32:** 301-308.

Alpkvist E, Klapper I (2007). A multidimensional multispecies continuum model for heterogeneous biofilm development. *B Math Biol* **69:** 765-789.

Amaretti A, Bernardi T, Tamburini E, Zanoni S, Lomma M, Matteuzzi D *et al* (2007). Kinetics and metabolism of *Bifidobacterium adolescentis* MB 239 growing on glucose, galactose, lactose, and galactooligosaccharides. *Appl Environ Microb* **73:** 3637-3644.

Anderl JN, Zahller J, Roe F, Stewart PS (2003). Role of nutrient limitation and stationary-phase existence in *Klebsiella pneumoniae* biofilm resistance to ampicillin and ciprofloxacin. *Antimicrob Agents Ch* **47:** 1251-1256.

Axelsson A, Persson B (1988). Determination of effective diffusion coefficients in calcium alginate gel plates with varying yeast cell content. *Appl Biochem Biotech* **18:** 231-250.

Baranyi J, Roberts TA (1994). A dynamic approach to predicting bacterial growth in food. *Int J Food Microbiol* **23:** 277-294.

Barken KB, Pamp SJ, Yang L, Gjermansen M, Bertrand JJ, Klausen M *et al* (2008). Roles of type IV pili, flagellum-mediated motility and extracellular DNA in the formation of mature multicellular structures in *Pseudomonas aeruginosa* biofilms. *Environ Microbiol* **10:** 2331-2343.

Bates DM, Watts DG (2007). *Nonlinear Regression Analysis and its Applications*. John Wiley & Sons: New York.

Bayoudh S, Othmane A, Mora L, Ben Ouada H (2009). Assessing bacterial adhesion using DLVO and XDLVO theories and the jet impingement technique. *Colloid Surface B* **73:** 1-9.

Bayston R (1999). Biofilms in medicine and disease: An overview. In: Wimpenny J, Gilbert P, Walker J, Brading M, Bayston R (eds). *Biofilms: The Good, The Bad and The Ugly*. BioLine: Cardiff. pp 1-6.

Begley M, Hill C, Gahan CGM (2006). Bile salt hydrolase activity in probiotics. *Appl Environ Microb* **72:** 1729-1738.

Belenguer A, Duncan SH, Calder AG, Holtrop G, Louis P, Lobley GE *et al* (2006). Two routes of metabolic cross-feeding between *Bifidobacterium adolescentis* and butyrate-producing anaerobes from the human gut. *Appl Environ Microb* **72:** 3593-3599.

Bernalier-Donadille A (2010). Fermentative metabolism by the human gut microbiota. *Gastroen Clin Biol* **34:** S16-S22.

Beuling EE, Van Dusschoten D, Lens P, Van Den Heuvel JC, Van As H, Ottengraf SPP (1998). Characterization of the diffusive properties of biofilms using pulsed field gradient-nuclear magnetic resonance. *Biotechnol Bioeng* **60:** 283-291.

Beuling EE, van den Heuvel JC, Ottengraf SPP (2000). Diffusion coefficients of metabolites in active biofilms. *Biotechnol Bioeng* **67:** 53-60.

Beyenal H, Lewandowski Z (2002). Internal and external mass transfer in biofilms grown at various flow velocities. *Biotechnol Prog* **18:** 55-61.

Boessmann M, Staudt C, Neu TR, Horn H, Hempel DC (2003). Investigation and modeling of growth, structure and oxygen penetration in particle supported biofilms. *Chem Eng Technol* **26:** 219-222.

Boks NP, Norde W, van der Mei HC, Busscher HJ (2008). Forces involved in bacterial adhesion to hydrophilic and hydrophobic surfaces. *Microbiology* **154:** 3122-3133.

Boland T, Latour RA, Sutzenberger FJ (2000). Molecular basis of bacterial adhesion. In: An YH, Friedman RJ (eds). *Handbook of Bacterial Adhesion: Principles, Methods and Appllcations*. Humana Press Inc.: Totowa. pp 29-41.

Boles BR, Thoendel M, Singh PK (2005). Rhamnolipids mediate detachment of *Pseudomonas aeruginosa* from biofilms. *Mol Microbiol* **57:** 1210-1223.

Bornhorst GM, Singh RP (2012). Bolus formation and disintegration during digestion of food carbohydrates. *Compr Rev Food Sci F* **11:** 101-118.

Borruel N, Carol M, Casellas F, Antolin M, De Lara F, Espin E *et al* (2002). Increased mucosal tumour necrosis factor α production in Crohn's disease can be downregulated *ex vivo* by probiotic bacteria. *Gut* **51:** 659-664.

Bouhnik Y, Vahedi K, Achour L, Attar A, Salfati J, Pochart P *et al* (1999). Short-chain fructo-oligosaccharide administration dose-dependently increases fecal bifidobacteria in healthy humans. *J Nutr* **129:** 113-116.

Briandet R, Lacroix-Gueu P, Renault M, Lecart S, Meylheuc T, Bidnenko E *et al* (2008). Fluorescence correlation spectroscopy to study diffusion and reaction of bacteriophages inside biofilms. *Appl Environ Microb* **74:** 2135-2143.

Bridier A, Dubois-Brissonnet F, Boubetra A, Thomas V, Briandet R (2010). The biofilm architecture of sixty opportunistic pathogens deciphered using a high throughput CLSM method. *J Microbiol Meth* **82:** 64-70.

Brownawell AM, Caers W, Gibson GR, Kendall CWC, Lewis KD, Ringel Y *et al* (2012). Prebiotics and the health benefits of fiber: Current regulatory status, future research, and goals. *J Nutr* **142:** 962-974.

Bryers JD, Drummond F (1998). Local macromolecule diffusion coefficients in structurally non-uniform bacterial biofilms using fluorescence recovery after photobleaching (FRAP). *Biotechnol Bioeng* **60:** 462-473.

Bublin M, Radauer C, Knulst A, Wagner S, Scheiner O, Mackie AR *et al* (2008). Effects of gastrointestinal digestion and heating on the allergenicity of the kiwi allergens Act d 1, actinidin, and Act d 2, a thaumatin-like protein. *Mol Nutr Food Res* **52:** 1130-1139.

Bull JJ, Harcombe WR (2009). Population dynamics constrain the cooperative evolution of cross-feeding. *PLoS ONE* **4:** e4115.

Burgess CM, Smid EJ, van Sinderen D (2009). Bacterial vitamin B2, B11 and B12 overproduction: An overview. *Int J Food Microbiol* **133:** 1-7.

Cao H, Li X, Jiang B, Sun J, Zhang Y (2004). Evaluation of the influence of extracellular polymeric substances on the mass transport of substrate within multispecies biofilms. *Chinese J Chem Eng* **12:** 590-594.

Carbonaro M, Maselli P, Nucara A (2012). Relationship between digestibility and secondary structure of raw and thermally treated legume proteins: A Fourier transform infrared (FT-IR) spectroscopic study. *Amino Acids* **43:** 911-921.

Carey MC, Small D, Bliss C (1983). Lipid digestion and absorption. *Annu Rev Physiol* **45:** 651-677.

Chamberlain AHL (1992). The role of adsorbed layers in bacterial adhesion. In: Melo LF, Bott TR, Fletcher M, Capdeville B (eds). *Biofilms — Science and Technology*. Springer Netherlands. pp 59-67.

Chang I, Gilbert ES, Eliashberg N, Keasling JD (2003). A three-dimensional, stochastic simulation of biofilm growth and transport-related factors that affect structure. *Microbiology* **149:** 2859-2871.

Chassard C, Bernalier-Donadille A (2006). H2 and acetate transfers during xylan fermentation between a butyrate-producing xylanolytic species and hydrogenotrophic microorganisms from the human gut. *FEMS Microbiol Lett* **254:** 116-122.

Chen J, Liang RH, Liu W, Li T, Liu CM, Wu SS *et al* (2013). Pectic-oligosaccharides prepared by dynamic high-pressure microfluidization and their in vitro fermentation properties. *Carbohyd Polym* **91:** 175-182.

Chen M-Y, Lee D-J, Tay J-H, Show K-Y (2007). Staining of extracellular polymeric substances and cells in bioaggregates. *Appl Microbiol Biot* **75:** 467-474.

Cherbut C (2002). Inulin and oligofructose in the dietary fibre concept. *Brit J Nutr* **87:** S159-162.

Chresand TJ, Dale BE, Hanson SL (1988). A stirred bath technique for diffusivity measurements in cell matrices. *Biotechnol Bioeng* **32:** 1029-1036.

Coconnier MH, Bernet MF, Kernéis S, Chauvière G, Fourniat J, Servin AL (1993). Inhibition of adhesion of enteroinvasive pathogens to human intestinal Caco-2 cells by *Lactobacillus acidophilus* strain LB decreases bacterial invasion. *FEMS Microbiol Lett* **110:** 299-305.

Conly JM, Stein K, Worobetz L, Rutledge-Harding S (1994). The contribution of vitamin K_2 (menaquinones) produced by the intestinal microflora to human nutritional requirements for vitamin K. *Am J Gastroenterol* **89:** 915-923.

Cookson AL, Woodward MJ (1999). The role of fimbriae in adhesion of verocytotoxic *Escherichia Coli* (VTEC). In: Wimpenny J, Gilbert P, Walker J, Brading M, Bayston R (eds). *Biofilms: The Good, The Bad and The Ugly*. BioLine: Cardiff. pp 73-80.

Cookson AL, Cooley WA, Woodward MJ (2002). The role of type 1 and curli fimbriae of shiga toxin-producing *Escherichia coli* in adherence to abiotic surfaces. *Int J Med Microbiol* **292:** 195-205.

Cornu M, Billoir E, Bergis H, Beaufort A, Zuliani V (2011). Modeling microbial competition in food: Application to the behavior of *Listeria monocytogenes* and lactic acid flora in pork meat products. *Food Microbiol* **28:** 639-647.

Costabile A, Kolida S, Klinder A, Gietl E, Buerlein M, Frohberg C *et al* (2010). A double-blind, placebo-controlled, cross-over study to establish the bifidogenic effect of a very-long-chain inulin extracted from globe artichoke (*Cynara scolymus*) in healthy human subjects. *Brit J Nutr* **104:** 1007-1017.

Costerton JW, Rozee KR, Cheng KJ (1983). Colonization of particulates, mucous, and intestinal tissue. *Prog Food Nutr Sci* **7:** 91-105.

Costerton JW, Cheng KJ, Geesey GG, Ladd TI, Nickel JC, Dasgupta M *et al* (1987). Bacterial biofilms in nature and disease. *Annu Rev Microbiol* **41:** 435-464.

Crank J (1975). *The Mathematics of Diffusion*, Second edn. Oxford University Press: New York.

Crittenden R, Laitila A, Forssell P, Matto J, Saarela M, Mattila-Sandholm T *et al* (2001). Adhesion of bifidobacteria to granular starch and its implications in probiotic technologies. *Appl Environ Microb* **67:** 3469-3475.

Cummings JH, Pomare EW, Branch WJ, Naylor CPE, Macfarlane GT (1987). Short chain fatty acids in human large intestine, portal, hepatic and venous blood. *Gut* **28:** 1221-1227.

Cummings JH, MacFarlane GT (1997). Role of intestinal bacteria in nutrient metabolism. *Clin Nutr* **16:** 3-11.

Danese PN, Pratt LA, Kolter R (2000). Exopolysaccharide production is required for development of *Escherichia coli* K-12 biofilm architecture. *J Bacteriol* **182:** 3593-3596.

Davenport HW (1982). *Physiology of the Digestive Tract*, 5th edn. Year Book Medical Publishers, Inc.: Chicago.

Davey ME, Caiazza NC, O'Toole GA (2003). Rhamnolipid surfactant production affects biofilm architecture in *Pseudomonas aeruginosa* PAO1. *J Bacteriol* **185:** 1027-1036.

Davey MJ, Landman KA, McGuinness MJ, Jin HN (2002). Mathematical modeling of rice cooking and dissolution in beer production. *AIChE J* **48:** 1811-1826.

Davies DG, Parsek MR, Pearson JP, Iglewski BH, Costerton JW, Greenberg EP (1998). The involvement of cell-to-cell signals in the development of a bacterial biofilm. *Science* **280:** 295-298.

De Beer D, Stoodley P, Lewandowski Z (1996). Liquid flow and mass transport in heterogeneous biofilms. *Water Res* **30:** 2761-2765.

De Beer D, Stoodley P, Lewandowski Z (1997). Measurement of local diffusion coefficients in biofilms by microinjection and confocal microscopy. *Biotechnol Bioeng* **53:** 151-158.

De Filippo C, Cavalieri D, Di Paola M, Ramazzotti M, Poullet JB, Massart S *et al* (2010). Impact of diet in shaping gut microbiota revealed by a comparative study in children from Europe and rural Africa. *Proc Natl Acad Sci USA* **107:** 14691-14696.

De Kerchove AJ, Elimelech M (2008). Calcium and magnesium cations enhance the adhesion of motile and nonmotile *Pseudomonas aeruginosa* on alginate films. *Langmuir* **24:** 3392-3399.

De Ruyter PGGA, Kuipers OP, De Vos WM (1996). Controlled gene expression systems for *Lactococcus lactis* with the food-grade inducer nisin. *Appl Environ Microbiol* **62:** 3662-3667.

De Vuyst L, Leroy F (2011). Cross-feeding between bifidobacteria and butyrate-producing colon bacteria explains bifdobacterial competitiveness, butyrate production, and gas production. *Int J Food Microbiol* **149:** 73-80.

Degnan BA, Macfarlane GT (1995). Arabinogalactan utilization in continuous cultures of *Bifidobacterium longum*: Effect of co-culture with *Bacteroides thetaiotaomicron*. *Anaerobe* **1:** 103-112.

Dereli RK, Ersahin ME, Ozgun H, Ozturk I, Jeison D, van der Zee F *et al* (2012). Potentials of anaerobic membrane bioreactors to overcome treatment limitations induced by industrial wastewaters. *Bioresource Technol* **122:** 160-170.

Donlan RM (2002). Biofilms: Microbial life on surfaces. *Emerg Infect Dis* **8:** 881-890.

Duncan SH, Louis P, Flint HJ (2004). Lactate-utilizing bacteria, isolated from human feces, that produce butyrate as a major fermentation product. *Appl Environ Microb* **70:** 5810-5817.

Dunne WM, Jr. (2002). Bacterial adhesion: Seen any good biofilms lately? *Clin Microbiol Rev* **15:** 155-166.

Eberl HJ, Parker DF, Vanloosdrecht MCM (2001). A new deterministic spatio-temporal continuum model for biofilm development. *J Theor Med* **3:** 161-175.

Epstein N (1989). On tortuosity and the tortuosity factor in flow and diffusion through porous media. *Chem Eng Sci* **44:** 777-779.

Eyssen H (1973). Role of the gut microflora in metabolism of lipids and sterols. *Proc Nutr Soc* **32:** 59-63.

Falony G, Vlachou A, Verbrugghe K, De Vuyst L (2006). Cross-feeding between *Bifidobacterium longum* BB536 and acetate-converting, butyrate-producing colon bacteria during growth on oligofructose. *Appl Environ Microbiol* **72:** 7835-7841.

Falony G (2009). Butyrogenic effect of inulin-type fructans: Kinetics of cross-feeding between colon bacteria. PhD thesis, Vrije Universiteit Brussel, Brussels.

Falony G, Calmeyn T, Leroy F, De Vuyst L (2009a). Coculture fermentations of *Bifidobacterium* species and *Bacteroides thetaiotaomicron* reveal a mechanistic insight into the prebiotic effect of inulin-type fructans. *Appl Environ Microb* **75:** 2312-2319.

Falony G, Lazidou K, Verschaeren A, Weckx S, Maes D, De Vuyst L (2009b). In vitro kinetic analysis of fermentation of prebiotic inulin-type fructans by *Bifidobacterium* species reveals four different phenotypes. *Appl Environ Microb* **75:** 454-461.

Fan LS, Leyva-Ramos R, Wisecarver KD, Zehner BJ (1990). Diffusion of phenol through a biofilm grown on activated carbon particles in draft-tube three-phase fluidized-bed bioreactor. *Biotechnol Bioeng* **35:** 279-286.

Ferrua MJ, Singh RP (2010). Modeling the fluid dynamics in a human stomach to gain insight of food digestion. *J Food Sci* **75:** R151-R162.

Ferrua MJ, Kong F, Singh RP (2011). Computational modeling of gastric digestion and the role of food material properties. *Trends Food Sci Technol* **22:** 480-491.

Flegal KM, Carroll MD, Ogden CL, Curtin LR (2010). Prevalence and trends in obesity among US adults, 1999-2008. *JAMA* **303:** 235-241.

Flemming H, Neu T, Wozniak D (2007). The EPS matrix: The "house of biofilm cells". *J Bacteriol* **189:** 7945 - 7947.

Flemming HC, Leis A, Strathmann M, Leon-Morales F (2005). The matrix reloaded - An interactive milieu. In: McBain A, Allison D, Pratten J, Spratt D, Upton M, Verran J (eds). *Biofilms: Persistence and Ubiquity*. The Biofilm Club: Manchester. pp 67-81.

Fletcher M (1988). Attachment of *Pseudomonas fluorescens* to glass and influence of electrolytes on bacterium-substratum separation distance. *J Bacteriol* **170:** 2027-2030.

Flint HJ, Scott KP, Louis P, Duncan SH (2012). The role of the gut microbiota in nutrition and health. *Nat Rev Gastroenterol* **9:** 577-589.

Franck A (2002). Technological functionality of inulin and oligofructose. *Brit J Nutr* **87:** S287-291.

Furrie E, Macfarlane S, Kennedy A, Cummings JH, Walsh SV, O'Neil DA *et al* (2005). Synbiotic therapy (*Bifidobacterium longum*/Synergy 1) initiates resolution of inflammation in patients with active ulcerative colitis: A randomised controlled pilot trial. *Gut* **54:** 242-249.

Gibson GR, Beatty ER, Wang X, Cummings JH (1995). Selective stimulation of bifidobacteria in the human colon by oligofructose and inulin. *Gastroenterology* **108:** 975-982.

Gilks WR, Richardson A, Spiegelhalter DJ (1996). *Markov Chain Monte Carlo in Practice*. Chapman & Hall: London.

Ginter E, Simko V (2010). Diabetes type 2 pandemic in 21st century. *Bratisl Med J* **111:** 134-137.

Giroux HJ, Constantineau S, Fustier P, Champagne CP, St-Gelais D, Lacroix M *et al* (2013). Cheese fortification using water-in-oil-in-water double emulsions as carrier for water soluble nutrients. *Int Dairy J* **29:** 107-114.

Glancey A, McBain AJ, Gilbert P (2007). Intestinal biofilms in health and neoplastic disease. In: Gilbert P, Allison D, Brading M, Pratten J, Spratt D, Upton M (eds). *Biofilms: Coming of Age*. The Biofilm Club: Manchester. pp 107-117.

Go PMNYH, Van Dieijen-Visser MP, Davies BI, Lens J, Brombacher PJ (1988). Microbial flora and bile acid metabolism in patients with an ileal reservoir. *Scand J Gastroentero* **23:** 229-236.

Goel P, Sneyd J, Friedman A (2006). Homogenization of the cell cytoplasm: The calcium bidomain equations. *Multiscale Model Sim* **5:** 1045-1062.

Goetze O, Steingoetter A, Menne D, Van Der Voort IR, Kwiatek MA, Boesiger P *et al* (2007). The effect of macronutrients on gastric volume responses and gastric emptying in humans: A

magnetic resonance imaging study. *American Journal of Physiology - Gastrointestinal and Liver Physiology*. pp G11-G17.

Goller CC, Romeo T (2008). Environmental Influences on Biofilm Development. In: Romeo T (ed). *Bacterial Biofilms*. Springer: Berlin. pp 37-66.

Gomi Y-I, Fukuoka M, Takeuchi S, Mihori T, Watanabe H (1996). Effect of temperature and moisture content on water diffusion coefficients in rice starch/water mictures. *Food Sci Technol Int* **2:** 171-173.

Gomi Y-I, Fukuoka M, Mihori T, Watanabe H (1998). The rate of starch gelatinization as observed by PFG-NMR measurement of water diffusivity in rice starch/water mixtures. *J Food Eng* **36:** 359-369.

Goulter RM, Gentle IR, Dykes GA (2009). Issues in determining factors influencing bacterial attachment: A review using the attachment of *Escherichia coli* to abiotic surfaces as an example. *Lett Appl Microbiol* **49:** 1-7.

Granato D, Branco GF, Nazzaro F, Cruz AG, Faria JA (2010). Functional foods and nondairy probiotic food development: Trends, concepts, and products. *Compr Rev Food Sci F* **9:** 292-302.

Grimshaw KEC, King RM, Nordlee JA, Hefle SL, Warner JO, Hourihane JOB (2003). Presentation of allergen in different food preparations affects the nature of the allergic reaction – A case series. *Clin Exp Allergy* **33:** 1581-1585.

Gristina A (2004). Biomaterial-centered infection: Microbial adhesion versus tissue integration. *Clin Orthop Relat R***:** 4-12.

Gristina AG (1987). Biomaterial-centered infection: Microbial adhesion versus tissue integration. *Science* **237:** 1588-1595.

Guarner F, Malagelada JR (2003). Gut flora in health and disease. *Lancet* **361:** 512-519.

Guinee TP, Fox PF (1983). Sodium chloride and moisture changes in Romano-type cheese during salting. *J Dairy Res* **50:** 511-518.

Guiot E, Georges P, Brun A, Fontaine-Aupart MP, Bellon-Fontaine MN, Briandet R (2002). Heterogeneity of diffusion inside microbial biofilms determined by fluorescence correlation spectroscopy under two-photon excitation. *Photochem Photobio* **75:** 570-578.

Guo MR, Fox PF, Flynn A, Kindstedt PS (1995). Susceptibility of β-lactoglobulin and sodium caseinate to proteolysis by pepsin and trypsin. *J Dairy Sci* **78:** 2336-2344.

Hamilton JP, Xie G, Raufman J-P, Hogan S, Griffin TL, Packard CA *et al* (2007). Human cecal bile acids: Concentration and spectrum. *Am J Physiol Gastrointest Liver Physiol* **293:** G256-G263.

Hammer BK, Bassler BL (2003). Quorum sensing controls biofilm formation in *Vibrio cholerae*. *Mol Microbiol* **50:** 101-104.

Hang PT, Brindley GW (1970). Methylene blue absorption by clay minerals. Determination of surface areas and cation exchange capacities (clay-organic studies XVIII). *Clay Clay Miner* **18:** 203-212.

Hasty DL, Ofek I, Courtney HS, Doyle RJ (1992). Multiple adhesins of streptococci. *Infect Immun* **60:** 2147-2152.

Hermanowicz SW (2001). A simple 2D biofilm model yields a variety of morphological features. *Math Biosci* **169:** 1-14.

Hermansson M (1999). The DLVO theory in microbial adhesion. *Colloid Surface B* **14:** 105-119.

Hicks S, Frankel G, Kaper JB, Dougan G, Phillips AD (1998). Role of intimin and bundle-forming pili in enteropathogenic *Escherichia coli* adhesion to pediatric intestinal tissue *in vitro*. *Infect Immun* **66:** 1570-1578.

Hinson RK, Kocher WM (1996). Model for effective diffusivities in aerobic biofilms. *J Environ Eng* **122:** 1023-1030.

Ho CS, Ju L-K (1988). Effects of microorganisms on effective oxygen diffusion coefficients and solubilities in fermentation media. *Biotechnol Bioeng* **32:** 313-325.

Hooper LV, Midwedt T, Gordon JI (2002). How host-microbial interactions shape the nutrient environment of the mammalian intestine. *Annu Rev Nutr* **22:** 283-307.

Hooper LV, MacPherson AJ (2010). Immune adaptations that maintain homeostasis with the intestinal microbiota. *Nat Rev Immunol* **10:** 159-169.

Hori K, Matsumoto S (2010). Bacterial adhesion: From mechanism to control. *Biochem Eng J* **48:** 424-434.

Horn H, Morgenroth E (2006). Transport of oxygen, sodium chloride, and sodium nitrate in biofilms. *Chem Eng Sci* **61:** 1347-1356.

Hosseini E, Grootaert C, Verstraete W, Van de Wiele T (2011). Propionate as a health-promoting microbial metabolite in the human gut. *Nutr Rev* **69:** 245-258.

Ishikawa T, Sato T, Mohit G, Imai Y, Yamaguchi T (2011). Transport phenomena of microbial flora in the small intestine with peristalsis. *J Theor Biol* **279:** 63-73.

Jacobs DM, Gaudier E, van Duynhoven J, Vaughan EE (2009). Non-digestible food ingredients, colonic microbiota and the impact on gut health and immunity: A role for metabolomics. *Curr Drug Metab* **10:** 41-54.

Janakiraman V, Englert D, Jayaraman A, Baskaran H (2009). Modeling growth and quorum sensing in biofilms grown in microfluidic chambers. *Ann Biomed Eng* **37:** 1206-1216.

Janssen M, Geeraerd AH, Logist F, De Visscher Y, Vereecken KM, Debevere J *et al* (2006). Modelling *Yersinia enterocolitica* inactivation in coculture experiments with *Lactobacillus sakei* as based on pH and lactic acid profiles. *Int J Food Microbiol* **111:** 59-72.

Jass J, Emerton ME, Robinson GB, Simpson HARW (1997). Adhesion of bone matrix cells and *Staphylococcus epidermidis* to surfaces. In: Wimpenny J, Handley P, Gilbert P, Lappin-Scott H, Jones m (eds). *Biofilms: Community Interactions and Control*. BioLine: Cardiff. pp 55-62.

Jenkinson HF, Nobbs AH, Jakubovics NS (2003). Adhesin-regulated biofilm communites. In: McBain A, Allison D, Brading M, Rickard A, Verran J, Walker J (eds). *Biofilm Communities: Order from Chaos?* BioLine: Cardiff. pp 97-103.

Jiménez E, Fernández L, Marín ML, Martín R, Odriozola JM, Nueno-Palop C *et al* (2005). Isolation of commensal bacteria from umbilical cord blood of healthy neonates born by cesarean section. *Curr Microbiol* **51:** 270-274.

Jiménez E, Delgado S, Fernández L, García N, Albújar M, Gómez A *et al* (2008a). Assessment of the bacterial diversity of human colostrum and screening of *staphylococcal* and *enterococcal* populations for potential virulence factors. *Res Microbiol* **159:** 595-601.

Jiménez E, Marín ML, Martín R, Odriozola JM, Olivares M, Xaus J *et al* (2008b). Is meconium from healthy newborns actually sterile? *Res Microbiol* **159:** 187-193.

Jones ML, Chen H, Ouyang W, Metz T, Prakash S (2004). Microencapsulated genetically engineered *Lactobacillus plantarum* 80 (pCBH1) for bile acid deconjugation and its implication in lowering cholesterol. *J Biomed Biotechnol* **2004:** 61-69.

Kamerman DK, Wilkinson MHF: In silico modelling of the human intestinal microflora. *International Conference on Computational Science (ICCS)*. Springer-Verlag 2002.

Kanmani P, Satish Kumar R, Yuvaraj N, Paari KA, Pattukumar V, Arul V (2013). Probiotics and its functionally valuable products-A review. *Crit Rev Food Sci* **53:** 641-658.

Kapellos GE, Alexiou TS, Payatakes AC (2007). A multiscale theoretical model for diffusive mass transfer in cellular biological media. *Math Biosci* **210:** 177-237.

Katsikogianni M, Missirlis YF (2004). Concise review of mechanisms of bacterial adhesion to biomaterials and of techniques used in estimating bacteria-material interactions. *Eur Cells Mat* **8:** 37-57.

Keener J, Sneyd J (1998). *Mathematical Physiology*. Springer-Verlag: New York.

Koch KL, Bitar KN, Fortunato JE (2012). Tissue engineering for neuromuscular disorders of the gastrointestinal tract. *World J Gastroentero* **18:** 6918-6925.

Kong F, Singh RP (2008). A model stomach system to investigate disintegration kinetics of solid foods during gastric digestion. *J Food Sci* **73:** E202-E210.

Kong F, Singh RP (2009a). Digestion of raw and roasted almonds in simulated gastric environment. *Food Biophys* **4:** 365-377.

Kong F, Singh RP (2009b). Modes of disintegration of solid foods in simulated gastric environment. *Food Biophys* **4:** 180-190.

Kong F, Oztop MH, Singh RP, McCarthy MJ (2011). Physical changes in white and brown rice during simulated gastric digestion. *J Food Sci* **76:** E450-E457.

Kong F, Singh RP (2011). Solid loss of carrots during simulated gastric digestion. *Food Biophys* **6:** 84-93.

Koo H, Xiao J, Klein MI, Jeon JG (2010). Exopolysaccharides produced by *Streptococcus mutans* glucosyltransferases modulate the establishment of microcolonies within multispecies biofilms. *J Bacteriol* **192:** 3024-3032.

Kreft JU, Picioreanu C, Wimpenny JWT, Van Loosdrecht MCM (2001). Individual-based modelling of biofilms. *Microbiology* **147:** 2897-2912.

Krishna R, Wesselingh JA (1997). The Maxwell-Stefan approach to mass transfer. *Chem Eng Sci* **52:** 861-911.

Kurokawa K, Itoh T, Kuwahara T, Oshima K, Toh H, Toyoda A *et al* (2007). Comparative metagenomics revealed commonly enriched gene sets in human gut microbiomes. *DNA Res* **14:** 169-181.

Lakhan SE, Kirchgessner A (2010). Gut inflammation in chronic fatigue syndrome. *Nutr Metab* **7:** 1-10.

Laspidou C, Rittmann B (2002). A unified theory for extracellular polymerica substances, soluble microbial products, and active and inert biomass. *J Water Res* **36:** 2711 - 2720.

Lebeer S, De Keersmaecker SCJ, Verhoeven TLA, Fadda AA, Marchal K, Vanderleyden J (2007). Functional analysis of *luxS* in the probiotic strain *Lactobacillus rhamnosus* GG reveals a central metabolic role important for growth and biofilm formation. *J Bacteriol* **189:** 860-871.

Leitch ECM, Walker AW, Duncan SH, Holtrop G, Flint HJ (2007). Selective colonization of insoluble substrates by human faecal bacteria. *Environ Microbiol* **9:** 667-679.

Lentle RG, Hemar Y, Hall CE, Stafford KJ (2005). Periodic fluid extrusion and models of digesta mixing in the intestine of a herbivore, the common brushtail possum (*Trichosurus vulpecula*). *J Comp Physiol [B]* **175:** 337-347.

Lentle RG, Janssen PWM (2008). Physical characteristics of digesta and their influence on flow and mixing in the mammalian intestine: A review. *J Comp Physiol [B]* **178:** 673-690.

Lentle RG, Janssen PWM (2010). Manipulating digestion with foods designed to change the physical characteristics of digesta. *Crit Rev Food Sci* **50:** 130-145.

Lewandowski Z (2000). Notes on biofilm porosity. *Water Res* **34:** 2620-2624.

Ley RE, Turnbaugh PJ, Klein S, Gordon JI (2006). Microbial ecology: Human gut microbes associated with obesity. *Nature* **444:** 1022-1023.

Li G, Wang Y, He R, Cao X, Lin C, Meng T (2009). Numerical simulation of predicting and reducing solid particle erosion of solid-liquid two-phase flow in a choke. *Pet Sci* **6:** 91-97.

Libicki SB, Salmon PM, Robertson CR (1988). Effective diffusive permeability of a nonreacting solute in microbial cell aggregates. *Biotechnol Bioeng* **32:** 68-85.

Lievin V, Peiffer I, Hudault S, Rochat F, Brassart D, Neeser JR *et al* (2000). *Bifidobacterium* strains from resident infant human gastrointestinal microflora exert antimicrobial activity. *Gut* **47:** 646-652.

Liu X, Lim JY, Donahue HJ, Dhurjati R, Mastro AM, Vogler EA (2007a). Influence of substratum surface chemistry/energy and topography on the human fetal osteoblastic cell line hFOB 1.19: Phenotypic and genotypic responses observed in vitro. *Biomaterials* **28:** 4535-4550.

Liu Y, Strauss J, Camesano TA (2007b). Thermodynamic investigation of *Staphylococcus epidermidis* interactions with protein-coated substrata. *Langmuir* **23:** 7134-7142.

Long G, Zhu P, Shen Y, Tong M (2009). Influence of extracellular polymeric substances (EPS) on deposition kinetics of bacteria. *Environ Sci Technol* **43:** 2308-2314.

Lucas JSA, Cochrane SA, Warner JO, Hourihane JOB (2008). The effect of digestion and pH on the allergenicity of kiwifruit proteins. *Pediatr Allergy Immu* **19:** 392-398.

Luckey TD (1972). Introduction to intestinal microecology. *Am J Clin Nutr* **25:** 1292-1294.

MacDonald TT, Monteleone G (2005). Immunity, inflammation, and allergy in the gut. *Science* **307:** 1920-1925.

Macfarlane GT, Cummings JH (1991). The colonic flora, fermentation and large bowel digestive function. In: Philips SF, Pemberton JH, Shorter RG (eds). *The Large Intestine: Physiology, Pathophysiology, and Disease*. Raven Press, Ltd.: New York. pp 51-92.

Macfarlane GT, Gibson GR, Cummings JH (1992). Comparison of fermentation reactions in different regions of the human colon. *J Appl Bacteriol* **72:** 57-64.

Macfarlane GT, Macfarlane S (2007). Models for intestinal fermentation: Association between food components, delivery systems, bioavailability and functional interactions in the gut. *Curr Opin Biotechnol* **18:** 156-162.

Macfarlane GT, Steed H, Macfarlane S (2008). Bacterial metabolism and health-related effects of galacto-oligosaccharides and other prebiotics. *J Appl Microbiol* **104:** 305-344.

Macfarlane GT, Blackett KL, Nakayama T, Steed H, Macfarlane S (2009). The gut microbiota in inflammatory bowel disease. *Curr Pharm Design* **15:** 1528-1536.

Macfarlane S, McBain AJ, Macfarlane GT (1997). Consequences of biofilm and sessile growth in the large intestine. *Adv Dent Res* **11:** 59-68.

Macfarlane S, Macfarlane GT (2006). Composition and metabolic activities of bacterial biofilms colonizing food residues in the human gut. *Appl Environ Microbiol* **72:** 6204-6211.

Macfarlane S, Dillon JF (2007). Microbial biofilms in the human gastrointestinal tract. *J Appl Microbiol* **102:** 1187-1196.

Madhu AN, Giribhattanavar P, Narayan MS, Prapulla SG (2009). Probiotic lactic acid bacterium from kanjika as a potential source of vitamin B_{12}: Evidence from LC-MS, immunological and microbiological techniques. *Biotechnol Lett* **32:** 1-4.

Mah T-FC, O'Toole GA (2001). Mechanisms of biofilm resistance to antimicrobial agents. *Trends Microbiol* **9:** 34-39.

Malagelada JR, Longstreth GF, Summerskill WHJ, Go VLW (1976). Measurement of gastric functions during digestion of ordinary solid meals in man. *Gastroenterology* **70:** 203-210.

Marciani L, Gowland PA, Fillery-Travis A, Manoj P, Wright J, Smith A *et al* (2001). Assessment of antral grinding of a model solid meal with echo-planar imaging. *Am J Physiol* **280:** G844-G849.

Marteau P, Pochart P, Dore J, Bera-Maillet C, Bernalier A, Corthier G (2001). Comparative study of bacterial groups within the human cecal and fecal microbiota. *Appl Environ Microb* **67:** 4939-4942.

Marvasi M, Visscher PT, Casillas Martinez L (2010). Exopolymeric substances (EPS) from *Bacillus subtilis* : Polymers and genes encoding their synthesis. *FEMS Microbiol Lett* **313:** 1-9.

Maxwell JC (1892). *A Treatise on Electricity and Magnetism*, Third edn, vol. 1. Clarendon Press: Oxford.

McLean JS, Ona ON, Majors PD (2008). Correlated biofilm imaging, transport and metabolism measurements via combined nuclear magnetic resonance and confocal microscopy. *ISME J* **2:** 121-131.

Meyer D, Stasse-wolthuis M (2009). The bifidogenic effect of inulin and oligofructose and its consequences for gut health. *Euro J Clin Nutr* **63:** 1277-1289.

Mirande C, Kadlecikova E, Matulova M, Capek P, Bernalier-Donadille A, Forano E *et al* (2010). Dietary fibre degradation and fermentation by two xylanolytic bacteria *Bacteroides xylanisolvens* XB1A^T and *Roseburia intestinalis* XB6B4 from the human intestine. *J Appl Microbiol* **109:** 451-460.

Mishellany-Dutour A, Peyron MA, Croze J, François O, Hartmann C, Alric M *et al* (2011). Comparison of food boluses prepared in vivo and by the AM2 mastication simulator. *Food Qual Prefer* **22:** 326-331.

Missirlis YF, Katsikogianni M (2007). Theoretical and experimental approaches of bacteria-biomaterial interactions. *Materwiss Werksttech* **38:** 983-994.

Mitchell DA, Do DD, Greenfield PF, Doelle HW (1991). A semimechanistic mathematical model for growth of *Rhizopus oligosporus* in a model solid-state fermentation system. *Biotechnol Bioeng* **38:** 353-362.

Mlobeli NT (1996). Batch culture stidies of *Bifidobacterium bifidum*. Master thesis, Massey University, Palmerston North.

Mlobeli NT, Gutierrez NA, Maddox IS (1998). Physiology and kinetics of *Bifidobacterium bifidum* during growth on different sugars. *Appl Microbiol Biot* **50:** 125-128.

Mota M, Teixeira JA, Yelshin A (2002). Immobilized particles in gel matrix-type porous media. Nonhomogeneous cell distribution. *Biotechnol Prog* **18:** 807-814.

Mounier J, Monnet C, Vallaeys T, Arditi R, Sarthou AS, Hélias A *et al* (2008). Microbial interactions within a cheese microbial community. *Appl Environ Microb* **74:** 172-181.

Muñoz-Quezada S, Bermudez-Brito M, Chenoll E, Genovés S, Gomez-Llorente C, Plaza-Diaz J *et al* (2013). Competitive inhibition of three novel bacteria isolated from faeces of breast milk-fed infants against selected enteropathogens. *Brit J Nutr* **109:** S63-S69.

Muñoz-Tamayo R, Laroche B, Walter T, Doré J, Leclerc M (2010). Mathematical modelling of carbohydrate degradation by human colonic microbiota. *J Theor Biol* **266:** 189-201.

Muñoz-Tamayo R, Laroche B, Walter É, Doré J, Duncan SH, Flint HJ *et al* (2011). Kinetic modelling of lactate utilization and butyrate production by key human colonic bacterial species. *FEMS Microbiol Ecol* **76:** 615-624.

Nepelska M, Cultrone A, Béguet-Crespel F, Le Roux K, Doré J, Arulampalam V *et al* (2012). Butyrate produced by commensal bacteria potentiates phorbol esters induced AP-1 response in human intestinal epithelial cells. *PLoS ONE* **7:** e52869.

Neu TR (1996). Significance of bacterial surface-active compounds in interaction of bacteria with interfaces. *Microbiol Rev* **60:** 151-166.

Nielsen PH, Jahn A (1999). Extraction of EPS. In: Wingender J, Neu TR, Flemming H-C (eds). *Microbial Extracellular Polymeric Substances*. Springer: Berlin. pp 49-72.

O'Keefe SJD (2008). Nutrition and colonic health: The critical role of the microbiota. *Curr Opin Gastroen* **24:** 51-58.

O'May GA, Reynolds N, Smith AR, Kennedy A, Macfarlane GT (2005). Effect of pH and antibiotics on microbial overgrowth in the stomachs and duodena of patients undergoing percutaneous endoscopic gastrostomy feeding. *J Clin Microbiol* **43:** 3059-3065.

O'Toole PW, Claesson MJ (2010). Gut microbiota: Changes throughout the lifespan from infancy to elderly. *Int Dairy J* **20:** 281-291.

Ölveczky BP, Verkman AS (1998). Monte Carlo analysis of obstructed diffusion in three dimensions: Application to molecular diffusion in organelles. *Biophys J* **74:** 2722-2730.

Oubekka SD, Briandet R, Waharte F, Fontaine-Aupart MP, Steenkeste K: Image-based fluorescence recovery after photobleaching (FRAP) to dissect vancomycin diffusion-reaction processes in *Staphylococcus aureus* biofilms. *Clinical and Biomedical Spectorscopy and Imaging II*; Munich. 2011.

Özdemir Ö (2010). Various effects of different probiotic strains in allergic disorders: An update from laboratory and clinical data. *Clin Exp Immunol* **160:** 295-304.

Panico S, Mattiello A (2010). Epidemiology of cardiovascular diseases in women in Europe. *Nutr Metab Cardiovasc Dis* **20:** 379-385.

Pashley RM, McGuiggan PM, Ninham BW, Evans DF (1985). Attractive forces between uncharged hydrophobic surfaces: Direct measurements in aqueous solution. *Science* **229:** 1088-1089.

Payne MR, Morison KR (1999). A multi-component approach to salt and water diffusion in cheese. *Int Dairy J* **9:** 887-894.

Pell RJ, Kowalski BR (1991). A test of three fitting criteria for multiresponse non-linear modeling. *J Chemometr* **5:** 375-387.

Penders J, Thijs C, Vink C, Stelma FF, Snijders B, Kummeling I *et al* (2006). Factors influencing the composition of the intestinal microbiota in early infancy. *Pediatrics* **118:** 511-521.

Perez PF, Doré J, Leclerc M, Levenez F, Benyacoub J, Serrant P *et al* (2007). Bacterial imprinting of the neonatal immune system: Lessons from maternal cells? *Pediatrics* **119**.

Peters BM, Jabra-Rizk MA, O'May GA, William Costerton J, Shirtliff ME (2012). Polymicrobial interactions: Impact on pathogenesis and human disease. *Clin Microbiol Rev* **25:** 193-213.

Peyron MA, Mishellany A, Woda A (2004). Particle size distribution of food boluses after mastication of six natural foods. *J Dent Res* **83:** 578-582.

Phillips RE (1968). Water diffusivity of germinating soybean, corn, and cotton seed. *Agron J* **60:** 568-571.

Phillips RJ (2000). A hydrodynamic model for hindered diffusion of proteins and micelles in hydrogels. *Biophys J* **79:** 3350-3353.

Picioreanu C, Kreft JU, Van Loosdrecht MCM (2004). Particle-based multidimensional multispecies biofilm model. *Appl Environ Microb* **70:** 3024-3040.

Poschet F, Vereecken KM, Geeraerd AH, Nicolaï BM, Van Impe JF (2005). Analysis of a novel class of predictive microbial growth models and application to coculture growth. *Int J Food Microbiol* **100:** 107-124.

Probert HM, Gibson GR (2002). Bacterial biofilms in the human gastrointestinal tract. *Curr Iss Intest Microbiol* **3:** 23-27.

Rahman NK, Bakar MZA, Hekarl Uzir M, Kamaruddin AH (2009). Modelling on the effect of diffusive and convective substrate transport for biofilm. *Math Biosci* **218:** 130-137.

Rajagopalan S, Rockstraw DA, Munson-McGee SH (1997). Modeling substrate particle degradation by *Bacillus coagulans* biofilm. *Bioresource Technol* **61:** 175-183.

Ramnani P, Gaudier E, Bingham M, Van Bruggen P, Tuohy KM, Gibson GR (2010). Prebiotic effect of fruit and vegetable shots containing Jerusalem artichoke inulin: A human intervention study. *Brit J Nutr* **104:** 233-240.

Rao AV, Bested A, Beaulne T, Katzman M, Iorio C, Berardi J *et al* (2009). A randomized, double-blind, placebo-controlled pilot study of a probiotic in emotional symptoms of chronic fatigue syndrome. *Gut Pathogens* **1:** 6.

Rasmussen K, Lewandowski Z (1998). Microelectrode measurements of local mass transport rates in heterogeneous biofilms. *Biotechnol Bioeng* **59:** 302-309.

Renslow RS, Majors PD, McLean JS, Fredrickson JK, Ahmed B, Beyenal H (2010). *In situ* effective diffusion coefficient profiles in live biofilms using pulsed-field gradient nuclear magnetic resonance. *Biotechnol Bioeng* **106:** 928-937.

Rhoads DD, Wolcott RW, Cutting KF, Percival SL (2007). Evidenc of Biofilms in Wounds and Potential Ramifications. In: Gilbert P, Allison D, Brading M, Pratten J, Spratt D, Upton M (eds). *Biofilms: Coming of Age*. The Biofilm Club: Manchester. pp 131-143.

Ridlon JM, Kang D-J, Hylemon PB (2006). Bile salt biotransformations by human intestinal bacteria. *J Lipid Res* **47:** 241-259.

Rossi M, Corradini C, Amaretti A, Nicolini M, Pompei A, Zanoni S *et al* (2005). Fermentation of fructooligosaccharides and inulin by bifidobacteria: A comparative study of pure and fecal cultures. *Appl Environ Microb* **71:** 6150-6158.

Rüdiger SG, Carlén A, Meurman JH, Kari K, Olsson J (2002). Dental biofilms at healthy and inflamed gingival margins. *J Clin Periodontol* **29:** 524-530.

Saguy IS, Marabi A, Wallach R (2005). New approach to model rehydration of dry food particulates utilizing principles of liquid transport in porous media. *Trends Food Sci Technol* **16:** 495-506.

Sandiford S, Tagg J, Upton M (2007). Antimicrobial peptides as agents to combat coagulase megatie *Stapylococcal* biofilms. In: Gilbert P, Allison D, Brading M, Pratten J, Spratt D, Upton M (eds). *Biofilms: Coming of Age*. The Biofilm Club: Manchester. pp 145-156.

Satokari R, Grönroos T, Laitinen K, Salminen S, Isolauri E (2009). *Bifidobacterium* and *Lactobacillus* DNA in the human placenta. *Lett Appl Microbiol* **48:** 8-12.

Saulnier DM, Kolida S, Gibson GR (2009). Microbiology of the human intestinal tract and approaches for its dietary modulation. *Curr Pharm Design* **15:** 1403-1414.

Saxton MJ (1987). Lateral diffusion in an archipelago. The effect of mobile obstacles. *Biophys J* **52:** 989-997.

Saxton MJ (1994). Anomalous diffusion due to obstacles: A Monte Carlo study. *Biophys J* **66:** 394-401.

Schneider RP (1996). Conditioning film-induced modification of substratum physicochemistry - Analysis by contact Angles. *J Colloid Interface Sci* **182:** 204-213.

Sela DA, Price NPJ, Mills DA (2010). Carbohydrate metabolism of the bifidobacteria. In: Mayo B, van Sinderen D (eds). *Bifidobacteria: Genomics and Molecular Aspecs*. Caister Academic Press: Norfolk. pp 46-48.

Selman JD, Rice P, Abdul-Rezzak RK (1983). A study of the apparent diffusion coefficients for solute losses from carrot tissue during blanching in water. *J Food Technol* **18:** 427-440.

Sharp MD, McMahon DJ, Broadbent JR (2008). Comparative evaluation of yogurt and low-fat cheddar cheese as delivery media for probiotic *Lactobacillus casei*. *J Food Sci* **73:** M375-M377.

Shipman JA, Cho KH, Siegel HA, Salyers AA (1999). Physiological characterization of SusG, an outer membrane protein essential for starch utilization by *Bacteroides thetaiotaomicron*. *J Bacteriol* **181:** 7206-7211.

Shipman JA, Berleman JE, Salyers AA (2000). Characterization of four outer membrane proteins involved in binding starch to the cell surface of *Bacteroides thetaiotaomicron*. *J Bacteriol* **182:** 5365-5372.

Shorten PR, Membré JM, Pleasants AB, Kubaczka M, Soboleva TK (2004). Partitioning of the variance in the growth parameters of *Erwinia carotovora* on vegetable products. *Int J Food Microbiol* **93:** 195-208.

Shorten PR, Sneyd J (2009). A mathematical analysis of obstructed diffusion within skeletal muscle. *Biophys J* **96:** 4764-4778.

Siegel JA, Urbain JL, Adler LP, Charkes ND, Maurer AH, Krevsky B *et al* (1988). Biphasic nature of gastric emptying. *Gut* **29:** 85-89.

Singh H, Ye A (2013). Structural and biochemical factors affecting the digestion of protein-stabilized emulsions. *Curr Opin Colloid In* **18:** 360-370.

Staudt C, Horn H, Hempel DC, Neu TR (2004). Volumetric measurements of bacterial cells and extracellular polymeric substance glycoconjugates in biofilms. *Biotechnol Bioeng* **88:** 585-592.

Stoodley P, DeBeer D, Lewandowski Z (1994). Liquid flow in biofilm systems. *Appl Environ Microb* **60:** 2711-2716.

Suau A, Bonnet R, Sutren M, Godon J-J, Gibson GR, Collins MD *et al* (1999). Direct analysis of genes encoding 16S rRNA from complex communities reveals many novel molecular species within the human gut. *Appl Environ Microbiol* **65:** 4799-4807.

Suslina TA (2005). On homogenization for a periodic elliptic operator in a strip. *St Petersburg Math J* **16:** 237-257.

Sutherland IW (2001a). The biofilm matrix - An immobilized but dynamic microbial environment. *Trends Microbiol* **9:** 222-227.

Sutherland IW (2001b). Biofilm exopolysaccharides: A strong and sticky framework. *Microbiology* **147:** 3-9.

Syarief AM, Gustafson RJ, Morey RV (1987). Moistrue diffusion coefficients for yellow-dent corn components. *T Am Soc Agr Eng* **30:** 522-528.

Tallon MJ (2009). *Probiotics success strategies in food and drinks*. Business Insights Ltd.

Tannock GW, Ghazally S, Walter J, Loach D, Brooks H, Cook G *et al* (2005). Ecological behavior of *Lactobacillus reuteri* 100-23 is affected by mutation of the *luxS* gene. *Appl Environ Microb* **71:** 8419-8425.

Thomas LA, Veysey MJ, French G, Hylemon PB, Murphy GM, Dowling RH (2001). Bile acid metabolism by fresh human colonic contents: A comparison of caecal versus faecal samples. *Gut* **49:** 835-842.

Toms AP, Farghal A, Kasmai B, Bagnall A, Malcolm PN (2011). Physiology of the small bowel: A new approach using MRI and proposal for a new metric of function. *Med Hypotheses* **76:** 834-839.

Tydeman EA, Parker ML, Wickham MSJ, Rich GT, Faulks RM, Gidley MJ *et al* (2010). Effect of carrot (*Daucus carota*) microstructure on carotene bioaccessibilty in the upper gastrointestinal tract. 1. In vitro simulations of carrot digestion. *J Agr Food Chem* **58:** 9847-9854.

Van der Meulen R, Adriany T, Verbrugghe K, De Vuyst L (2006a). Kinetic analysis of bifidobacterial metabolism reveals a minor role for succinic acid in the regeneration of NAD+ through Its growth-associated production. *Appl Environ Microbiol* **72:** 5204-5210.

Van der Meulen R, Makras L, Verbrugghe K, Adriany T, De Vuyst L (2006b). *In vitro* kinetic analysis of oligofructose consumption by *Bacteroides* and *Bifidobacterium* spp. indicates different degradation mechanisms. *Appl Environ Microb* **72:** 1006-1012.

Van Impe JF, Poschet F, Geeraerd AH, Vereecken KM (2005). Towards a novel class of predictive microbial growth models. *Int J Food Microbiol* **100:** 97-105.

Van Oss CJ, Good RJ, Chaudhury MK (1986). The role of van der Waals forces and hydrogen bonds in "hydrophobic interactions" between bipolymers and low energy surfaces. *J Colloid Interface Sci* **111:** 378-390.

Van Oss CJ, Chaudhury MK, Good RJ (1988). Interfacial Lifshitz-van der Waals and polar interactions in macroscopic systems. *Chem Rev* **88:** 927-941.

Van Oss CJ (1989). Energetics of cell-cell and cell-biopolymer interactions. *Cell Biochem Biophys* **14:** 1-16.

Van Wey AS, Cookson AL, Roy NC, McNabb WC, Soboleva TK, Shorten PR (2011). Bacterial biofilms associated with food particles in the human large bowel. *Mol Nutr Food Res* **55:** 969-978.

Van Wey AS, Cookson AL, Soboleva TK, Roy NC, McNabb WC, Bridier A *et al* (2012). Anisotropic nutrient transport in three-dimensional single species bacterial biofilms. *Biotechnol Bioeng* **109:** 1280-1292.

Van Wey AS, Shorten PR (Accepted). Mathematical models of food degradation in the human stomach. In: Boland M, Golding M, Singh H (eds). *Food Structures, Digestion and Health*. Elsevier.

Van Wey AS, Cookson AL, Roy NC, McNabb WC, Soboleva TK, Shorten PR (Submitted-a). Monoculture parameters successfully predict the coculture growth of *Bacteroides thetaiotaomicron* and *Bifidobacterium*. *ISME J*.

Van Wey AS, Cookson AL, Roy NC, McNabb WC, Soboleva TK, Wieliczko RJ *et al* (Submitted-b). A mathematical model of the effect of pH and food matrix composition on fluid transport into foods: An application in gastric digestion and cheese brining. *Food Res Int*.

Venugopalan VP, Kuehn M, Hausner M, Springael D, Wilderer PA, Wuertz S (2005). Architecture of a nascent *Sphingomonas* sp. biofilm under varied hydrodynamic conditions. *Appl Environ Microb* **71:** 2677-2686.

Verschueren M, Engles WJM, Straatsman J, van den Berg G, de Jong P (2007). Modelling Gouda ripening to predict flavour development. In: Weinmer BC (ed). *Improving the Flavour in Cheese*. Woodhead Publishing: Philadelphia. pp 537-562.

Vu B, Chen M, Crawford RJ, Ivanova EP (2009). Bacterial extracellular polysaccharides involved in biofilm formation. *Molecules* **14:** 2535-2554.

Wada J, Ando T, Kiyohara M, Ashida H, Kitaoka M, Yamaguchi M *et al* (2008). *Bifidobacterium bifidum* lacto-N-biosidase, a critical enzyme for the degradation of human milk oligosaccharides with a type 1 structure. *Appl Environ Microb* **74:** 3996-4004.

Waggoner PE, Parlange J-Y (1976). Water uptake and water diffusivity of seeds. *Plant Physiol* **57:** 153-156.

Waharte F, Steenkeste K, Briandet R, Fontaine-Aupart MP (2010). Diffusion measurements inside biofilms by image-based fluorescence recovery after photobleaching (FRAP) analysis with a commercial confocal laser scanning microscope. *Appl Environ Microb* **76:** 5860-5869.

Walker AW, Duncan SH, Harmsen HJM, Holtrop G, Welling GW, Flint HJ (2008). The species composition of the human intestinal microbiota differs between particle-associated and liquid phase communities. *Environ Microbiol* **10:** 3275-3283.

Wang Q, Zhang T (2010). Review of mathematical models for biofilms. *Solid State Comm* **150:** 1009-1022.

Wang Z, Liu Y, Tay J (2007). Biodegradability of extracellular polymeric substances produced by aerobic granules. *Appl Microbiol Biot* **74:** 462 - 466.

Wanner O, Eberl HJ, Morgenroth E, Noguera DlR, Picioreanu C, Rittmann BE *et al* (2006). *Mathematical Modeling of Biofilms*. IWA Publishing: London.

Wiesmann R, Zimelka W, Baumgärtl H, Götz P, Buchholz R (1994). Investigation of oxygen transfer through the membrane of polymer hollowspheres by oxygen micro-electrodes. *J Biotech* **32:** 221-229.

Wilkinson MHF (2002). Model intestinal microflora in computer simulation: A simulation and modeling package for host-microflora interactions. *IEEE T Bio-Med Eng* **49:** 1077-1085.

Wintermute EH, Silver PA (2010). Emergent cooperation in microbial metabolism. *Mol Syst Biol* **6**.

Wolfaardt GM, Lawrence JR, Korber DR (1999). Function of EPS. In: Wingender J, Neu TR, Flemming H-C (eds). *Microbial Extracellular Polymeric Substances*. Springer: Berlin. pp 171-200.

Wood BD, Whitaker S (1999). Cellular growth in biofilms. *Biotechnol Bioeng* **64:** 656-670.

Wood BD, Whitaker S (2000). Multi-species diffusion and reaction in biofilms and cellular media. *Chem Eng Sci* **55:** 3397-3418.

Wood BD, Quintard M, Whitaker S (2002). Calculation of effective diffusivities for biofilms and tissues. *Biotechnol Bioeng* **77:** 495-516.

Xavier JB, Picioreanu C, van Loosdrecht MCM (2004). Assessment of three-dimensional biofilm models through direct comparison with confocal microscopy imaging. *Wat Sci Tech* **49:** 177-185.

Xu J, Mahowald MA, Ley RE, Lozupone CA, Hamady M, Martens EC *et al* (2007). Evolution of symbiotic bacteria in the distal human intestine. *PLoS Biol* **5:** e156.

Yamamoto S (1999). Effects of glycerol on the drying of gelatin and sugar solutions. *Dry Technol* **17:** 1681-1695.

Yang S, Lewandowski Z (1995). Measurement of local mass transfer coefficient in biofilms. *Biotechnol Bioeng* **48:** 737-744.

Yerly J, Hu Y, Jones SM, Martinuzzi RJ (2007). A two-step procedure for automatic and accurate segmentation of volumetric CLSM biofilm images. *J Microbiol Meth* **70:** 424-433.

Younes H, Coudray C, Bellanger J, Demigné C, Rayssiguier Y, Rémésy C (2001). Effects of two fermentable carbohydrates (inulin and resistant starch) and their combination on calcium and magnesium balance in rats. *Brit J Nutr* **86:** 479-485.

Zhang TC, Bishop PL (1994). Density, porosity, and pore structure of biofilms. *Water Res* **28:** 2267-2277.

Zhu J, Mekalanos JJ (2003). Quorum sensing-dependent biofilms enhance colonization in *Vibrio cholerae*. *Dev Cell* **5:** 647-656.

Appendix A

The 60 strains of bacteria used to determine EDC values both perpendicular and parallel to the substratum. For complete details about the origin of the bacteria used in this study, please refer to the work of Bridier et al (2010). The strains in bold were used to determine the effects of EPS on nutrient transport within biofilms.

Species	Strain	Species	Strain
Salmonella enterica	**S24 (ser. St Paul)**	*Listeria monocytogenes*	**EGDe**
	I26 (ser. Agona)		CIP 104794
	S2 (ser. Brandenburg)		CIP 103573
	S19 (ser. Duby)		CIP 103575
	S59 (ser. Dublin)		CIP 78 39
	S38 (ser. Enteritidis)		370P-Lm
	S12 (ser. Hadar)		Lm 162
	S55 (ser. Indiana)		Lm 481
	ATCC 13311 (ser. Typhimurium)		LO28
	S34 (ser. Typhimurium)		BUG1641
Escherichia coli	**PHL 565 (MG1655)**	*Pseudomonas aeruginosa*	**ATCC 15442**
	163P-Ec		PSE.1.2
	186P-Ec		ATCC 10145
	RS218		ATCC 14210
	ATCC 8739		ATCC 49189
	ESC.1.13		ATCC 9027
	ESC.1.16		ATCC 15692
	ESC.1.24		ATCC 9721
	ESC.1.30		ATCC 14207
	ESC.1.33		ATCC 51447
Staphylococcus aureus	**ATCC 6538**	*Enterococcus faecalis*	**ATCC 19433**
	CIP 57.10		ATCC 51188
	ATCC 9144		ATCC 33012
	ATCC 29213		ATCC 49477
	ATCC 27217		ATCC 33186
	ATCC 25923		ATCC 27959
	ATCC 29247		ATCC 700802
	ATCC 8096		ATCC 29212
	ATCC 43300		ATCC 29302
	STA.1.5		ATCC 51299